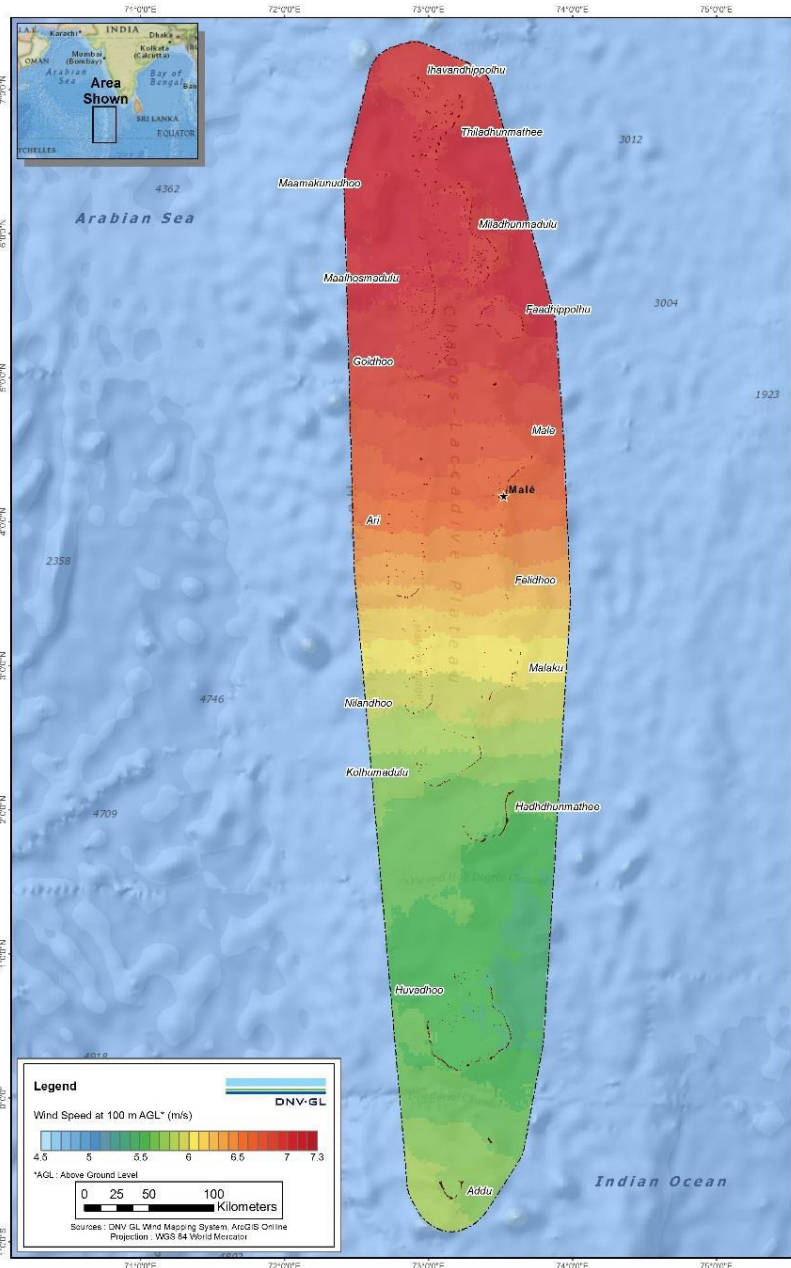


# Wind Resource Mapping in the Maldives

## MESOSCALE WIND MODELING REPORT

JULY 2015



This report was prepared by [DNV GL](#), under contract to [The World Bank](#).

It is one of several outputs from the wind **resource mapping component of the activity “Renewable Energy Resource Mapping and Geospatial Planning – Maldives”** [Project ID: P146018]. This activity is funded and supported by the Energy Sector Management Assistance Program (ESMAP), a multi-donor trust fund administered by The World Bank, under a global initiative on Renewable Energy Resource Mapping. Further details on the initiative can be obtained from the [ESMAP website](#).

This document is an **interim output** from the above-mentioned project. Users are strongly advised to exercise caution when utilizing the information and data contained, as this has not been subject to full peer review. The final, validated, peer reviewed output from this project will be the Maldives Wind Atlas, which will be published once the project is completed.

Copyright © 2015 International Bank for Reconstruction and Development / THE WORLD BANK  
Washington DC 20433  
Telephone: +1-202-473-1000  
Internet: [www.worldbank.org](http://www.worldbank.org)

This work is a product of the consultants listed, and not of World Bank staff. The findings, interpretations, and conclusions expressed in this work do not necessarily reflect the views of The World Bank, its Board of Executive Directors, or the governments they represent.

The World Bank does not guarantee the accuracy of the data included in this work and accept no responsibility for any consequence of their use. The boundaries, colors, denominations, and other information shown on any map in this work do not imply any judgment on the part of The World Bank concerning the legal status of any territory or the endorsement or acceptance of such boundaries.

The material in this work is subject to copyright. Because The World Bank encourages dissemination of its knowledge, this work may be reproduced, in whole or in part, for non-commercial purposes as long as full attribution to this work is given. Any queries on rights and licenses, including subsidiary rights, should be addressed to World Bank Publications, The World Bank Group, 1818 H Street NW, Washington, DC 20433, USA; fax: +1-202-522-2625; e-mail: [pubrights@worldbank.org](mailto:pubrights@worldbank.org). Furthermore, the ESMAP Program Manager would appreciate receiving a copy of the publication that uses this publication for its source sent in care of the address above, or to [esmap@worldbank.org](mailto:esmap@worldbank.org).

RENEWABLE ENERGY WIND MAPPING FOR THE MALDIVES

# Mesoscale Wind Modeling Report 1- Interim wind atlas for the Maldives

The World Bank

**Document No.:** 702909-AUME-R-01-D

**Issue:** D, **Status:** FINAL

**Date:** 02 July 2015



## IMPORTANT NOTICE AND DISCLAIMER

1. This document is intended for the sole use of the Customer as detailed on the front page of this document to whom the document is addressed and who has entered into a written agreement with the DNV GL entity issuing this document ("DNV GL"). To the extent permitted by law, neither DNV GL nor any group company (the "Group") assumes any responsibility whether in contract, tort including without limitation negligence, or otherwise howsoever, to third parties (being persons other than the Customer), and no company in the Group other than DNV GL shall be liable for any loss or damage whatsoever suffered by virtue of any act, omission or default (whether arising by negligence or otherwise) by DNV GL, the Group or any of its or their servants, subcontractors or agents. This document must be read in its entirety and is subject to any assumptions and qualifications expressed therein as well as in any other relevant communications in connection with it. This document may contain detailed technical data which is intended for use only by persons possessing requisite expertise in its subject matter.
2. This document is protected by copyright and may only be reproduced and circulated in accordance with the Document Classification and associated conditions stipulated or referred to in this document and/or in DNV GL's written agreement with the Customer. This document may not be disclosed in any prospectus or stock exchange listing without the express and prior written consent of DNV GL. A Document Classification permitting the Customer to redistribute this document shall not thereby imply that DNV GL has any liability to any recipient other than the Customer.
3. This document may be printed or download provided that: no documents or related graphics in this document are modified in any way; no graphics in the document are used separately from the corresponding text; DNV GL's copyright and trade mark notices and any permission noted appear in all copies; no attempt is made to interfere with the intended and efficient functioning of the document, and no attempt is made to reverse engineer, disassemble, or decompile the document or any information herein, and no process or procedure is made to derive the source code of any software included herein.
4. This document has been produced from information relating to dates and periods referred to in this document. This document does not imply that any information is not subject to change. Except and to the extent that checking or verification of information or data is expressly agreed within the written scope of its services, DNV GL shall not be responsible in any way in connection with erroneous information or data provided to it by the Customer or any third party, or for the effects of any such erroneous information or data whether or not contained or referred to in this document.
5. Any energy forecasts estimates or predictions are subject to factors not all of which are within the scope of the probability and uncertainties contained or referred to in this document and nothing in this document guarantees any particular wind speed or energy output.

## KEY TO DOCUMENT CLASSIFICATION

Strictly Confidential	:	For disclosure only to named individuals within the Customer's organisation.
Private and Confidential	:	For disclosure only to individuals directly concerned with the subject matter of the document within the Customer's organisation.
Commercial in Confidence	:	Not to be disclosed outside the Customer's organisation.
DNV GL only	:	Not to be disclosed to non-DNV GL staff
Customer's Discretion	:	Distribution for information only at the discretion of the Customer (subject to the above Important Notice and Disclaimer and the terms of DNV GL's written agreement with the Customer).
Published	:	Available for information only to the general public (subject to the above Important Notice and Disclaimer).

Project name: Renewable Energy Wind Mapping for the Maldives DNV GL - Energy  
 Report title: Mesoscale Wind Modeling Report 1 Renewables Advisory  
 Customer: The World Bank, 9665 Chesapeake Drive, Suite 435  
 1818 H Street, N.W. San Diego, CA 92123  
 Washington, DC 20433 Tel: 703-795-8103  
 Contact person: Abdulaziz Faghi Enterprise No.: 94-3402236  
 Date of issue: 02 July 2015  
 Project No.: 702909  
 Document No.: 702909-AUME-R-01-D  
 Issue/Status: D/FINAL

Task and objective: Present the results of the interim mesoscale wind mapping for the Maldives, including a detailed summary of assumptions and methodology used.

Prepared by:  <hr/> Mark Purcell Engineer, Renewables Advisory	Verified by:  <hr/> Daran Rife Global Head of Mesoscale Modeling	Approved by:  <hr/> Richard Whiting Service Line Leader, Project Development
<hr/> Jessica Ma Global Specialist – Mesoscale Modeling	<hr/> Trenton Gilbert Head of Section, Developer Support Services (Pacific), Renewables Advisory	
<hr/> Caroline Donohue GIS Analyst, Environmental and Permitting Services		

- Strictly Confidential
- Private and Confidential
- Commercial in Confidence
- DNV GL only
- Customer's Discretion
- Published

Keywords:  
 World Bank, ESMAP, ASTAE, Maldives, wind,  
 mesoscale, mapping, methodology, GIS

© Garrad Hassan America, Inc. All rights reserved.

Reference to part of this report which may lead to misinterpretation is not permissible.

Issue	Date	Reason for Issue	Prepared by	Verified by	Approved by
A	13 February 2015	Draft	MP/JM/CD	DR/TG	RW
B	08 May 2015	Final	MP/JM/CD	DR/TG	RW
C	2 July 2015	Final, repaginated	MP/JM/CD	DR/TG	RW

## Table of contents

1 INTRODUCTION .....	7
1.1 Background .....	7
1.2 Project description.....	8
2 METHODOLOGY – DNV GL WIND MAPPING SYSTEM.....	9
3 RESULTS.....	10
3.1 Preliminary and Unvalidated Wind Speed Map.....	10
3.2 Preliminary and Unvalidated Wind Speed Uncertainty Index.....	14
3.3 Preliminary and Unvalidated Wind Energy Map.....	17
3.4 Preliminary and Unvalidated Seasonal and Diurnal Trends .....	21
3.5 Preliminary and Unvalidated Estimates of Interannual Variability.....	23
3.6 Interim Wind Atlas (*.lib files) .....	25
4 REFERENCES .....	26
APPENDIX A – DETAILED METHODOLOGY .....	27
APPENDIX B – PRELIMINARY AND UNVALIDATED MESOSCALE OUTPUTS .....	52

## List of tables

Table 3-1 Representative energy loss factors applied.....	17
Table 3-2 “12 x 24” matrix of energy production (% of annual mean energy production) .....	21

## List of figures

Figure 2-1 Mesoscale computational grid configuration used for the DNV GL WMS simulations.....	9
Figure 3-1 Preliminary and unvalidated mesoscale annual mean wind speed map at 100 m AGL, .....	12
Figure 3-2 Preliminary and unvalidated mesoscale annual mean wind speed map at 10 m AGL, .....	13
Figure 3-3 The multiphysics ensemble approach .....	14
Figure 3-4 Preliminary and unvalidated wind speed uncertainty index.....	16
Figure 3-5 Preliminary and unvalidated annual mean wind energy map created using the DNV GL Wind Mapping System .....	19
Figure 3-6 Hypothetical maximum wind turbine capacity for inhabited islands across the Maldives.....	20
Figure 3-7 Seasonal variation of energy production for four selected grid cells.....	22
Figure 3-8 Seasonal flow patterns for Sep 2013-Sep 2014 over the Maldives.....	23
Figure 3-9 Preliminary and unvalidated interannual variability index (IAVI) for wind speed .....	24



# 1 INTRODUCTION

The results described in this report are derived from interim output and are **preliminary** and **unvalidated**, and they **have not been subjected to full peer review**. DNV GL does not guarantee the accuracy of the maps, data, and visualizations presented in this report, and accepts no responsibility whatsoever for any consequence of their use. Wind speed values shown in tables and maps should not be relied upon in an absolute sense. Rather they should be strictly interpreted as indicative (e.g., elevated windiness near mountaintops and escarpments). Users are strongly urged to exercise caution when using the information and data contained within this report.

During Phase 2 of this project, measurements will be collected from a number of representative sites throughout the country over a 24 month period, and these will be used in Phase 3 to develop a final, validated, peer-reviewed suite of outputs from this project, which will be made available at the project's completion.


The World Bank (the "Client") has retained Garrad Hassan America, Inc. ("DNV GL") to provide a validated mesoscale wind atlas for the Maldives, including associated deliverables and wind energy development training courses. A new 2-km-resolution mesoscale wind atlas has been generated by DNV GL for the entire country of the Maldives, providing a comprehensive up-to-date estimate of the potential resource. It is based on a complete 10-year simulation of the local and regional wind flows, and will serve as the foundation to a broader program of sustainable development of renewable energy in the Maldives, while dramatically increasing the awareness of the available resources within the country to both policy makers and potential investors.

A unique characteristic of this new 2 km resolution interim wind atlas is the availability of hourly output over the entire 10-year simulation period, which represents the full range of wind and thermal stratification conditions over the Maldives. It will allow the monthly, seasonal, yearly, and interannual variation in the wind resource to be quantified. This unprecedented level of granularity leads to more accurate results because it enables the diurnal variation of processes in the planetary boundary layer (PBL), as well as the local forcing, to be well represented and sets the benchmark for renewable energy mapping over the coming years.

## 1.1 Background

The Maldives is in the early stages of exploring the resource potential of wind power. To date there are no utility scale wind turbines operating in the country. Single-purpose meteorological masts dedicated to the high quality measurement of wind resource have not been deployed extensively in the country, presenting a significant barrier to policymakers interested in evaluating the potential for supply diversity and distributed generation that wind energy projects can deliver.

The Maldives does not possess any native, non-renewable energy resources (oil, natural gas, coal) and therefore relies heavily on the importation of fuels to provide power generation, transportation, lighting and food preparation. Diesel is the dominant fuel source which provides all of the electricity generation, fishing fleet, and sea transport. Aviation fuel is another major import.



To decrease the dependency on imported fuels, the Maldives Government is planning to transform the energy sector with a target of achieving carbon neutrality. The Maldives has good prospects for solar and wind energy, but these resources have not been extensively measured or exploited for any significant electricity generation to date.

## 1.2 Project description

The key goal of this project is to provide Maldives' policy makers and stakeholders with accurate and valuable knowledge of the national wind resource which can be of direct practical use, both for formulating energy policy and implementing wind projects. The installation and operation of high quality wind measurement equipment throughout the country will also strengthen local capacity to support future development of wind projects in the Maldives.

The primary deliverable supporting the above goal will be a well-validated national mesoscale wind resource atlas that will greatly improve the awareness and understanding of the locations with the greatest potential for wind energy. When used in combination with a Geographic Information System (GIS), this forms a highly valuable planning tool which facilitates energy strategy planning for policy makers and stimulates commercial wind development by removing an important knowledge barrier.

This Mesoscale Wind Modeling Report documents the preliminary mesoscale modeling approach and results, and has been used as a primary input into the identification of suitable measurement locations (as described in the Candidate Site Identification Report [1]) to support the validation of the atlas.



## 2 METHODOLOGY – DNV GL WIND MAPPING SYSTEM

The new interim wind atlas has been generated using the DNV GL Wind Mapping System (WMS). WMS is a dynamical downscaling system developed to generate high-resolution mesoscale wind maps for any part of the world. Full details for the methods and inputs to the WMS appear in Appendix A – Detailed Methodology. The WMS configuration for this project employs telescoping, one-way interacting computational grids to achieve a resolution of 2 km across all of the Maldives (See Figure 2-1).

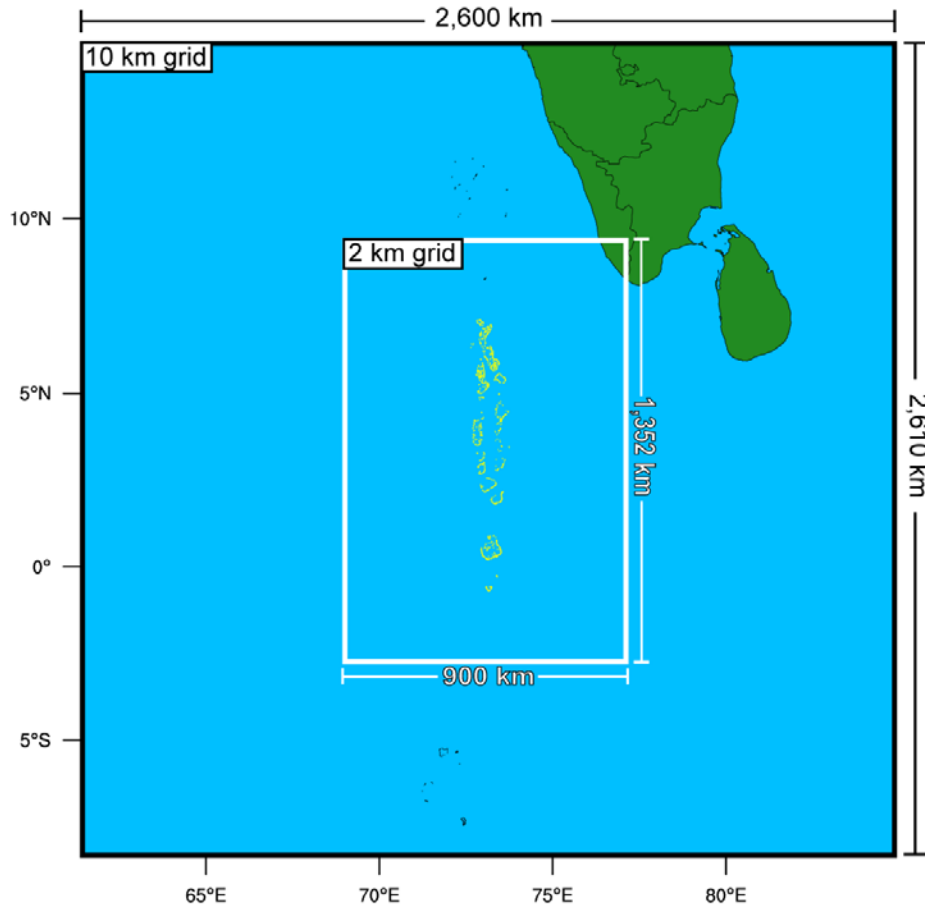


**Figure 2-1 Mesoscale computational grid configuration used for the DNV GL WMS simulations**

A complete hourly time series with the 10 km resolution grid is first generated over the entire 10 year period (01 September 2004 to 31 August 2014). Next, a nested 2 km grid is used to generate an hourly time series over the last year of the 10 km resolution simulation (01 September 2013 to 31 August 2014). These outputs provide the basis for the high resolution downscaling performed with the DNV GL Analog Ensemble, which is further described in Appendix A, to yield a complete 10-year times series at 2 km resolution over the entire country.

The preliminary wind speed map, and other associated derived outputs are presented and discussed in the following sections.

## 3 RESULTS

### 3.1 Preliminary and Unvalidated Wind Speed Map

Figure 3-1 and Figure 3-2 show the interim atlas for 100 m and 10 m above ground level (AGL) based on a complete 10-year, hourly simulation at 2 km resolution. The atlas provides comprehensive up-to-date quantitative maps of the long-term wind resource across the country. A number of interesting features of the wind climate in the Maldives emerge from this map:

#### Geographical variation

The Maldives stretch approximately 860 km between about 7.1° North to 0.7° South. The northern most atoll lies 500 km from the southern tip of India. The Palk Strait between India and Sri Lanka is a significant wind corridor where the flow of air is channeled between the two land masses. This geographical enhancement leads to strong mean wind speeds (about 10 m/s) at the narrowest part of the strait. This acceleration occurs during both the northeast and southwest monsoons, and the effect extends to northern and central parts of the Maldives. It is clear that the best wind resource lies mainly in the northern section of the country. Lower mean wind speeds prevail within the equatorial zone as shown in Figure 3-1, which is often typified by light and variable conditions termed the “doldrums”.

#### Monsoons

The climate within the Maldives regions is influenced by two distinct monsoons:

- Northeast monsoon (Iruvai) occurring from January to March;
- Southwest monsoon (Hulhangu) occurring from May to November'

The months of April and December are “transition months” between the two dominant phases of the monsoon.


Iruvai is typified by dry conditions and clear skies, while Hulhangu ushers in the wet season. The Hulhangu monsoon is generally accompanied by rough seas and strong winds.

#### Topographical impacts

The Maldives are situated within the Indian Ocean, southwest of the southern-most tip of India, and the entire country sits effectively at sea level. Thus, there is no topographical enhancement of the winds in this region, as most islands rise less than 1 m above sea level, and only few have elevations approaching 3 m above sea level. While the majority of islands occupy a land area smaller than 0.5 km<sup>2</sup>, a few atolls have a total land area as large as 20 km<sup>2</sup>.

#### Impacts of vegetation and urban areas

Many islands are comprised of fairly dense vegetation, or patches of vegetation which impart increased frictional drag on the near surface wind. There are also several islands which are completely urbanized. This creates increased drag on the near-surface wind speeds relative to the surrounding water points, and this effect is most evident in the 10 m and 50 m AGL preliminary wind speed maps. The impacts of surface friction gradually reduce with height and are less evident in wind speed maps for heights above 50 m.



It is noted that thermally driven land/sea winds are not expected to have a significant impact on the wind regime in the Maldives, due to the relatively small size of most land areas.

### **Variation of wind speed with height**

The variation of wind speed with height over the study area is consistent with that which would be encountered in an area that is predominantly ocean. This includes small variations in wind speed with height over most of the study area (with typical reductions of approximately 10 % between 100 m and 10 m), but more substantial variations in those areas denoted as land (with typical reductions of 20 to 30 % between 100 m and 10 m).

### **Area for detailed study**

In coordination with The World Bank, DNV GL has restricted the extent of the study area to approximately 25 km from any landmass within the Maldives. This covers the territorial waters of the country (12 nautical miles from the coastline by definition, or approximately 22.2 km). The rationale is to exclude areas where development is not feasible, since the sea floor drops sharply to several thousand meters in all directions from the atolls. The selected study area is shown by the dashed line in Figure 3-1.

While the new atlas represents the best possible estimate of the wind resource within the region using the latest advances in mesoscale modeling, it does have inherent limitations. Small or localized landscape features are poorly resolved or not resolved at all. For instance, the smallest islands and urban areas are not resolved by this dataset. As a general rule of thumb, the WRF model is capable of resolving spatial variations in the wind field at scales ranging from about 3-7 grid lengths [2]. In the present case, this equates to features with length scales of about 15 km and larger. Thus, an essential future step is to further downscale these results using a microscale model to account for the impacts of very localized features. Such modeling will be undertaken during Phase 3 of the project, and will incorporate the validation using ground based measurements collected during Phase 2.

A full set of wind speed maps at heights of 10 m, 50 m, 80 m, 100 m, and 200 m (AGL) are shown in Appendix B – Preliminary and Unvalidated Mesoscale Outputs.

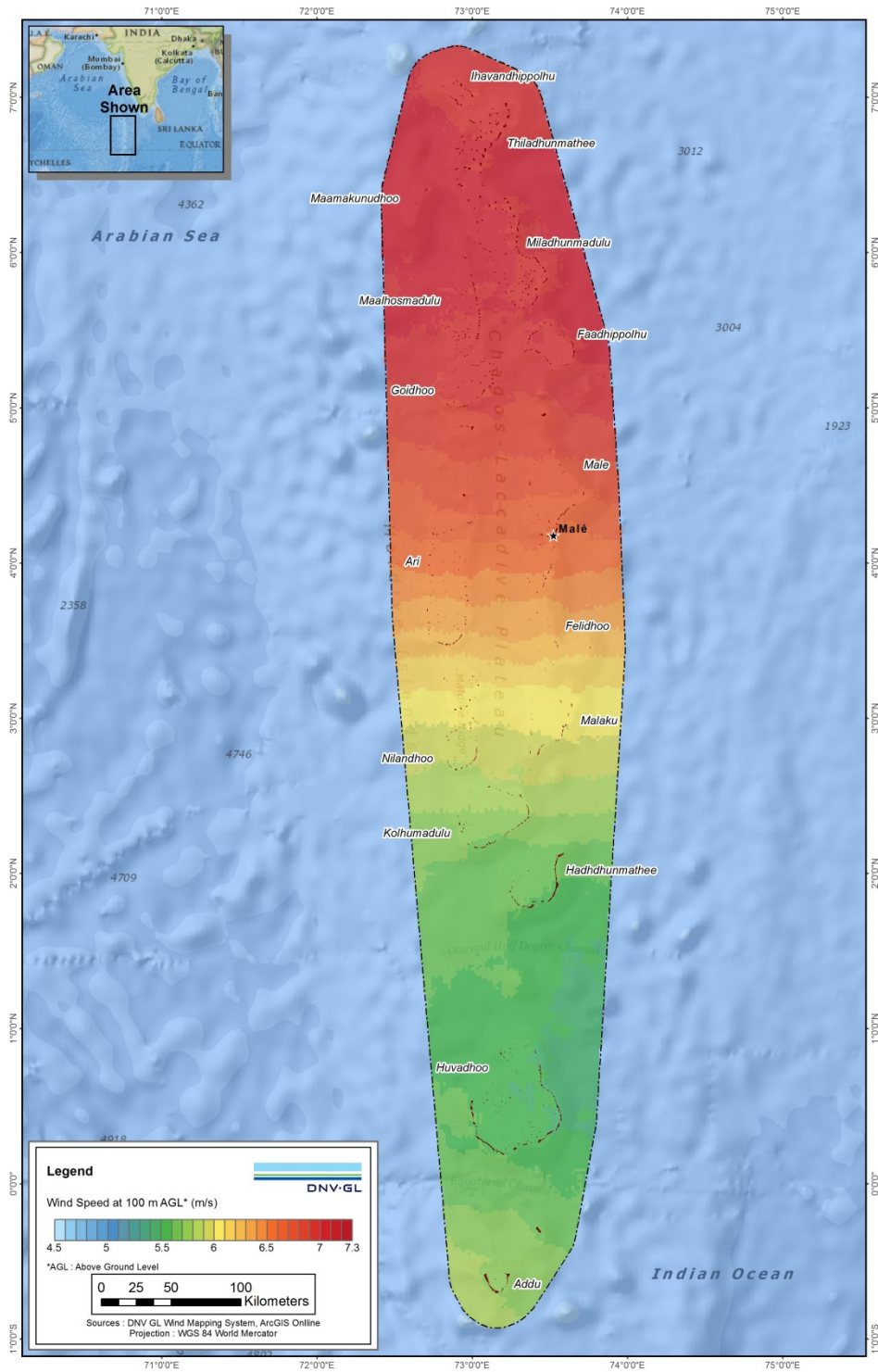


**Figure 3-1 Preliminary and unvalidated mesoscale annual mean wind speed map at 100 m AGL, created using the DNV GL Wind Mapping System.**

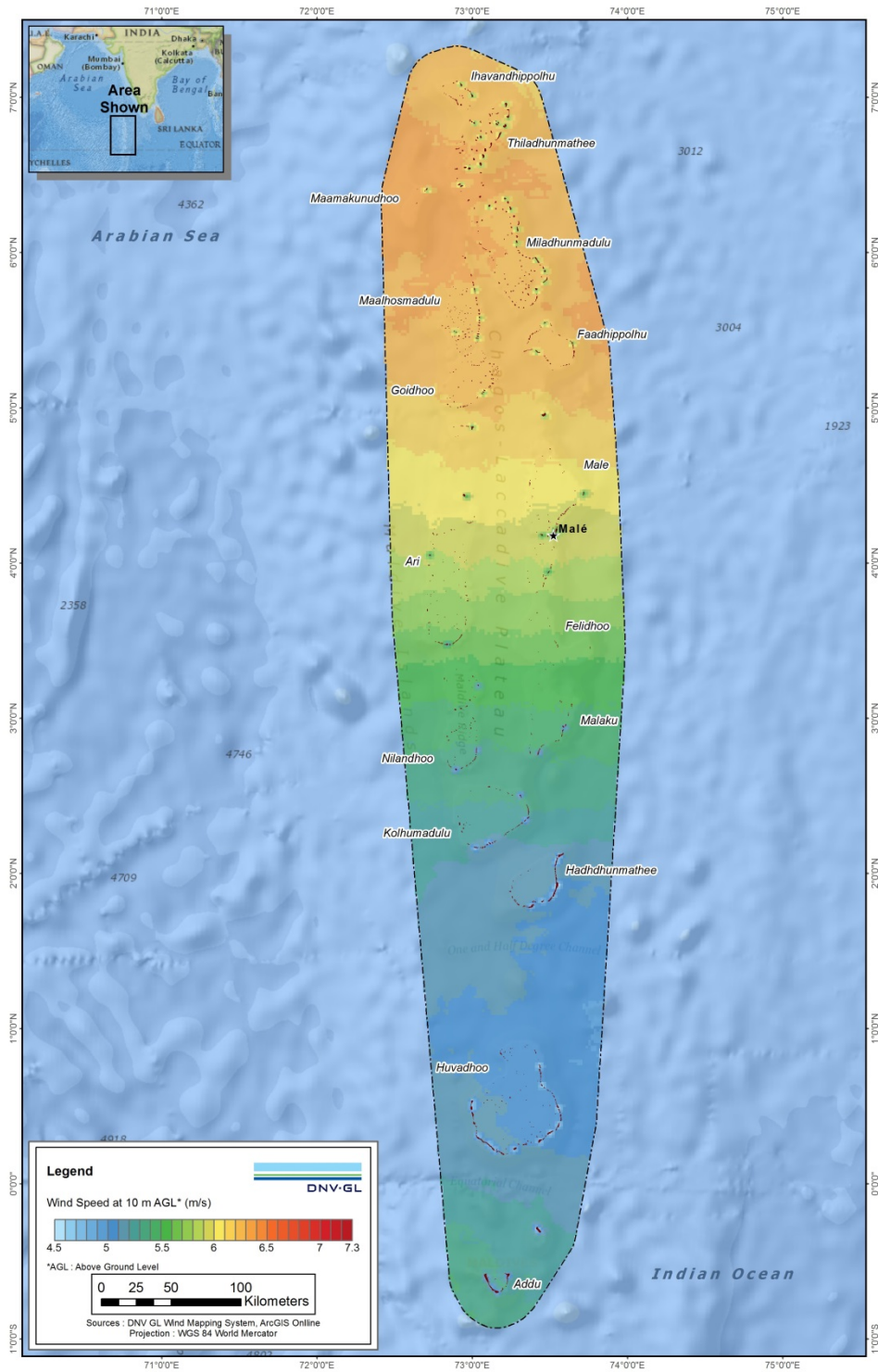


**Figure 3-2 Preliminary and unvalidated mesoscale annual mean wind speed map at 10 m AGL, created using the DNV GL Wind Mapping System.**

### 3.2 Preliminary and Unvalidated Wind Speed Uncertainty Index

It is well known that mesoscale model simulations have a number of inherent and unavoidable limitations and uncertainties, including the input datasets, the lateral boundary conditions, the numerical approximations used in the dynamical core of the model, and the imperfect representation of the complex physical processes that strongly drive the winds within the boundary layer.

DNV GL has employed a Monte Carlo method to mitigate these limitations, and to provide statistically defined estimates of the meteorological uncertainty in the mesoscale results. The “multiphysics ensemble”, illustrated in Figure 3-3, amounts to constructing several unique versions of the model by selecting different suites of physical process parameterizations or input datasets, and each model version is then used to perform a separate parallel downscaled simulation. For this project, DNV GL has selected 10 ensemble members for this analysis. Each of the ensemble simulations provides an equally plausible representation of the wind climate, within the likely range of meteorological uncertainty. See Appendix A – Detailed Methodology for more details.

The “ensemble spread” or standard deviation among the ensemble of simulations provides an objective estimate of the meteorological uncertainty, allowing us to place a statistically defined error bar on the resource estimate for any point within the numerical wind map/atlas.

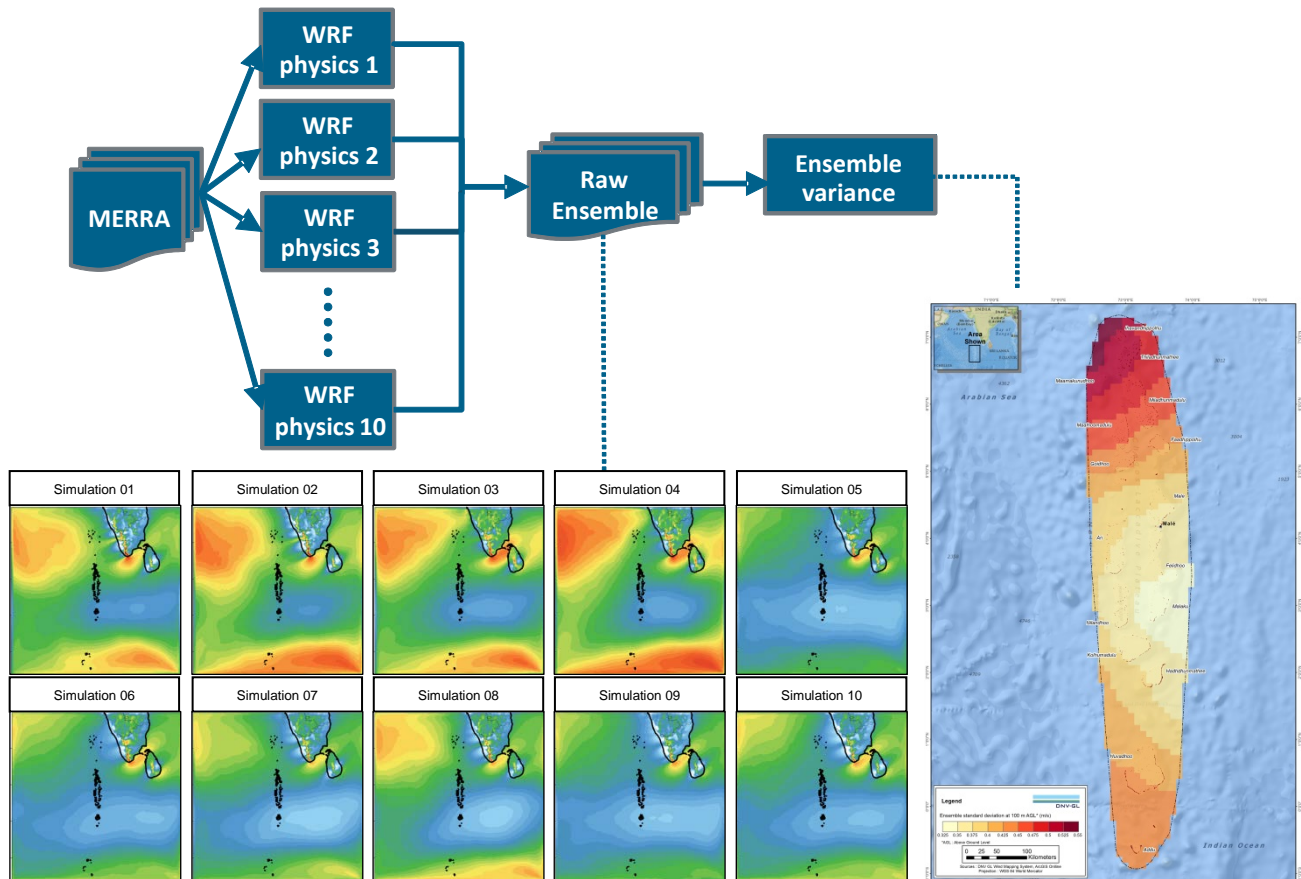



Figure 3-3 The multiphysics ensemble approach



The preliminary wind speed uncertainty index is defined as the standard deviation of the ten multiphysics mesoscale ensemble member solutions, as shown in Figure 3-4. Areas with a high index value, and therefore high standard deviation, indicate where there is a lack of consensus between the ten multiphysics ensemble members. This highlights the apparent difficulty in accurately modeling the wind flows in these areas. During Phase 3 of the project, ground-based measurements and microscale modeling will be used to refine the uncertainty index.

Interestingly, uncertainty index values are not strictly a function of wind speed. For example the uncertainty index values are relatively high in the southern Maldives where average wind speeds are lowest. Lower uncertainty index values are exhibited in the center of the Maldives near the Malaku Atoll, where the simulated wind speeds are modest. The highest overall uncertainty index values lie in the north west corner of the Maldives at the Ihavandhippolhu Atoll which may be partly attributed cyclonic activity in the Northwest Indian Ocean. Examination of the seasonal and annual wind flows in this area (see Section 3.4) indicates a varying magnitude of the seasonal monsoons and the cyclones generated in the Northwest Indian Ocean, which are more common in the months between May to June and September to January.

One point of difference in the ensemble members is the degree to which the high wind speeds channeled through the Palk Strait penetrate out into the Maldives. Several of the ensemble members indicate a very extensive effect, with higher wind speeds influencing the middle and north of the Maldives, while a number of other members indicate that the effect will dissipate quickly before reaching the Maldives. This dissimilarity between the 10 ensemble members likely results from the winds in this region being more difficult to predict and is a cause of the larger uncertainty modeled in the north of the Maldives.

This requires further study, and the measurements collected during Phase 2 of the project, together with microscale modeling, will be key to understanding and developing a more refined uncertainty index. The wind speed uncertainty index has been used along with other important parameters to guide the recommendations for the Candidate Site Identification Report [1].

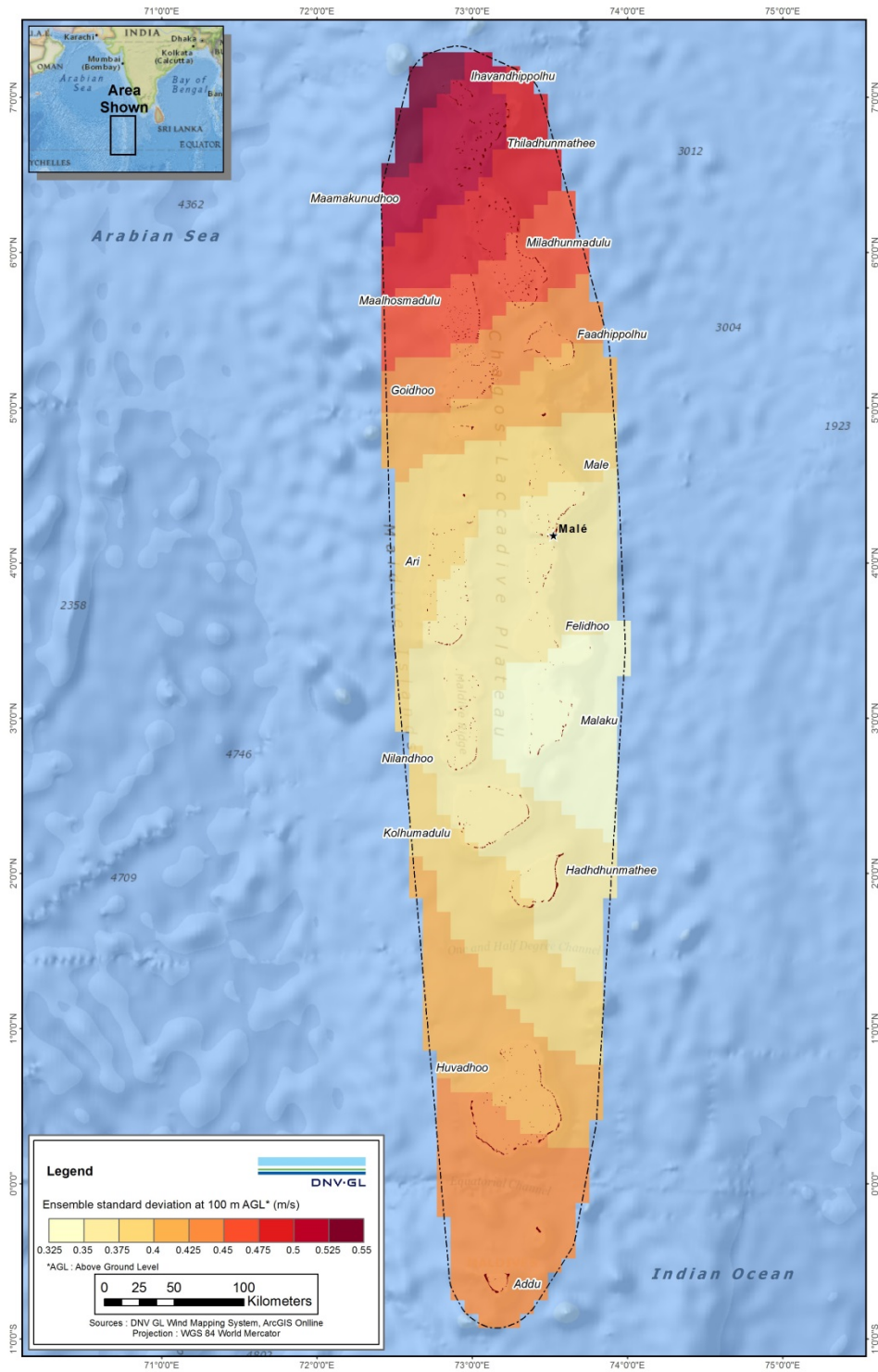


**Figure 3-4 Preliminary and unvalidated wind speed uncertainty index created with the DNV GL Wind Mapping System**



### 3.3 Preliminary and Unvalidated Wind Energy Map

The preliminary wind energy map is presented in Figure 3-5. Here the values represent the approximate net annual energy production (GWh/annum) that would be produced by a single 'generic wind turbine', if it were to experience the long-term mean wind conditions simulated in the 2 km preliminary mesoscale wind map at 100 m.

The methodology used is outlined as follows. For each *hourly* record from the 10-year simulation, the simulated air density and wind speed value at 100 m AGL are combined with a power curve at each 2 km grid cell. This results in a database of (24 hours × 3650 days = 87,600) hourly power values specific to the speed and density at each time and grid cell location.

From this 10-year hourly power time series, the mean annual gross energy in GWh for each 2km grid point for each individual year is calculated. The individual yearly results at each grid point are then combined to give the long-term mean energy output.


Finally, the values presented here include consideration of a set of high-level starting assumptions for typical energy losses which may be expected for wind farm development in this region. The list of losses applied to generate the preliminary wind energy map is shown in Table 3-1 below.

**Table 3-1 Representative energy loss factors applied**

<b>Loss Factor</b>	<b>Value</b>
Wake effect	95.0%
Availability	90.0%
Electrical efficiency	97.0%
Turbine Performance	98.5%
Environmental	99.0%
Curtailements	100.0%
<b>Total</b>	<b>80.9%</b>

This means that approximately one fifth of the extractable energy content of the calculated wind resource will be lost. While such losses can be lowered through selection of advanced turbine technology, good wind farm design and careful maintenance, they cannot be entirely eliminated on any wind farm. These losses lead to expected capacity factors of approximately 12 to 25 % across the Maldives for the generic wind turbine considered here. However, it is noted that for a given wind regime, the potential capacity factor can vary significantly depending on the rotor diameter, generator capacity and power curve of the turbine under consideration.

It is also noted that the generating capacity and hub height of this 'generic wind turbine' may not be feasible or practical for installation at every location within the Maldives and is used here only to provide an indication of the variation of the generating potential of the wind resource across the country. The 'annual energy production' results presented in Figure 3-5 should be viewed in conjunction with, and giving



consideration to, the 'hypothetical maximum turbine capacity' presented in Figure 3-6. The hypothetical maximum turbine capacity for each island was calculated using information on the historical peak load demand of each island and assuming a 50% renewable energy penetration compared to peak load. It is noted that although the generic wind turbine (with a capacity of 3 MW) could theoretically generate over 6 GWh/annum in areas of the north of the Maldives, the load in many of the islands in this region would only support the installation of turbines with capacities of 1 MW or less, with most islands only likely to support turbines with capacities of 200 kW or less. This means that the realisable energy generation is likely to be substantially lower across the majority of the Maldives, compared to that shown in Figure 3-5. The exception is the greater Male region, where there is potentially sufficient load to support the installation of multiple 3 MW turbines.

These calculations involve a number of assumptions, which are described in more detail in Appendix A, including a description of the generic wind turbine selected by DNV GL.

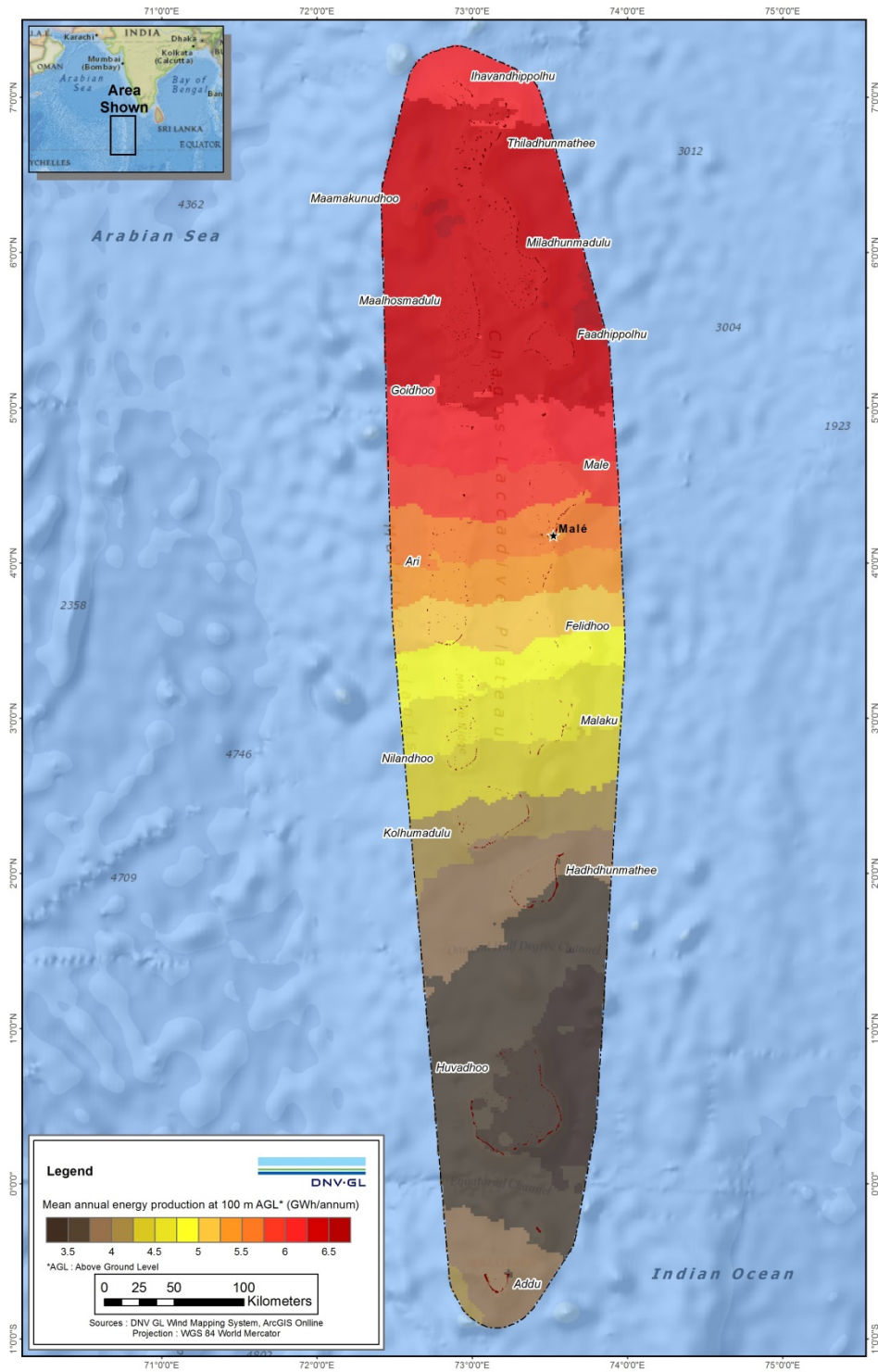


**Figure 3-5 Preliminary and unvalidated annual mean wind energy map created using the DNV GL Wind Mapping System**

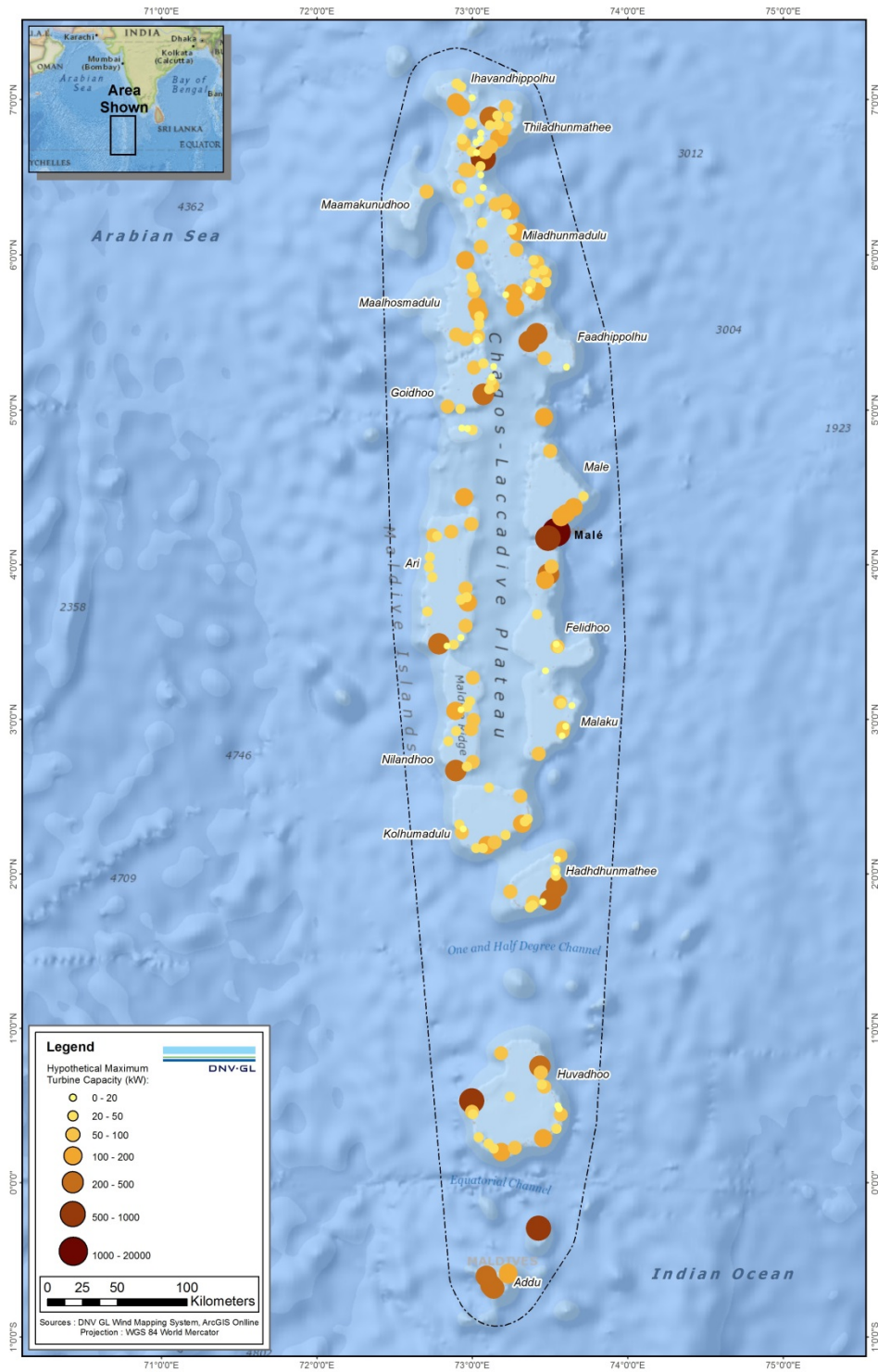


Figure 3-6 Hypothetical maximum wind turbine capacity for inhabited islands across the Maldives

### 3.4 Preliminary and Unvalidated Seasonal and Diurnal Trends

The time series simulation approach used for this project provides for a wealth of additional information, and the following section provides some highlights that are directly relevant to this project.

A “12 x 24” matrix for each 2 km grid point was created to estimate the diurnal variation in mean wind speed for each calendar month, as well as a 12 x 24 matrix of wind energy production. These data, from 30,634 grid cells, will be supplied to the Client prior to the Phase 1 workshop. An example of the matrix for energy production is shown in Table 3-2 below for a single location.

**Table 3-2 “12 x 24” matrix of energy production (% of annual mean energy production)**

Predicted hourly and monthly energy production as a percentage of mean annual energy production													
Generic 3MW power curve at 100 m AGL													
Hour	Energy production [%]												Total
	Jan	Feb	Mar	Apr	May	Jun	Jul	Aug	Sep	Oct	Nov	Dec	
00:00	0.34	0.26	0.22	0.28	0.52	0.44	0.26	0.35	0.51	0.50	0.32	0.33	4.32
01:00	0.35	0.26	0.21	0.26	0.49	0.39	0.23	0.33	0.48	0.48	0.28	0.33	4.09
02:00	0.35	0.27	0.21	0.26	0.50	0.40	0.24	0.31	0.48	0.47	0.31	0.33	4.12
03:00	0.33	0.26	0.20	0.26	0.53	0.39	0.22	0.29	0.48	0.48	0.28	0.32	4.04
04:00	0.33	0.27	0.19	0.26	0.51	0.43	0.23	0.29	0.47	0.47	0.28	0.32	4.05
05:00	0.30	0.24	0.20	0.25	0.45	0.38	0.20	0.28	0.44	0.44	0.28	0.30	3.77
06:00	0.29	0.23	0.17	0.24	0.47	0.38	0.19	0.27	0.45	0.45	0.26	0.29	3.69
07:00	0.26	0.21	0.17	0.24	0.46	0.38	0.21	0.27	0.44	0.45	0.26	0.27	3.62
08:00	0.28	0.22	0.17	0.23	0.47	0.38	0.19	0.28	0.46	0.48	0.28	0.27	3.72
09:00	0.27	0.22	0.19	0.23	0.50	0.39	0.21	0.30	0.50	0.51	0.29	0.26	3.87
10:00	0.29	0.23	0.19	0.24	0.54	0.39	0.20	0.28	0.50	0.52	0.30	0.29	3.97
11:00	0.27	0.22	0.18	0.24	0.52	0.40	0.18	0.29	0.50	0.51	0.30	0.27	3.88
12:00	0.28	0.23	0.19	0.25	0.49	0.37	0.18	0.29	0.49	0.51	0.28	0.29	3.82
13:00	0.29	0.24	0.21	0.27	0.54	0.40	0.20	0.30	0.54	0.53	0.31	0.31	4.13
14:00	0.29	0.24	0.21	0.28	0.56	0.41	0.22	0.33	0.54	0.55	0.31	0.30	4.23
15:00	0.31	0.25	0.21	0.28	0.57	0.41	0.20	0.32	0.55	0.56	0.30	0.31	4.26
16:00	0.34	0.26	0.22	0.29	0.57	0.41	0.23	0.34	0.56	0.55	0.30	0.32	4.41
17:00	0.36	0.27	0.21	0.29	0.61	0.43	0.25	0.36	0.58	0.56	0.31	0.33	4.56
18:00	0.36	0.26	0.21	0.29	0.64	0.48	0.28	0.40	0.59	0.59	0.32	0.30	4.70
19:00	0.33	0.23	0.18	0.29	0.61	0.49	0.28	0.38	0.57	0.54	0.29	0.30	4.49
20:00	0.31	0.23	0.20	0.31	0.65	0.50	0.27	0.38	0.58	0.57	0.34	0.29	4.63
21:00	0.32	0.23	0.20	0.30	0.65	0.48	0.27	0.37	0.58	0.57	0.32	0.32	4.60
22:00	0.33	0.23	0.21	0.30	0.60	0.46	0.27	0.38	0.57	0.54	0.30	0.34	4.54
23:00	0.35	0.24	0.22	0.29	0.61	0.44	0.27	0.37	0.56	0.54	0.32	0.33	4.53
Total	7.52	5.82	4.75	6.42	13.05	10.00	5.48	7.73	12.41	12.37	7.13	7.32	100.01

These data can be presented in a number of forms, and access to the underlying data allows the various stakeholders to customise charts and figures for their specific needs. For example, the above matrix can easily be distilled into a monthly profile of energy production as shown in Figure 3-7 for four locations within the Maldives.

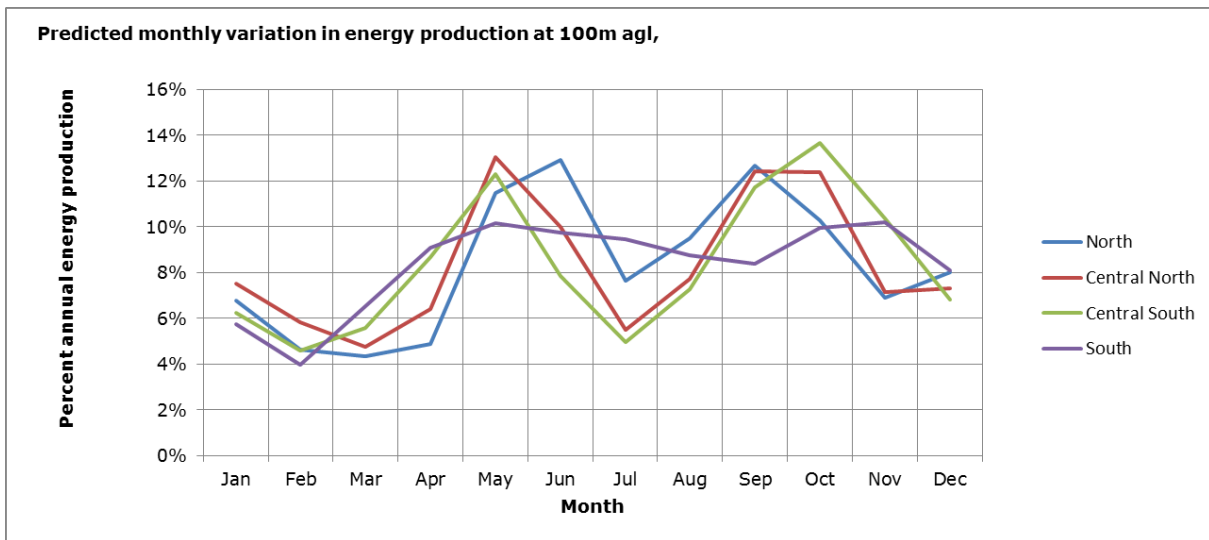


**Figure 3-7 Seasonal variation of energy production for four selected grid cells**

It is well known that the Maldives lie within the influence of the broad Indian Ocean monsoon circulation, which is prevalent throughout the year, but is particularly strong in the north of the country during June to November. For an understanding of this type of regional variation, the seasonal wind flow patterns simulated by the WMS are shown in Figure 3-8. It is clear that winds during the height of the northeast monsoon (Dec-Apr) are generally weak, as shown in the left two panels of the figure. However, the situation changes dramatically during the southwest monsoon (Jun-Nov), where the 2-km wind atlas indicates mean wind speeds of 7-8 m/s over the northern half of the Maldives.

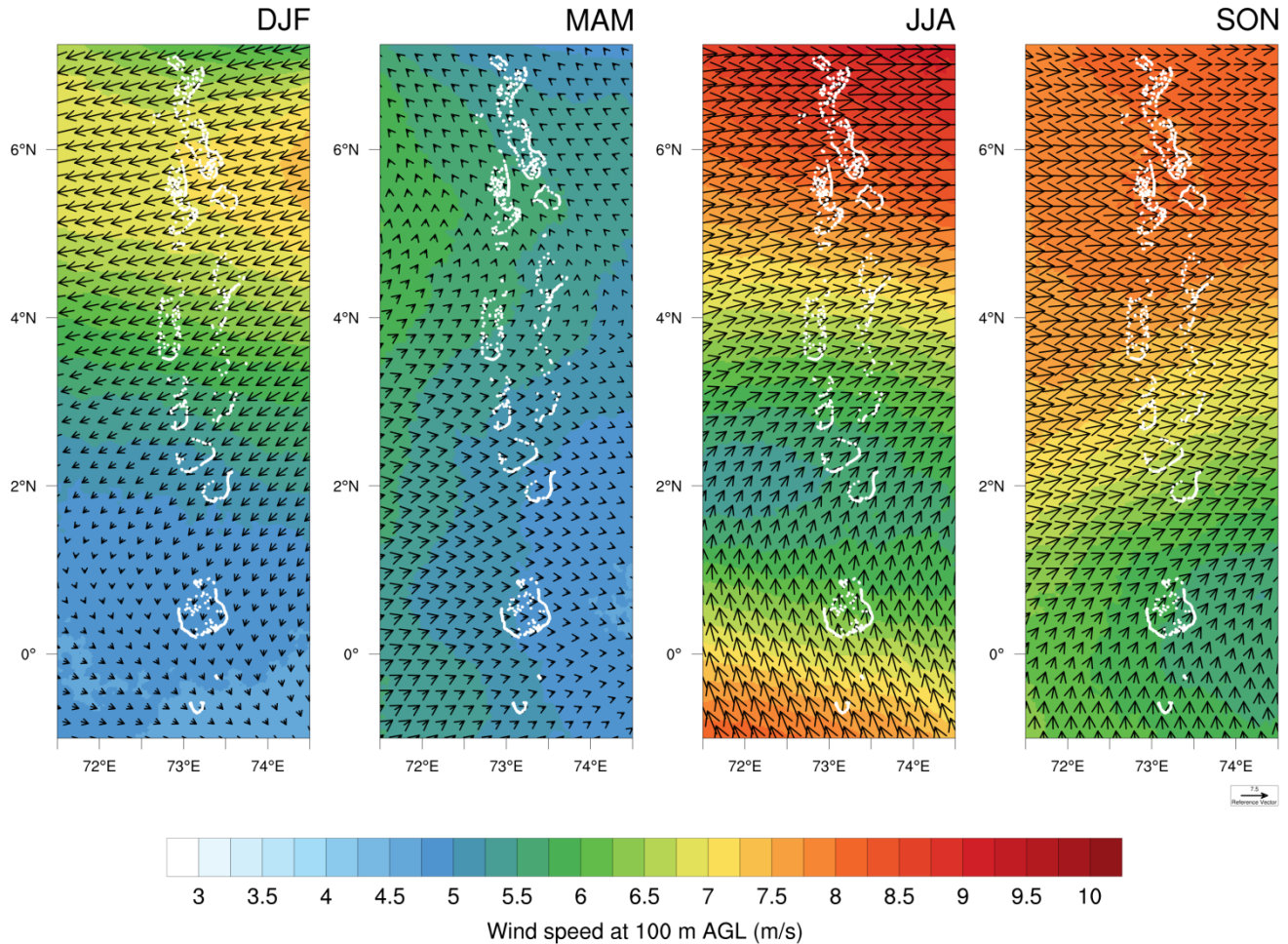


**Figure 3-8 Seasonal flow patterns for Sep 2013-Sep 2014 over the Maldives as simulated by the DNV GL Wind Mapping System**

### 3.5 Preliminary and Unvalidated Estimates of Interannual Variability

An Interannual Variability Index (IAVI) of wind speed and energy is derived from the WMS 10-year simulations and presented in Figure 3-9 for each 2 km grid point. The IAVI is defined as the standard deviation of the 10 samples available of simulated annual mean wind speed and annual energy production for each 2 km grid point.

Care should be taken when using this map, since a robust estimate of interannual variability typically requires at least 30 years of reliable reference data [3]. Furthermore, uncertainty models used for wind farm financing have almost exclusively used measurements to derive interannual variability rather than model-derived estimates. It is also important to note that these preliminary maps of IAVI are not yet validated. Once measurements become available to better understand the mesoscale model performance, the IAVI will be revised and improved.

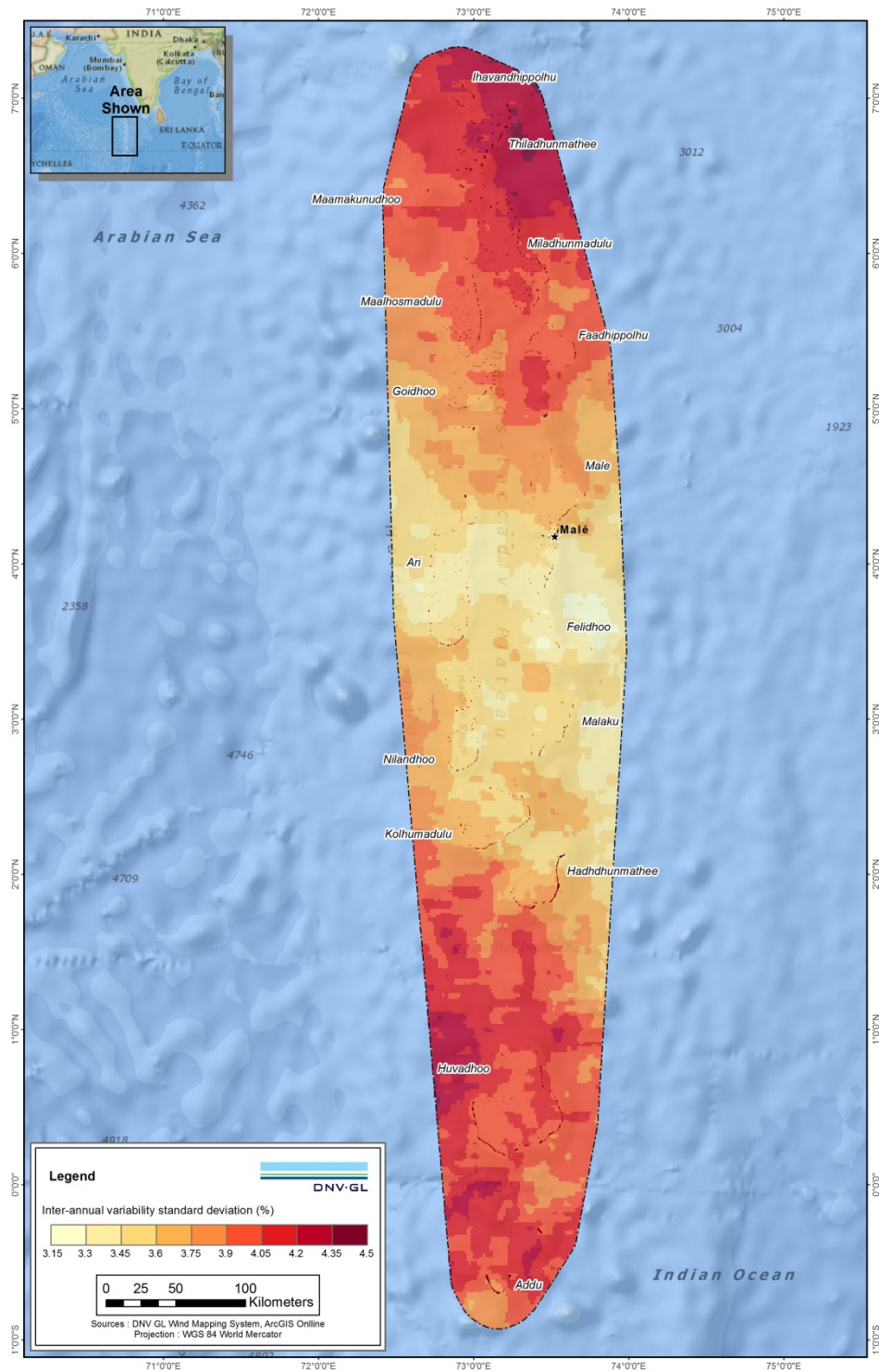


Figure 3-9 Preliminary and unvalidated interannual variability index (IAVI) for wind speed





### 3.6 Interim Wind Atlas (\*.lib files)

The hourly outputs of the WMS at each 2 km grid cell in the study domain are used to calculate the generalized wind climate statistics. This is done according to the industry-standard WASP-format “wind atlas” (“WASP-lib”) file, according to the European Wind Atlas method (Troen and Petersen, 1989). This was performed using the Danish Technical University (DTU) Generalized Wind Climate software package.

The full suite of \*.lib files will be delivered to the Client in advance of the Phase 1 workshop.



## 4 REFERENCES

- [1] Candidate Site Identification Report Maldives, DNV GL, February 2015, 702909-AUME-R-02-A.
- [2] W. C. Skamarock, 2004: Evaluating Mesoscale NWP Models Using Kinetic Energy Spectra. *Mon. Wea. Rev.*, **132**, 3019–3032. doi: <http://dx.doi.org/10.1175/MWR2830.1>
- [3] Raftery A., Tindal J. and Garrad A. (1997), Understanding the risks of financing windfarms, Proc. EWEA Wind Energy Conference, Dublin.



## APPENDIX A – DETAILED METHODOLOGY

### THE DNV GL WMS

#### Model configuration

The new interim wind atlas is generated using the DNV GL Wind Mapping System (WMS). WMS is a dynamical downscaling system developed to generate high-resolution mesoscale wind maps for any part of the world. At the heart of WMS is the Weather Research and Forecasting (WRF) model, a state-of-the-science open source mesoscale model developed and maintained by a consortium of more than 150 international agencies, laboratories, and universities (Skamarock et al. 2008). The WRF model has been employed successfully for a spectrum of applications ranging from operational weather forecasting (e.g., Hacker et al. 2011), to climate downscaling (e.g., Leung et al. 2009; Liang et al. 2012; Mearns et al. 2012). And because WRF is one of the most widely used mesoscale models in the renewable energy industry (e.g., Potter et al. 2008; Draxl et al. 2012; Parks et al. 2010), its performance for wind energy applications is well understood. For the application described herein, DNV GL's WMS utilizes WRF version 3.4.1 to create hourly analyses on a 2-km horizontal grid, with 36 vertical levels covering the period 01 September 2004 to 31 August 2014, inclusive. The result is a database of (10 years x 365 days x 24 hours) three-dimensional analyses. The physical process parameterizations are chosen for maximum numerical stability, and for producing the best overall representation of hub height winds within the Maldives. These choices are based on DNV GL's extensive validation studies conducted at more than 500 locations on every major continent, including a number of sites in India.

The WMS configuration uses telescoping, one-way interacting computational grids to provide complete coverage for the Maldives and the bordering regions (See Figure A-1). Their respective horizontal grid increments are 10 km and 2 km, and both grids use 36 vertically stretched terrain following levels, with approximately 13 levels within the lowest 1.5 km AGL.

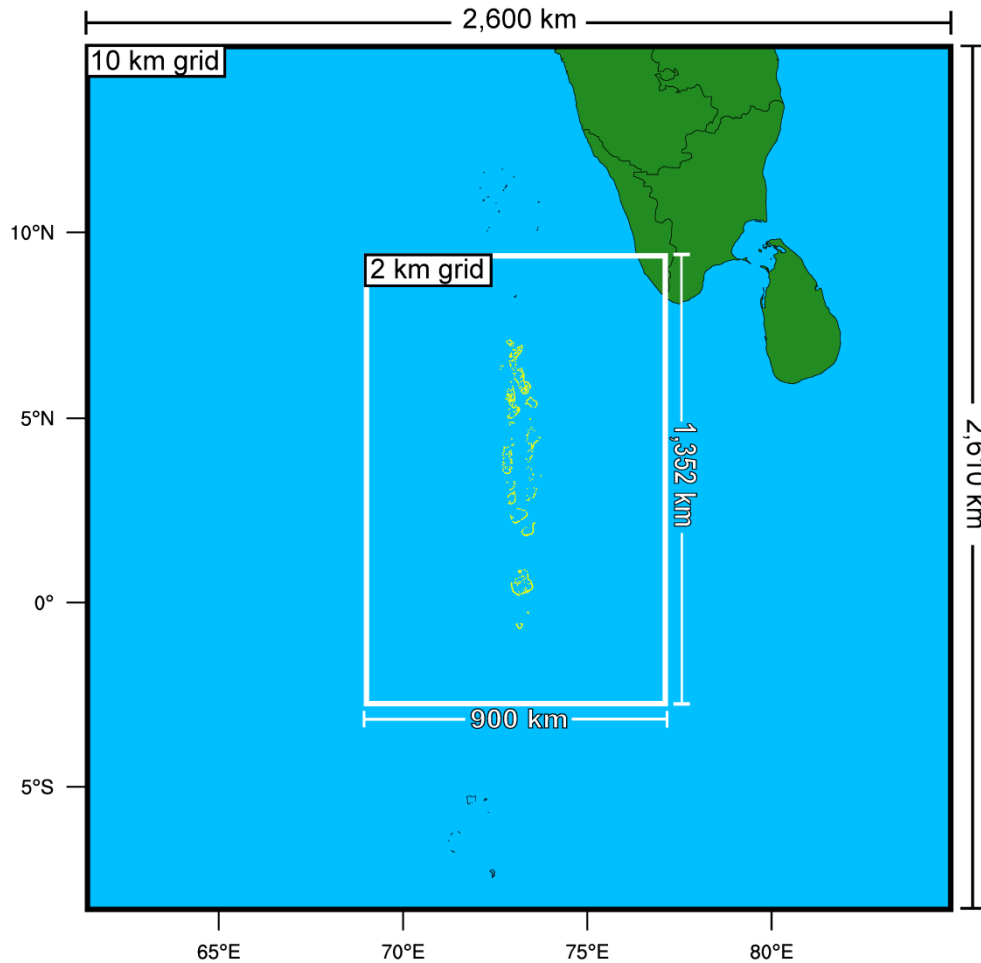



**Figure A-1 Mesoscale computational grid configuration used in the DNV GL WMS simulations**

The 10 km outer grid's mesh size is  $260 \times 261$ , and the nested 2 km grid's mesh size is  $450 \times 676$ . Both grids employ the recommended lateral boundary buffer zone.

### Model Inputs

The multitude of small islands that make up the Maldives presents an interesting challenge for mesoscaling modeling of the area. Only three individual islands of the Maldives would be large enough to warrant the classification of a 2 km resolution grid cell as "land". However, limiting the simulation of land to only these larger islands will under-represent the effect of surface friction on the near-surface wind field in and around the atoll chains. To properly represent the islands in the model, the 2 km land use database was algorithmically modified to incorporate the correct overall spatial distribution of land points according to the density of the atolls, while ensuring that the total land area of the atolls equaled the same as indicated by a high-resolution database of administrative boundaries. The outcome of this process is shown in Figure A-3, Figure A-4 and Figure A-5 below.



DNV GL notes that there appear to be some land areas (such as Thohdoo island) in the administrative dataset supplied by the Land and Survey Authority that do not agree with or are offset from other independent data sources. These minor disagreements may be caused by co-ordinate system or projection issues within the dataset, and so they were not used to define the model parameters discussed here. However, the Land and Survey Authority boundaries were used to prepare the figures presented in this report.

DNV GL typically uses the U.S. Geological Survey (USGS) Earth Resources Observing System (EROS) 1-km dataset (Loveland et al. 1995) to define the vegetation type, which in turn is used to specify the surface aerodynamic roughness length in the WRF model. However this database does not accurately resolve the islands of the Maldives. DNV GL applied land use, elevation, and aerodynamic roughness lengths as applicable to the grid cells defined "land". The majority of land grid cells were assigned a representative land-use category of "wooded wetland" (roughness length of 0.45 m). However, land grid cells covering substantial settlements were assigned the land use class of "urban and built up" (roughness length of 0.5 m). All other grid cells within the study area are water bodies (roughness length of 0.0001 m). This is shown in Figure A-2, Figure A-6, Figure A-7 and Figure A-8.

Additionally, all grid cells designated as land within the 2 km WRF domain were assigned a terrain elevation of 0.20 m as portrayed in Figure A-9, Figure A-10 and Figure A-11. A quantitative analysis of high-resolution digital elevation model (DEM) data for this region indicates that the vast majority of atolls have an elevation of 0.2 m or less. While there are a few islands with elevations between 1-3 m above sea level, their rise above the surrounding ocean points will have minimal impact on the surface wind field at the mesoscale, but will be more pronounced at the microscale. Even though the 2 km grid provides unprecedented resolution for wind maps within the Maldives, it is important to note that small islands, towns or reef features are poorly resolved or not resolved at all. As a general rule of thumb, the WRF model is capable of resolving spatial variations in the wind field at scales ranging from about 3-7 grid lengths (Skamarock 2004). In the present case, this equates to features with length scales of about 6-14 km and larger.

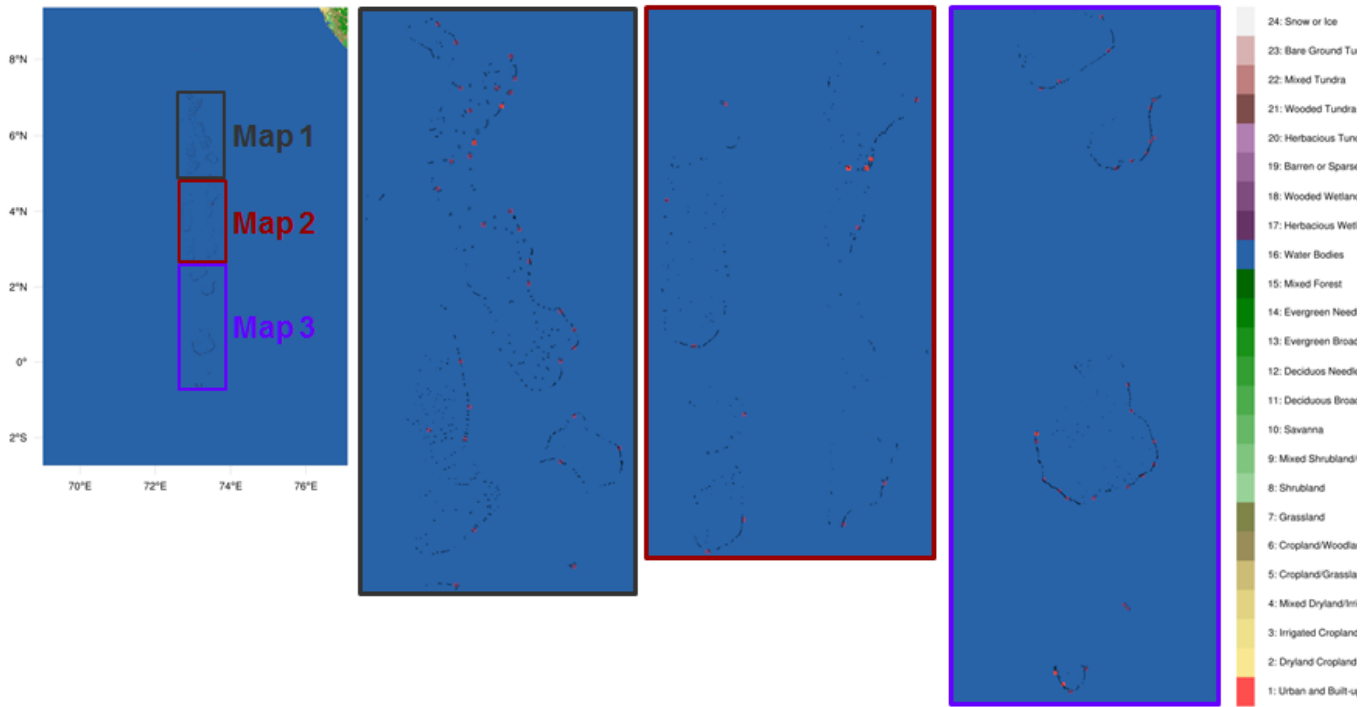


**Figure A-2 Land use types for the Maldives as setup within WRF land cover database**

Note: The global land cover database used within the WRF model contains 24 distinct categories. There are 3 classes within the Maldives (1: Urban and Built-up Land, 16: Water Bodies and 18: Wooded Wetland).

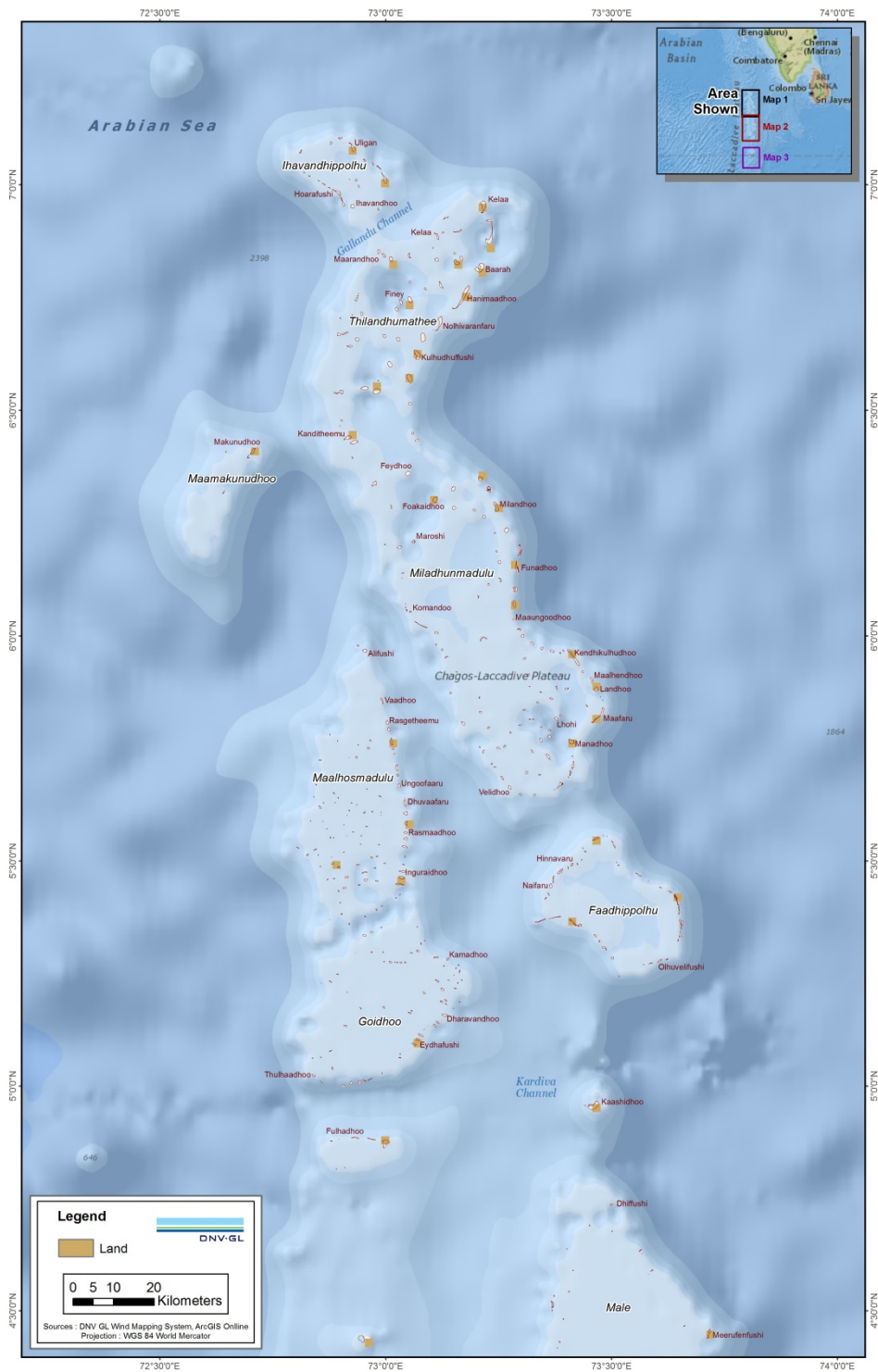


Figure A-3 Model land mask used in the WRF 2 km grid for the north of the Maldives

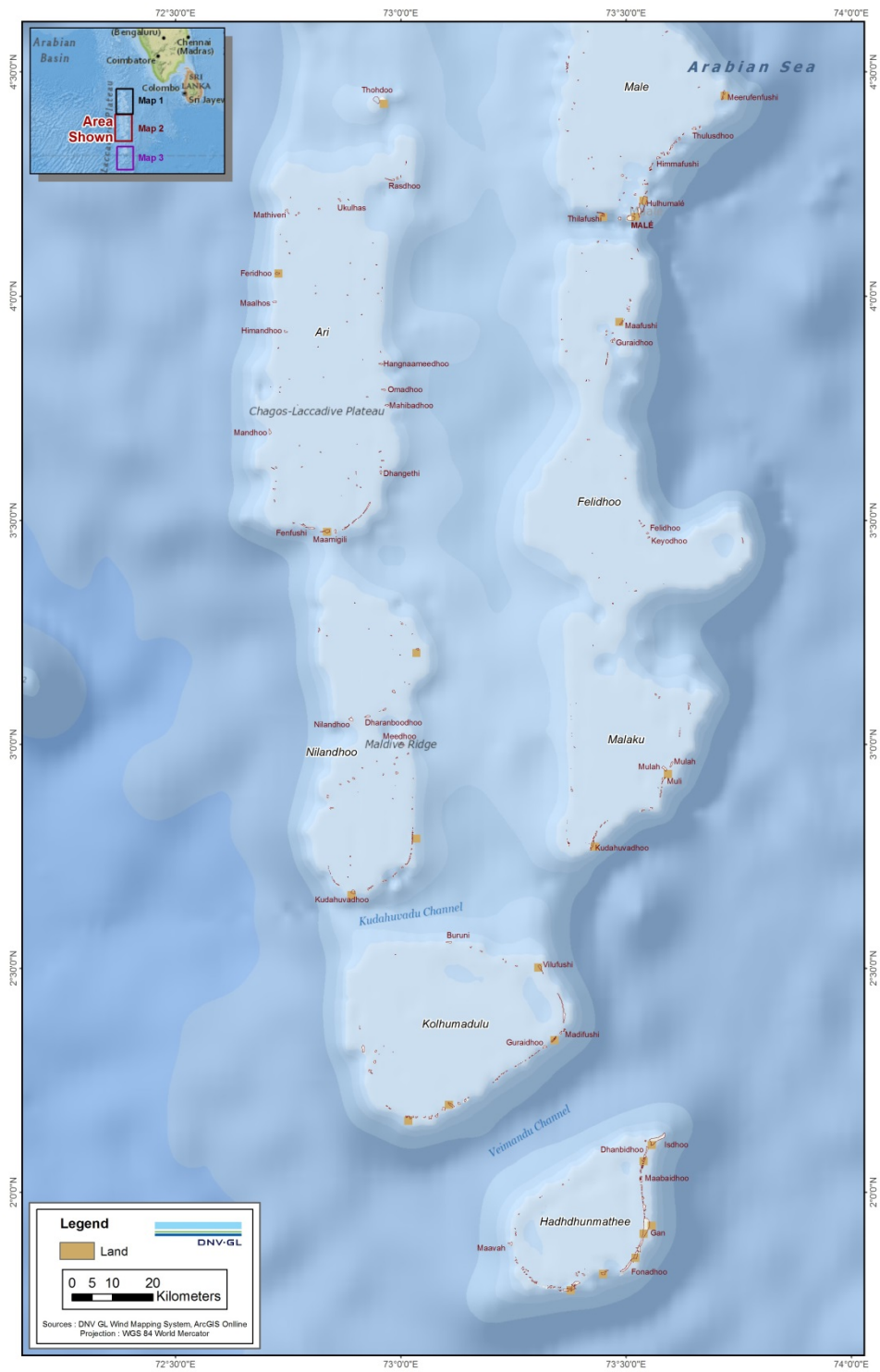


Figure A-4 Model land mask used in the WRF 2 km grid for the center of the Maldives



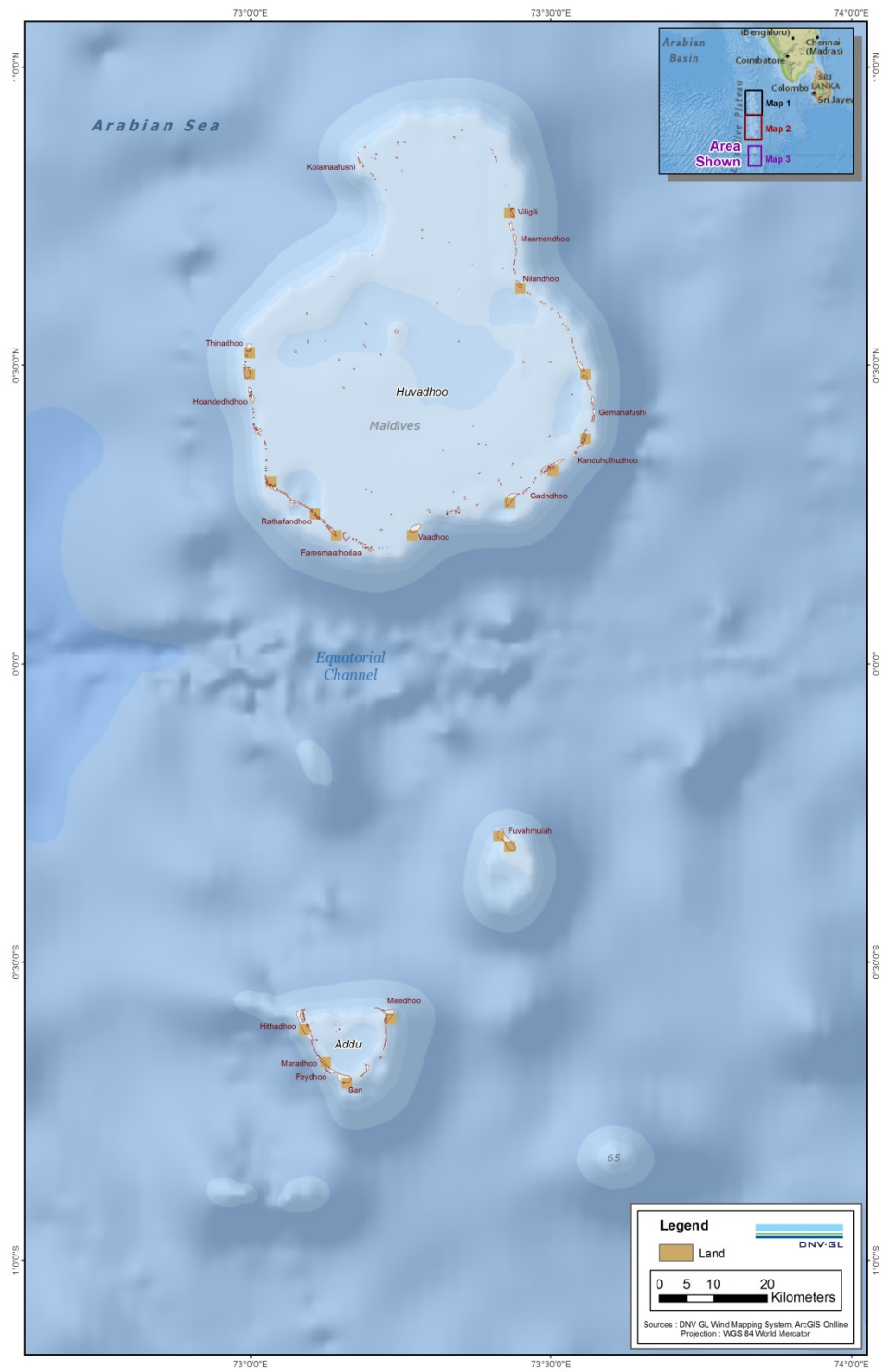


Figure A-5 Model land mask used in the WRF 2 km grid for the south of the Maldives

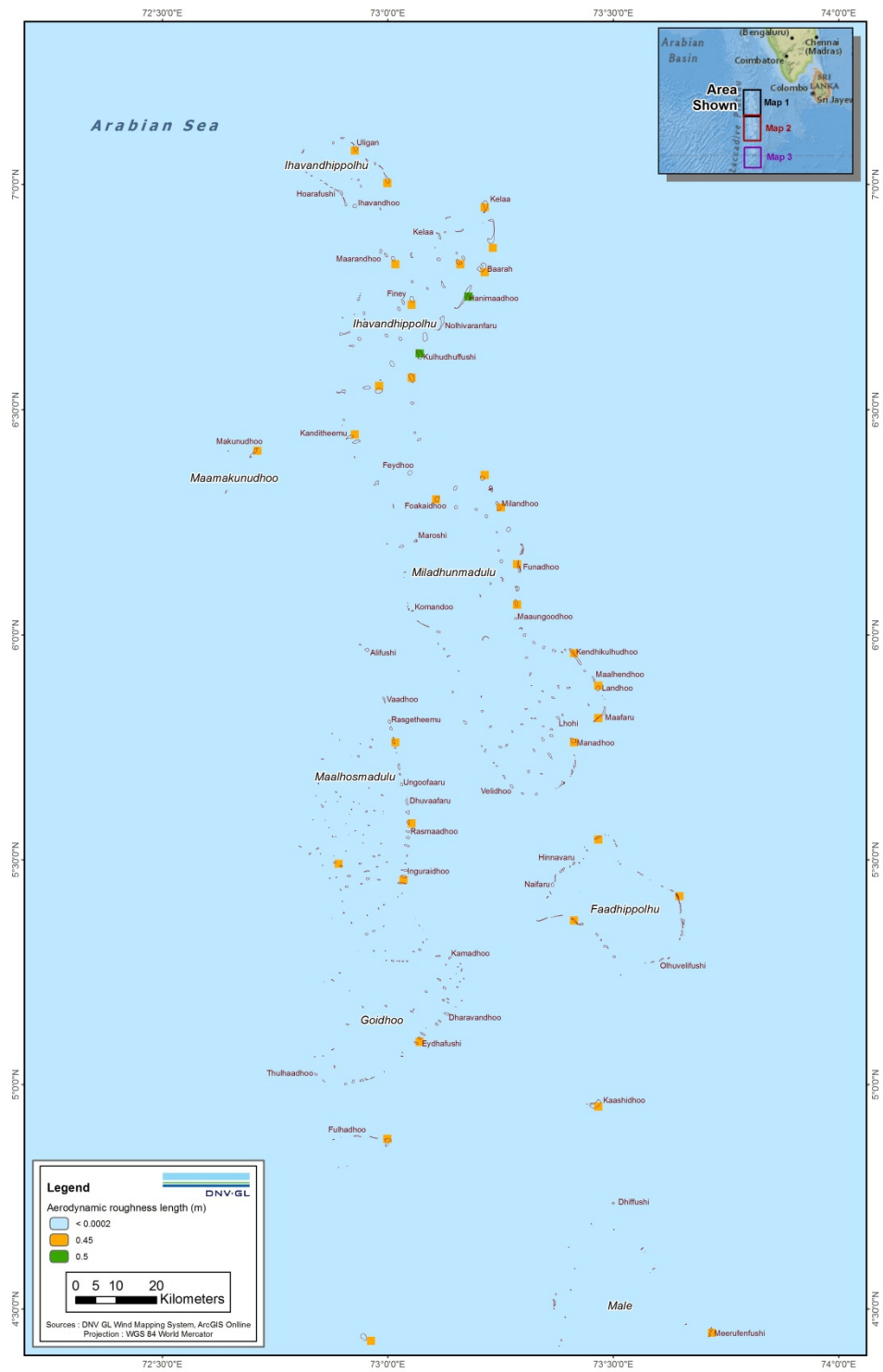


Figure A-6 Aerodynamic roughness length for the north of the Maldives



Figure A-7 Aerodynamic roughness length for the center of the Maldives

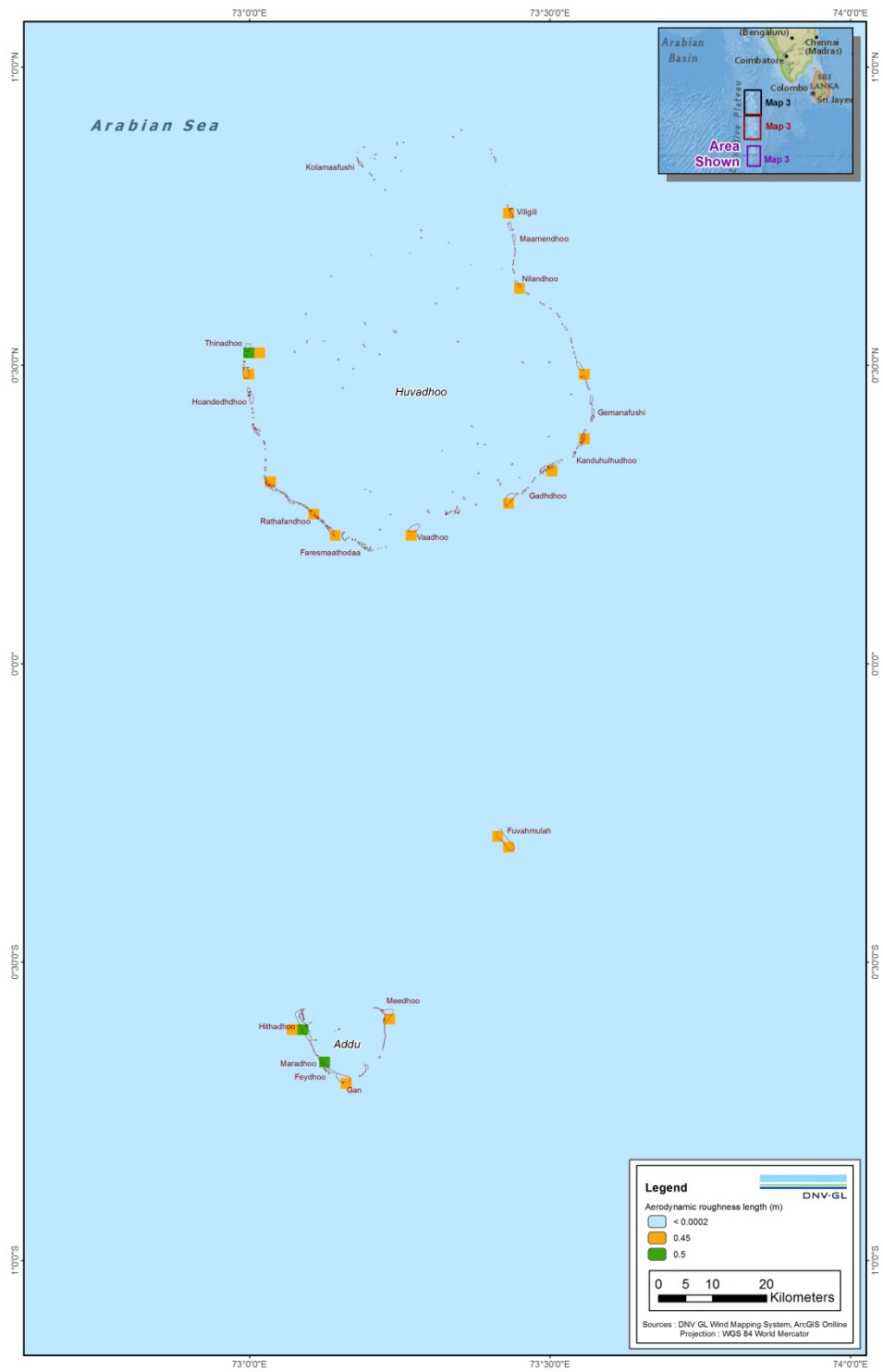


Figure A-8 Aerodynamic roughness length for the south of the Maldives

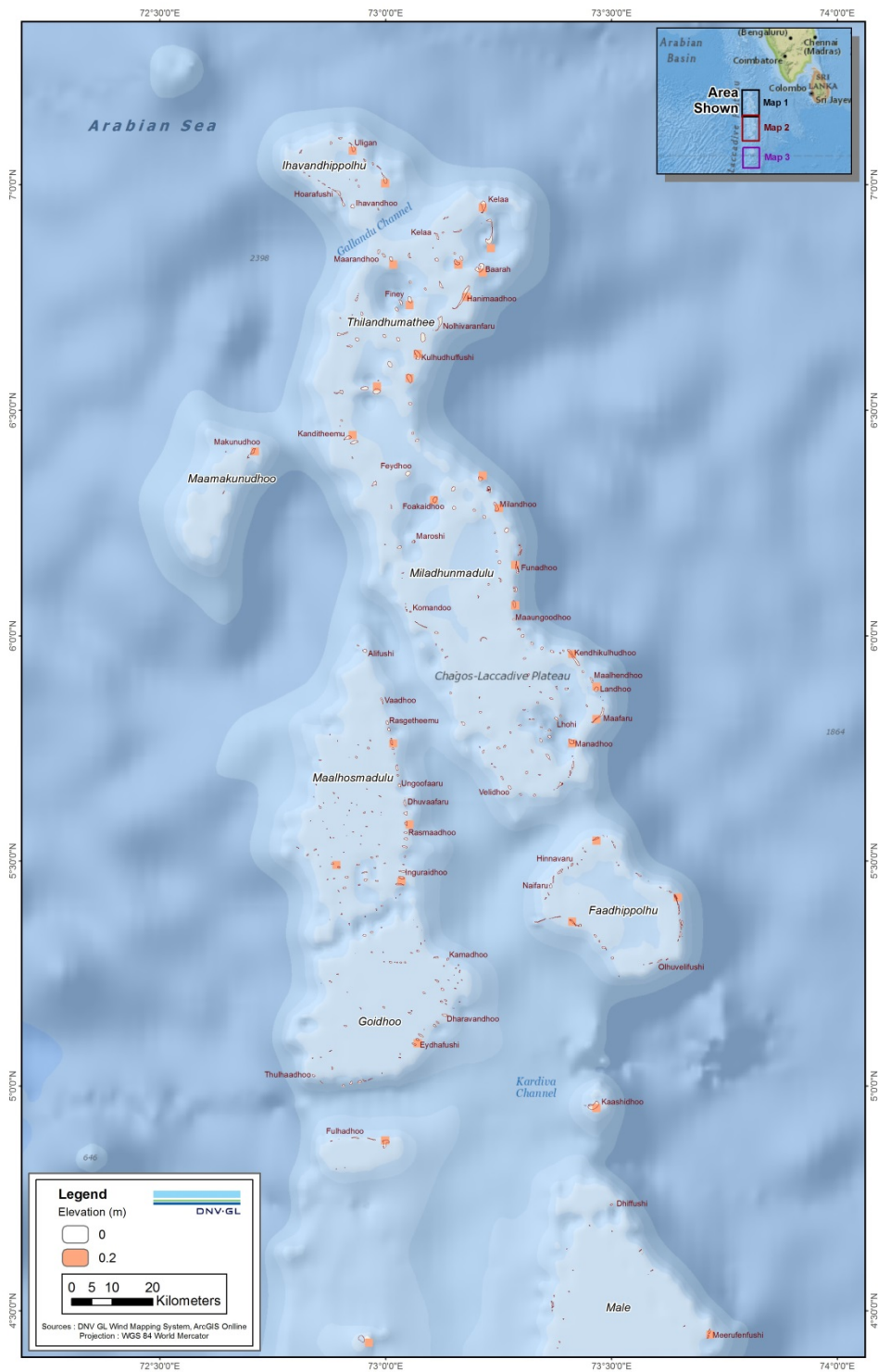


Figure A-9 Model terrain elevation (m) used in the WRF 2 km grid for the north of the Maldives

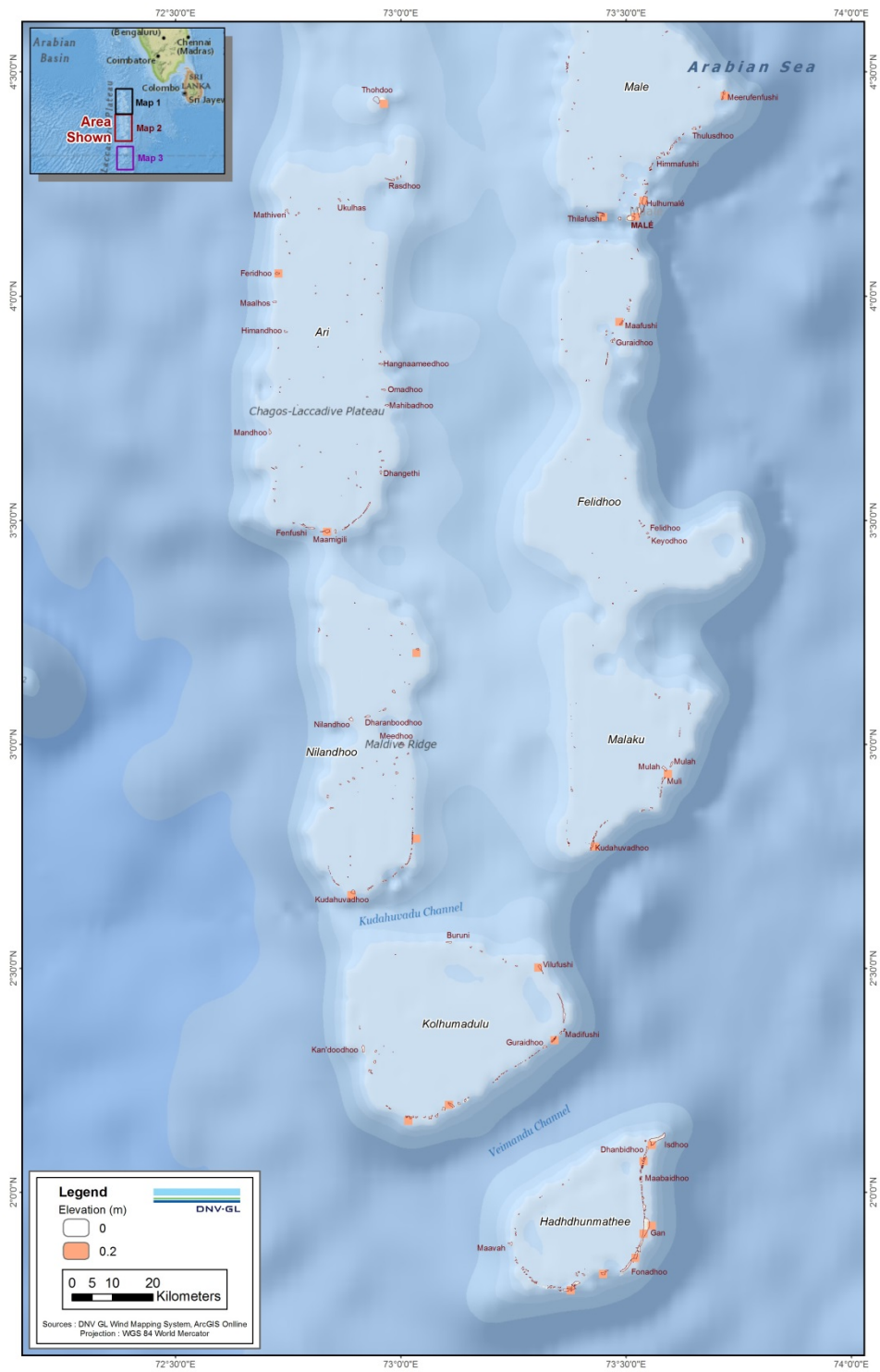


Figure A-10 Model terrain elevation (m) used in the WRF 2 km grid for the center of the Maldives

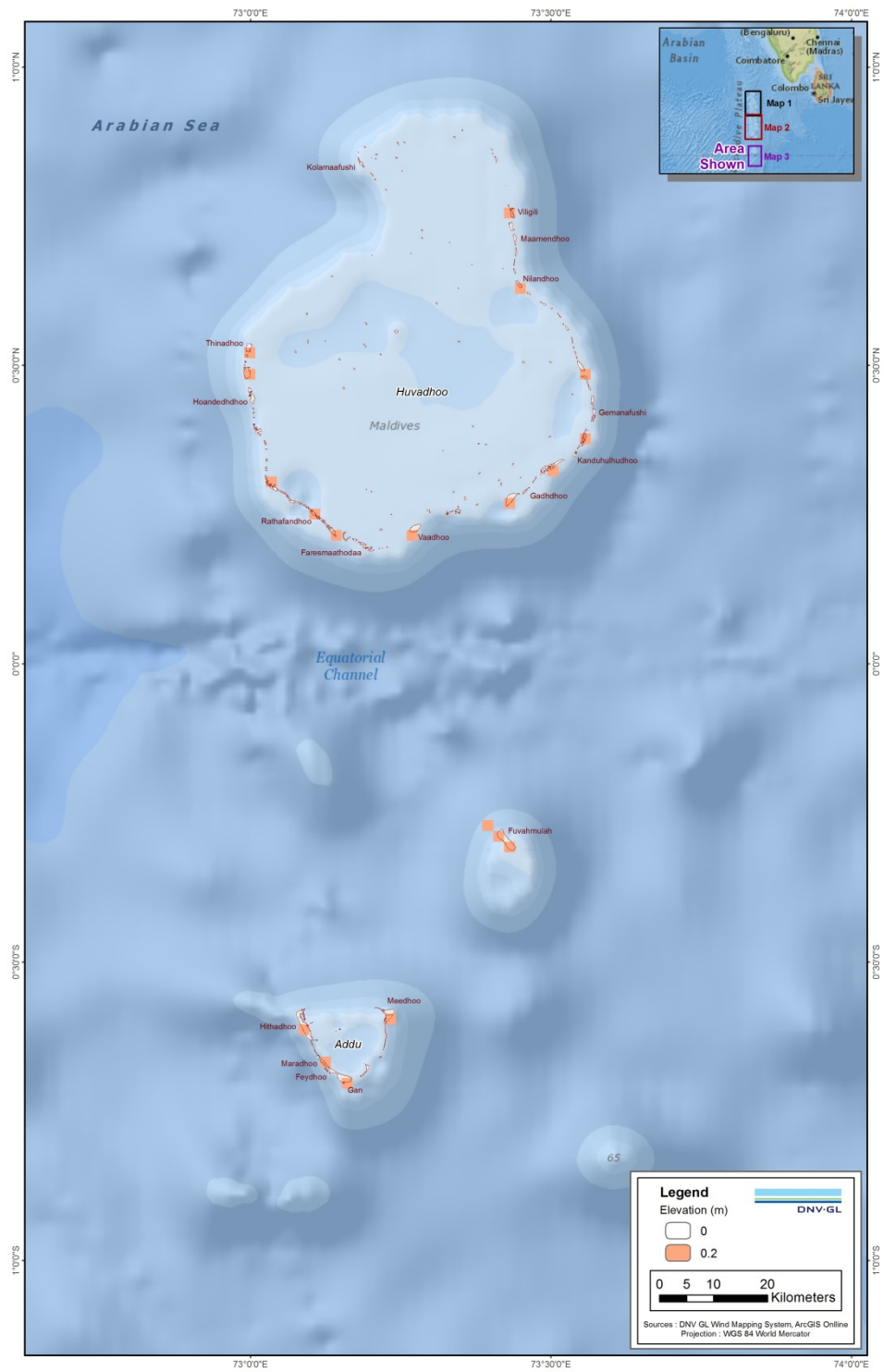



Figure A-11 Model terrain elevation (m) used in the WRF 2 km grid for the south of the Maldives



Initial land surface conditions for each simulation are based upon the National Aeronautics and Space Administration (NASA) Global Land Data Assimilation System (GLDAS; Rodell et al. 2004) dataset that is defined on a (0.25° × 0.25°) grid. The GLDAS fields used here are substrate soil moisture and temperature, ground skin temperature, and snow water equivalent. These fields are interpolated to all land grid points on each WRF grid. Sea surface temperatures (SSTs) are interpolated to ocean and lake grid points on each WRF model domain using the National Centers for Environmental Prediction (NCEP) global optimum interpolation SST (OISST) dataset (Reynolds et al. 2002) that is defined on a (0.25° × 0.25°) grid, and is updated daily throughout the entire 10-year simulation. These inputs are used in combination with an advanced and robust land surface model to properly represent the land-and sea-surface processes that strongly drive the boundary wind flows.

### **Initial and Lateral Boundary Conditions**

Individual simulations are initialized using the large-scale (0.5° latitude × 0.67° longitude grid) National Aeronautics and Space Administration's (NASA) Modern-Era Retrospective Analysis for Research and Applications reanalysis (MERRA; Rienecker et al. 2011). The MERRA analyses also provide the lateral boundary conditions every 6 hours during the simulations. This helps to preserve consistency amongst the large-scale features between the WMS and MERRA.

MERRA is a state-of-the-science third generation global reanalysis of the satellite era from 1979-present (Rienecker et al. 2011), with assimilation of an extensive set of global measurements. As described in Rife et al. (2013), assimilated data most relevant for wind energy applications are winds from rawinsondes, profilers, NEXRAD radar, land-based stations, aircraft, ship, and QuikSCAT scatterometer winds. An array of satellite-based measurements is also assimilated by MERRA, including data from the entire constellation of NASA Earth Observing System (EOS) satellites. DNV GL has extensively used MERRA for bankable wind resource assessments, and has a thorough understanding of its quality and suitability for use as a long-term reference. It exhibits substantially better correlations to measurements in a broad variety of locations compared to first and second generation reanalyses (such as the NCEP-NCAR reanalysis), making it a superior starting point for mesoscale downscaling. Additionally, the many active evaluations of MERRA appearing in the open peer-reviewed literature demonstrate that its quality is well understood.

### **Steps of the DNV GL WMS process**

There are 5 distinct steps in the overall WMS modeling process which are detailed below and described in the subsequent sections.

- Step 1: Determine period over which MERRA exhibits temporal consistency
- Step 2: Perform 10 km resolution simulations for most recent multi-year period, and 2 km resolution nested simulations for the most recent 365-day period
- Step 3: Perform analog ensemble (AnEn) downscaling to generate a complete 10-year time series at 2 km resolution
- Step 4 : Conduct generalized wind climate modeling for the interim wind atlas
- Step 5: Generate preliminary mesoscale wind speed uncertainty index map





### **Step 1: Determine period over which MERRA exhibits temporal consistency**

The process begins by determining the period over which MERRA exhibits temporal consistency within the client country. For bankable resource prediction applications it is vital that the data set used is consistent. DNV GL has conducted a formal temporal consistency analysis at the global level, using the World Meteorological Organization (WMO) change point analysis technique (Wang, 2008a, b), and finds that all reanalysis datasets are broadly consistent since about January 2000. However, because many developing countries lack dense networks of reliable long-term ground based measurements, the impact of the large changes in the global satellite observing systems over the past 30 years will have a much greater influence on the consistency and accuracy of reanalysis in these regions. Thus, it is important to establish the local and regional consistency of MERRA within the Maldivian region.

Ideally, comparisons between MERRA and reliable long-term ground based wind datasets would be conducted over the region to determine MERRA's temporal consistency. As stated in the TOR, the Maldives currently lacks reliable measurement data from ground based measurement stations. This prevents us from performing statistically robust and meaningful comparisons to measurements. As a result, the investigations reported here focus on analyses and statistical tests performed on MERRA itself, as well as comparisons between MERRA and another widely used and thoroughly vetted third generation global analysis: the European Centre for Medium-Range Weather Forecasts Interim Re-Analysis (ERA-Interim; Dee et al, 2011).

A detailed analysis was performed at 9 representative sites within the Maldives, as shown in Figure A-12. Locations were chosen to provide good geographical coverage of the country and wind conditions. The MERRA hourly time series data at 50 m above ground level (AGL) were obtained for each location from January 2000 to July 2014 (the most recent output available at the start of the project). This is a readily available vertical layer that is closest to the current standard hub heights. The hourly data was averaged to produce a monthly time series, and these were subjected to the WMO change point tests.

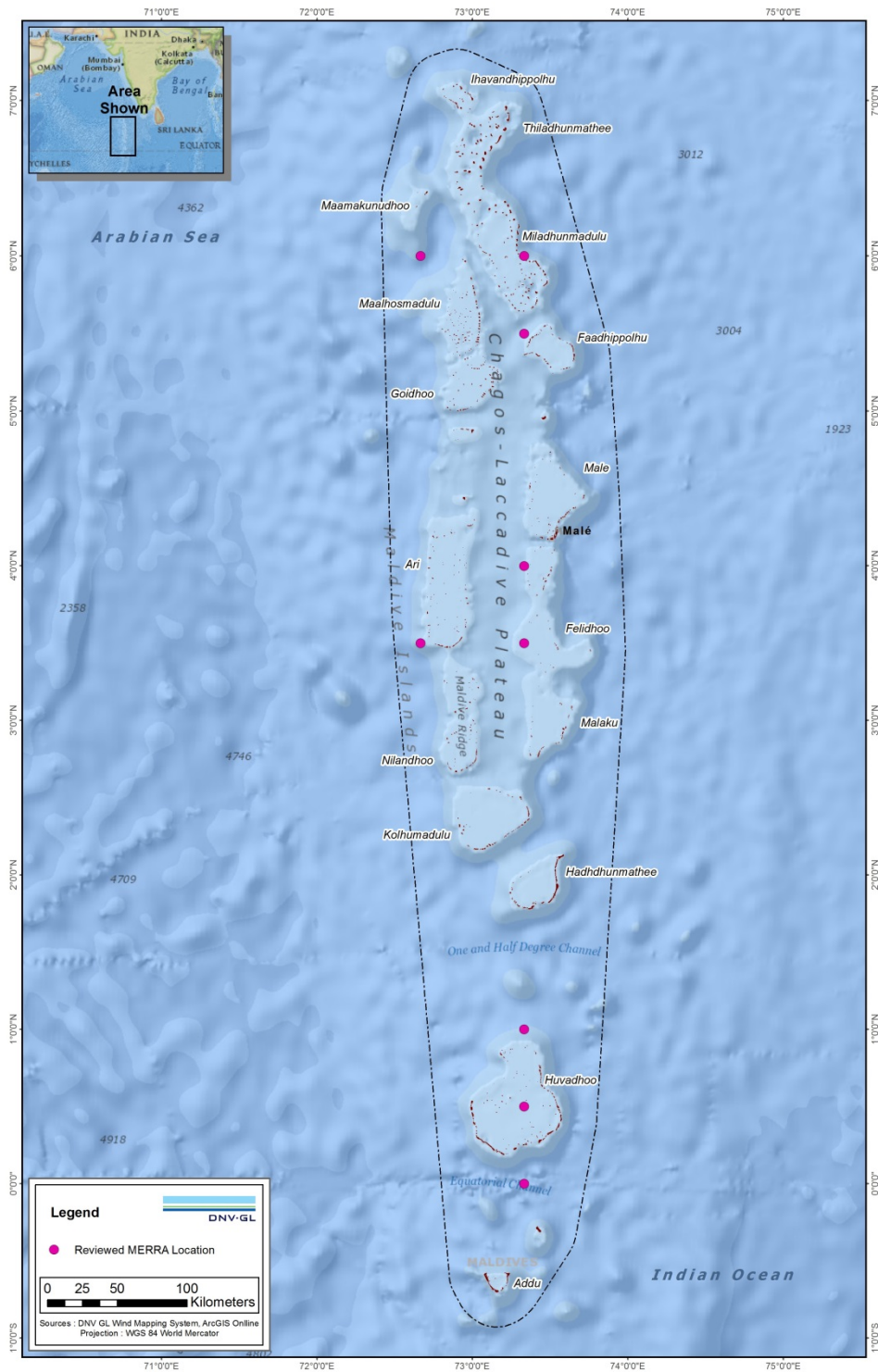


**Figure A-12 Map of the center point (purple dots) of the MERRA grid cell wind speed results used for the detailed change point analysis and tests**

The MERRA time series for all locations exhibited temporal consistency across the entire 2000-2014 period at the 99% confidence level. Figure A-13 shows the MERRA monthly mean wind speeds at 50 m AGL for a site in the central region of the Maldives. Overall, there appears to be a negative linear trend of approximately  $-0.05$  m/s/annum from 2000-2014 for this example. Similar order of magnitude trends are seen at other locations, indicating that the trend seen is not isolated to only one particular area of the Maldives.

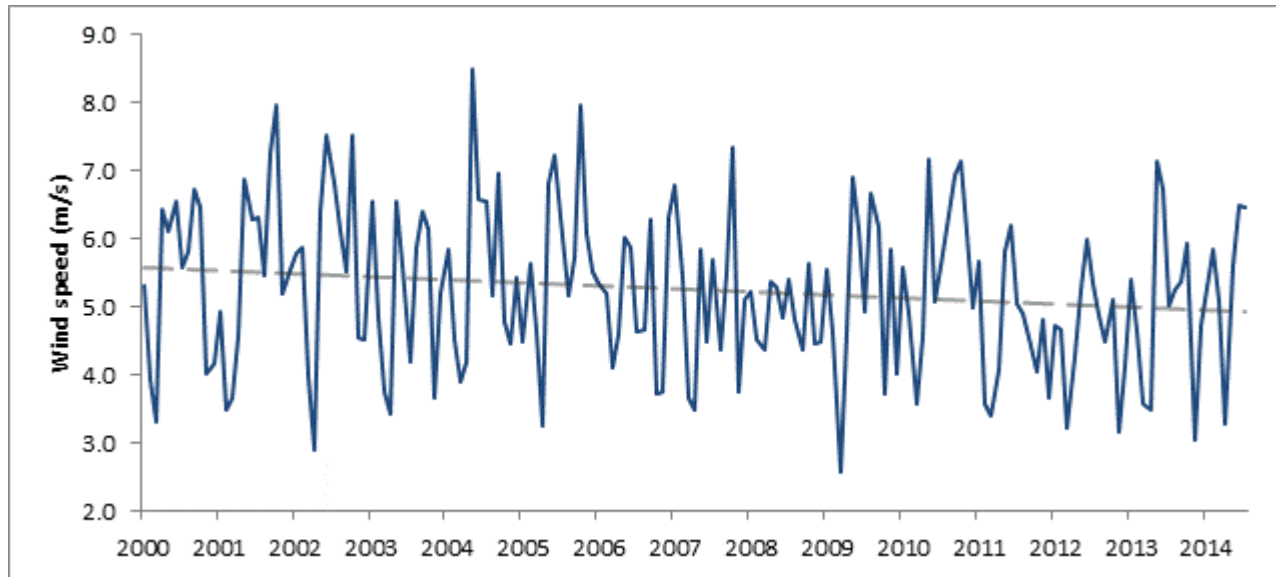


**Figure A-13 Monthly mean wind speeds at 50 m AGL for MERRA data sourced from a location representative of the center of the Maldives (3.5°N, 73.3°E)**

Another common approach is to compare the long-term temporal consistency with other available global reanalyses. In the present case, MERRA has been directly compared to the ERA-Interim reanalysis, which serves as a somewhat independent check of consistency. ERA-Interim data is obtained for grid cells closest to the MERRA study locations for the same 2000-2014 period. Visual comparisons of, and correlations between, normalized monthly mean wind speeds reveal good general agreement between MERRA and ERA-Interim at all sites, as illustrated for one example site in Figure A-14. However, whilst the ERA-Interim data also exhibits a negative linear trend, the magnitude of this trend is lower with a value of approximately  $-0.01$  m/s/annum. Negative long-term wind speed trends have been observed in this region in other studies (I.R. Young et al. 2011; J. Wentz et al. 2007) indicating that the presence of a negative long-term trend in the reanalyses is reasonable. Yet, it is difficult to confirm which of the reanalyses better reflects the real trend due to the absence of reliable long-term measured reference data sets in the Maldives. As such, DNV GL has selected the higher resolution MERRA dataset to initiate the mesoscale simulations used to generate the wind atlas. However, in order to quantify how differences between the two reanalyses may contribute to the uncertainty associated with the wind atlas, DNV GL has included both the MERRA and ERA-Interim reanalyses in the multiphysics multi-reanalysis ensemble runs carried out as part of this study, as discussed further in Step 5.

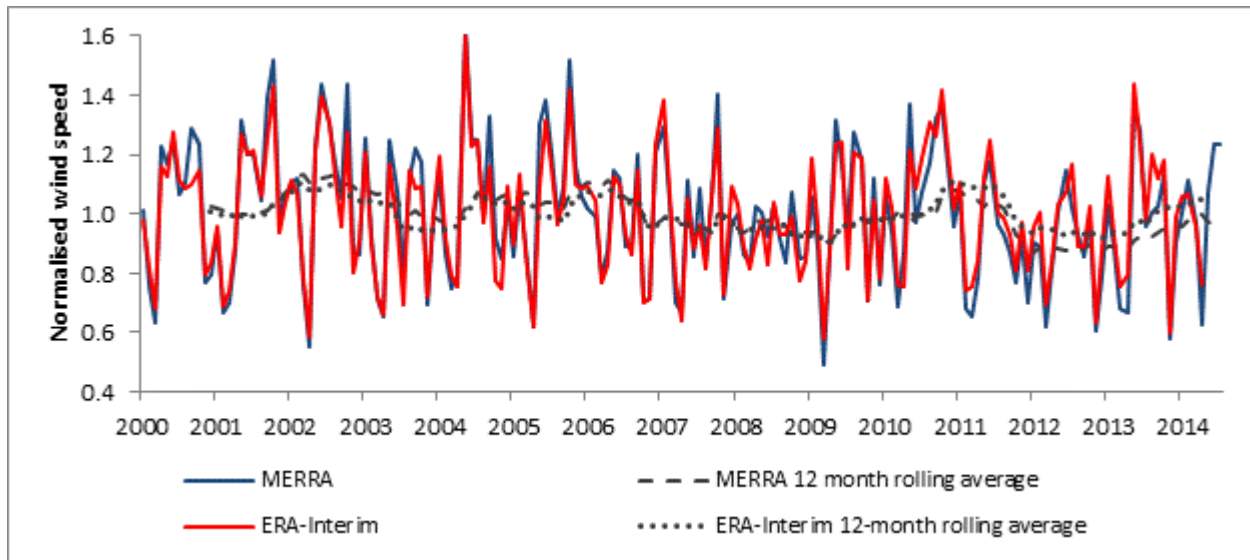


**Figure A-14 Monthly mean wind speed anomalies as represented by MERRA and ERA-Interim from the center of the Maldives (3.5°N, 73.3°E) for 2000-2014**

DNV GL has performed all reasonable checks to establish that the period used has no significant inconsistencies; however, it is reiterated that robust ground measurements represent the most reliable source of data to use in this verification process. As the performance of reanalysis datasets in the region become better understood, increased confidence can be placed on these results.

**Step 2: Perform 10 km resolution simulations for most recent multi-year period, and 2 km resolution nested simulations for the most recent 365-day period**

The mesoscale downscaling approach used for this project is based on a computationally efficient and statistically robust method for generating long-term dynamically downscaled datasets. A coarse resolution (10 km) mesoscale model is run for the entire period to be downscaled, while for only a fraction of that period a nested version of that same model is run at high (2 km) resolution. The period over which the coarse and high-resolution runs overlap is called the training period, while the remaining portion is termed downscaling period. For each time of the latter, the best matching coarse estimates (termed “analog”) over the training period are found. The downscaled solution is then constructed from the set of high-resolution values that correspond to the best matching coarse analogs. This method has been rigorously validated and published in open peer-reviewed scholarly journals (Delle Monache et al. 2011, 2013). It has been demonstrated to yield downscaled time series that closely approximate the standard “brute force” approach to dynamical downscaling, in terms of bias, root-mean-squared difference, and goodness-of-fit (Rife et al. 2014). Other properties of the time series are replicated very well by the analog method, including the autocorrelation and the hour-to-hour variability.

A complete hourly time series with the 10 km resolution grid is first generated over the entire 10 year period (01 September 2004 to 31 August 2014). Next, a nested 2 km grid is used to provide an hourly time series over the last year of the 10 km resolution simulation (01 September 2013 to 31 August 2014). These outputs provide the basis for the high resolution downscaling performed with the analog ensemble, which is further described in the following step, to yield a complete 10-year time series at 2 km resolution over the entire country.

### Step 3: Perform analog ensemble (AnEn) downscaling to generate a complete 10-year time series at 2 km resolution


As described above, a published and rigorously validated method is employed to downscale the 10-km gridded analyses to the 2-km grid. The new technique, termed the analog ensemble (AnEn), was originally developed by Delle Monache et al (2011) and further advanced in collaboration with project co-lead Rife (Delle Monache et al. 2013). The procedure is shown Figure A- 15. In this example, a 10 km WRF simulation at Sample Time 1 (filled black dot) is downscaled to 2 km resolution. The procedure first finds all dates in the 2013-2014 training period where the 10 km WRF hourly simulations are a close match to the 10 km solution at Sample Time 1 (open circles), and ranks them according to their similarity to Sample Time 1. Next, the 2 km WRF simulations for these ranked dates (open squares) are obtained and then a weighted mean of those 2 km simulations is used to form the analog ensemble mean prediction at Sample Time 1. This process is repeated for every hourly output time in the 2004-2014 period. For wind mapping applications, DNV GL have found that the optimal number of analogs is about 5, which are used to form a weighted average of the 2 km WRF simulations on those dates. As shown in Rife et al. (2014) this yields a result that closely matches the “brute force” mesoscale calculation in terms of goodness-of-fit ( $R^2$ ), bias, and root-mean-squared error for hourly wind speed and wind direction.

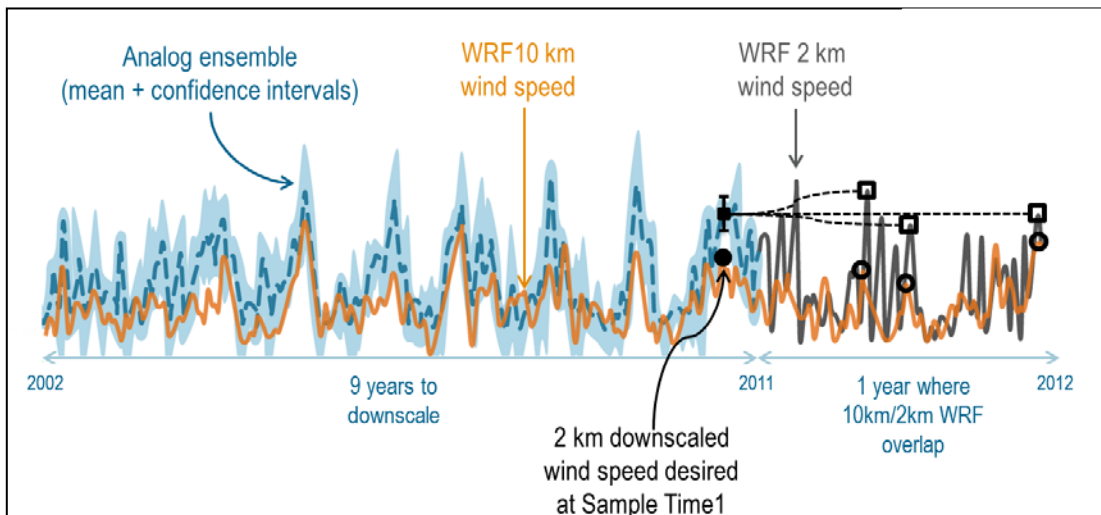


**Figure A- 15 Analog ensemble procedure. See text for explanation. Adapted from Delle Monache (2012).**

It is important to note that the analogs are sought independently for each analysis time and grid point, using the wind speed and wind direction at the five heights required in the TOR<sup>1</sup>, and the Obukhov length (a measure of vertical thermal stratification). Thus, when the search procedure is “localized” in both space and time, this greatly reduces the degrees of freedom and significantly increases the probability of finding well matching analogs. Additionally, it is not necessary to match all aspects of the gridded reanalysis, such as upper-level winds or temperatures. For example, Delle Monache et al. (2011a, 2013) found that many good analogs are found by matching only the wind speed, wind direction, temperature and pressure at a specific

<sup>1</sup> The TOR (Selection # 1139234) specifies that wind speed and wind direction are to be provided at the following heights AGL: 10 m, 50 m, 80 m, 100 m, and 200 m.



location and time. Rife et al. (2014) found that very good analogs are found using wind speed and wind direction only. In the present application, including the Obukhov length in the analog matching procedure ensures that analogs from the same thermal stability regime are chosen. Other authors have also demonstrated that analog-based approaches are highly effective if they include a localization strategy in space and time (Van den Dool 1989, 1994; Hamill and Whitaker 2006). It should also be noted that a set of sensitivity experiments revealed that the performance of the Analog Ensemble method is largely insensitive to the choice of year used for the truth data, regardless of whether the weather patterns during that year are impacted by large scale modes of variability such as the Monsoon, and the El Niño Southern Oscillation (Rife et al. 2014).

The complete multi-year integration performed for the simulations yields a continuous hourly time series that well represents the full range of wind and thermal stratification conditions over the Maldives. This is a dramatic improvement over previous wind mapping approaches used for World Bank funded projects. Previous methods used a random sampling technique, which has uncertainties as high as 45% for both wind speed and direction (Rife et al. 2013a). These uncertainties are entirely eliminated in the time-series approach used for this project whilst also allowing the inter-annual variation in the wind resource to be quantified. Also, because the proposed modeling approach creates a continuous hourly time series, updates to the wind atlas only require performing simulations over the most recent period. For example, the Phase 1 calculations are performed over the 01 September 2004 to 31 August 2014 period. If updates to the atlas are desired in 2015, say 01 July 2015, then DNV GL need only simulate the 01 September 2014 to 01 July 2015 period to bring the atlas database fully up-to-date. All the relevant wind statistics can then be easily re-calculated for the WASP-lib files, and the new statistics will fully incorporate the information from the most recent year of data. By contrast, the random sampling method would have to be fully re-run “from scratch”, and there is no guarantee that the most recent year’s information will be adequately represented in the new results, since for each calendar day, a year is randomly chosen, typically from among the most recent 15 years. For example, for 1 January the year 2005 might be chosen, and for 2 January the year 2009 may be chosen, and so on through 31 December (Rife et al. 2013a) to form a single “representative year”.


The result of these continuous hourly 10-year simulations is used to create the various outputs for the interim numerical wind atlas.

#### **Step 4: Generalized wind climate modeling for the interim wind atlas**

The hourly outputs of WMS at each grid point of the 2 km mesoscale domain are used to calculate the generalized wind climate wind statistics according to the industry-standard WASP-format “wind atlas” (“WASP-lib”) file, consistent with the European Wind Atlas method (Troen and Petersen, 1989). This was performed using the Danish Technical University (DTU) Generalized Wind Climate software package.

#### **Step 5: Preliminary mesoscale wind speed uncertainty index map**

It is well known that mesoscale model simulations have a number of inherent and unavoidable limitations and uncertainties, including the input datasets, the lateral boundary conditions, the numerical approximations used in the dynamical core of the model, and the imperfect representation of the complex physical processes that strongly drive the winds within the boundary layer. Monte Carlo methods have been developed to mitigate these errors, and provide statistically defined estimates of the uncertainty in the mesoscale results. Within the numerical weather prediction community such techniques are generically



termed “ensemble methods”. For this project a “multiphysics multi-reanalysis ensemble” was utilized. Five different versions of the model were constructed, each with a unique suite of physical process parameterizations. These five versions were initiated using MERRA as initial and lateral boundary conditions, and the same five versions were also initiated with ERA-Interim. This procedure is commonly referred to as a “multiphysics ensemble” to perform separate parallel downscaling simulations (e.g., Stensrud et al. 1999). By varying both the model versions and the input datasets to form the ensemble allows us to specifically quantify the uncertainty related to the necessarily imperfect representation of the physical processes such as land surface interactions, clouds, rainfall, and the errors and uncertainties in the input datasets. Errors in the input datasets arise because the atmosphere can never be completely and perfectly observed, either in terms of spatial coverage or accuracy of the instruments. The multiphysics ensemble approach has been proven extensively for over 20 years (Stensrud et al. 1999; Eckel and Mass 2005, Hacker et al. 2011; Lee et al. 2012, among others). The “ensemble spread” or standard deviation among the ensemble of simulations provides an objective estimate of the meteorological uncertainty, allowing us to place a statistically defined error bar on the resource estimate for any point within the numerical wind map/atlas.

The WRF model has a large list of options for each type of physical parameterization, and thus it is straightforward to create a significant number of ensemble members by simply varying these parameterizations. Because parameterizations employ a wide variety of formulations and assumptions about their representation of the physical processes, the individual simulations each will yield an equally plausible (and unique) representation of the atmospheric state at any instant, within the likely range of meteorological and numerical model uncertainty. Hacker et al. (2011) and Lee et al. (2012) provide excellent guidance for the unique sets of parameterizations that yield the best overall results within a multiphysics ensemble for boundary layer applications. For the Maldives project DNV GL made use of the approximate intersection of their configurations to select 5 total model versions (see Figure A-16). Again, these 5 model versions are run with both MERRA and ERA-Interim reanalysis datasets as input, totaling 10 multiphysics multi-reanalysis ensemble members. It is important to note that full range of uncertainty information due to errors in the physics is obtainable with as few as 8-10 ensemble members (e.g., Du et al. 1997; Clark et al. 2009, 2011; Lee et al. 2012; Wandashin et al. 2001).

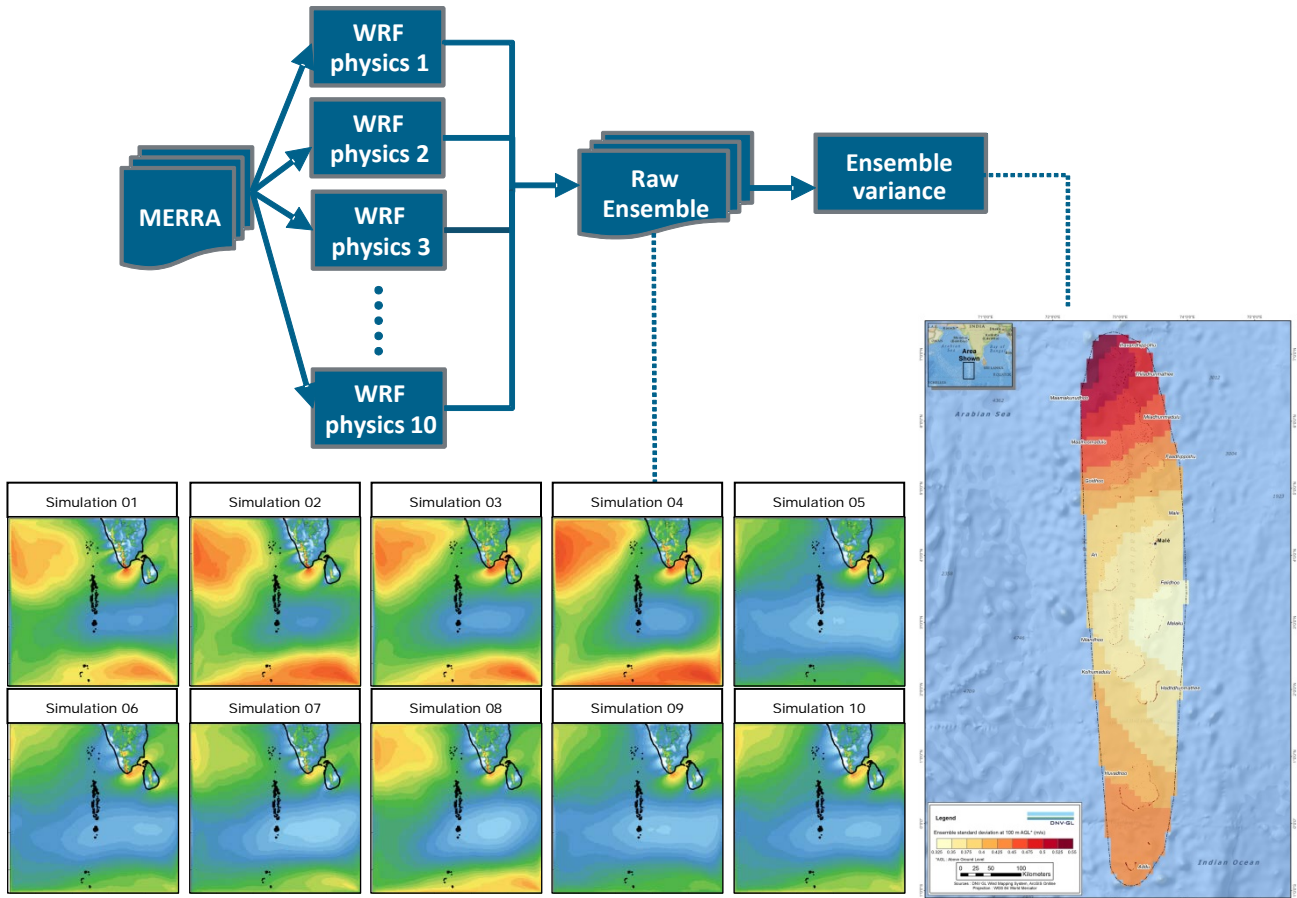


**Figure A-16 The multiphysics ensemble approach**

Since the aim of this process is to understand the overall uncertainties in the interim wind atlas at the regional level, the 10-member multiphysics ensemble simulations are performed on the 10 km outer grid over the Maldives and the surrounding region for one representative year. This representative year was one where the overall wind speeds and patterns are most similar to the long-term mean and was chosen based on the decade long 10 km WRF simulation used to create the interim wind atlas. This has the advantage of being very cost effective in terms of computational time and expense, and the results can be directly related to those on the 2 km grid, since the relationships between the 10 km and 2 km grids are well established during the AnEn downscaling stage.

An annual mean wind speed map is computed for each of the 10 ensemble member simulations and the standard deviation is computed among the 10 maps (termed the ensemble standard deviation). Given the lack of ground measurements to validate the wind atlas and the absence of microscale modeling undertaken at this stage of the project, the preliminary wind speed uncertainty index is initially set to be equal to the standard deviation of the 10 multi-physics mesoscale ensemble members. Areas with a high index value, and therefore high standard deviation indicate where there is a lack of consensus between the ten multi-



physics ensemble members, and shows the apparent increased difficulty in modeling the flows in these areas.

This dataset will provide tremendous value to stakeholders and commercial developers, as it provides the first available statistically defined uncertainty index for the estimated wind resource at each region within the map, thereby helping target the best placement of meteorological masts and potential wind farm sites. Indeed, the uncertainty map is a key input to the Candidate Site Identification Report as part of the Phase 1 deliverables. It will also help to significantly advance the current state-of-the-art in wind mapping, and helping the industry to understand the true value and utility of modern ensemble prediction methods, which have become the mainstay of many other fields, including weather forecasting and climate prediction. For example, all of the world's national weather prediction centers have well-established ensemble modeling systems that are used in daily operations to support a large variety of commercial and public sector requirements, including forecasting for operational wind and solar power plants.

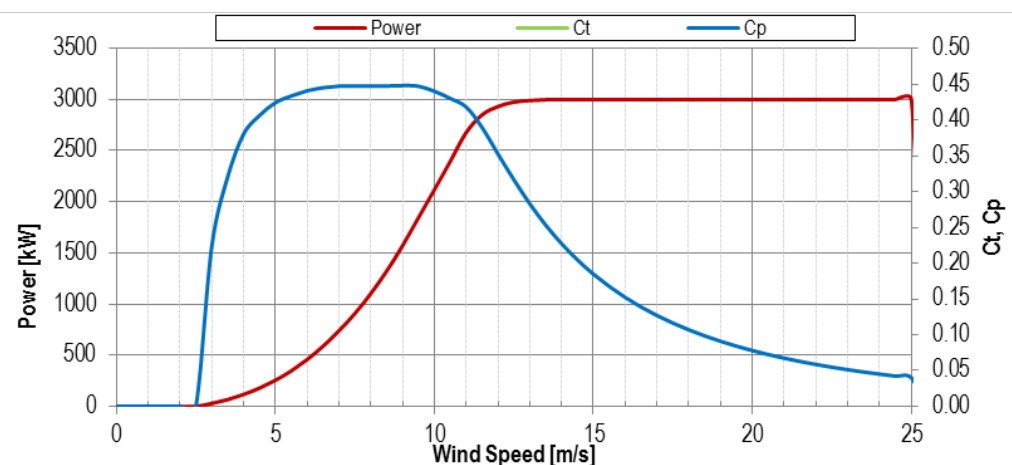
## GENERATING A POWER TIME SERIES

Many of the derived outputs required as part of this project require the generation of a power time series.

Firstly, a "generic wind turbine" must be defined. The TOR stipulates that generic pitch controlled wind turbine with 100 m rotor, 3 MW rated power and at 100 m hub height should be used. DNV GL has taken a range of power curves with similar dimensions from different manufacturers and averaged them to produce a single "generic" power curve that fulfils these criteria. Power curves at the standard 1.225 kg/m<sup>3</sup> air density have been used for this purpose. Through this process it was ensured that the power curve exhibits a reasonable peak power coefficient (maximum Cp of 0.45). The derived generic wind turbine power curve is shown below in Table A- 1.

**Table A- 1 power curve for generic wind turbine model**

Wind speed (m/s)	Power (kW)
2	0
3	29
4	117
5	255
6	458
7	738
8	1102
9	1571
10	2117
11	2677
12	2931
13	2990
14 - 25	3000



The details of this generic turbine are just one of the topics DNV GL is keen to solicit feedback on, from both Client and key Stakeholders alike as part of the Phase 1 workshop. Initial review of the preliminary wind speed map indicates that for much of the Maldives a larger rotor diameter turbine may be more appropriate. However, the characteristics of the turbine proposed here are considered to capture the salient features relating wind speed frequency distributions through to an energy value for initial planning purposes.

The next step involves computing a time series of density for every 2 km grid cell. The approach taken here was to first compute a 12 x 24 matrix of air density at each 2 km grid cell using the single year simulation from 01 September 2013 to 31 August 2014, rather than from the full 10-year simulation. The rationale for this approach is that the interannual variability of air density is low, as air density is a measure of total columnar mass of the atmosphere at any point. Although hourly and daily average values of air density may vary from one year to the next due to changes associated with transient weather systems, the seasonal and annual averages (e.g., the climatologic values), of air density will not, as the total atmospheric mass content neither increases or decreases (mass conservation). Indeed, the 10-year simulations from the DNV GL WMS show negligible interannual variability of monthly or seasonal values of air density.

Air density is computed according to the IEC 61400-12-1 standards<sup>2</sup>.

$$\rho = \frac{1}{T} \left( \frac{B}{R_o} - \phi P_w \left( \frac{1}{R_o} - \frac{1}{R_w} \right) \right)$$

Where:

B is the barometric pressure [Pa]

T is the absolute temperature [K]

$\phi$  is the relative humidity (range 0 to 1)

$R_o$  is the gas constant of dry air [287.05 J kg<sup>-1</sup> K<sup>-1</sup>]

$R_w$  is the gas constant of water vapour [461.5 J kg<sup>-1</sup> K<sup>-1</sup>]

$P_w$  is the vapour pressure [Pa].

The vapour pressure is calculated according to:  $P_w = 0.0000205 \exp(0.0631846 * T)$

The above parameters are derived directly from the DNV GL WMS model outputs with a resolution of 2 km and a height of 100 m AGL. Once the 12 x 24 matrix of air density values is created at each mesoscale grid point, a full 10 year time series of density at a height of 100 m AGL can be generated by using the 12 x 24 density table as a look up table for each individual hourly record.

Next, for each hourly record, the density value derived for the hour is used to create a power curve for the specific hour, for each 2 km grid cell, according to the recommendations of the IEC 61400-12-1 standard, and then the simulated wind speed at 100 m is used to calculate the power output from the density specific power curve. This is repeated for each hourly record in the 10-year time series across the entire country yielding a continuous 10 year time series of hourly power output in GW.

## REFERENCES

<sup>2</sup> IEC 61400-12-1 "Wind turbines – Part 12-1: Power Performance Measurement of Electricity Producing Wind Turbines", First edition, 2005-12.

- Clark, A. J., et al., 2011. *Mon. Wea. Rev.*, **139**, 1410–1418.
- Dee et al, 2011. *Q. J. Roy. Meteor. Soc.*, **137**, 553-597
- Delle Monache, L., et al., 2011. *Mon. Wea. Rev.*, **139**, 3554–3570.
- Delle Monache, L., 2012. AWEA Wind Resource & Project Energy Assessment Seminar, Pittsburgh, Pennsylvania.
- Delle Monache, L., et al., 2013. *Mon. Wea. Rev.*, **141**, 3498-3516.
- Draxl, C., et al., G., 2012. *Wind Energy*. doi: 10.1002/we.1555.
- Du, J., S. L. Mullen, and F. Sanders, 1997. *Mon. Wea. Rev.*, **125**, 2427–2459.
- Eckel, F. A., et al., 2005. *Wea. Forecasting*, **20**, 328–350.
- Hacker, J. P., et al., 2011. *Tellus A*, **63**, 625–641.
- Hamill, T., et al. 2006a. *Bull. Amer. Meteor. Soc.*, **87**, 33–46.
- Hamill, T., et al., 2006b. *Mon. Wea. Rev.*, **134**, 3209–3229.
- Lee, J. A., et al., 2012. *Mon. Wea. Rev.*, **140**, 2270–2286.
- Leung, L. R., and Y. Qian, 2009. *Geophys. Res. Lett.*, **36**, L03820, doi:10.1029/2008GL036445.
- Liang, Xin-Zhong, et al., 2012. *Bull. Amer. Meteor. Soc.*, **93**, 1363–1387.
- Mass, C., et al., 2002. *Bull. Amer. Meteor. Soc.*, **83**, 407–430.
- Mass, C. et al. 2008. *Wea. Forecasting*, **23**, 438–459.
- Mearns, L. O., et al., 2012. *Bull. Amer. Meteor. Soc.*, **93**, 1337–1362. Mullen, S., R. Buizza, 2002. *Wea. Forecasting*, **17**, 173–191.
- Parks, K., Y et al., 2011. NREL/SR-5500-52233, Golden, CO: National Renewable Energy Laboratory.
- Potter, A. W., et al., 2008. *Wind Engineering*, **32**, 325–338.
- Reynolds, et al., 2002. *J. Climate*, **15**, 1609–1625.
- Rienecker, M.M., et al., 2011. *J. Climate*, **24**, 3624–3648.
- Rife, D., et al., 2013a. *J. Appl. Meteor. Climatol.*, **42**, 47-63.
- Rife, D., et al., 2013b, *WindPower 2013 Conference*, Chicago, IL.
- Rife, D., et al., 2014, *WindPower 2014 Conference*
- Rodell, M., et al., 2004. *Bull. Amer. Meteor. Soc.*, **85**, 381–394.
- Skamarock, W. C. 2004: *Mon. Wea. Rev.*, **132**, 3019–3032
- Skamarock, W. C., et al., 2008. NCAR/TN-475+STR, 113 pp. [[http://www.mmm.ucar.edu/wrf/users/docs/arw\\_v3.pdf](http://www.mmm.ucar.edu/wrf/users/docs/arw_v3.pdf)].
- Stensrud, et al., 1999. *Mon. Wea. Rev.*, **127**, 433-446.
- Troen, I., and E. L. Petersen, 1989. Risø National Laboratory, 656 pp.
- Wandishin, et al., 2001. *Mon. Wea. Rev.*, **129**, 729–747.
- Wang, X. L., 2008: *J. Appl. Meteor. Climatol.*, **47**, 2423-2444.
- Wang, X. L., 2008b. *J. Atmos. Oceanic Tech.*, **25**, 368-384.



## APPENDIX B – PRELIMINARY AND UNVALIDATED MESOSCALE OUTPUTS

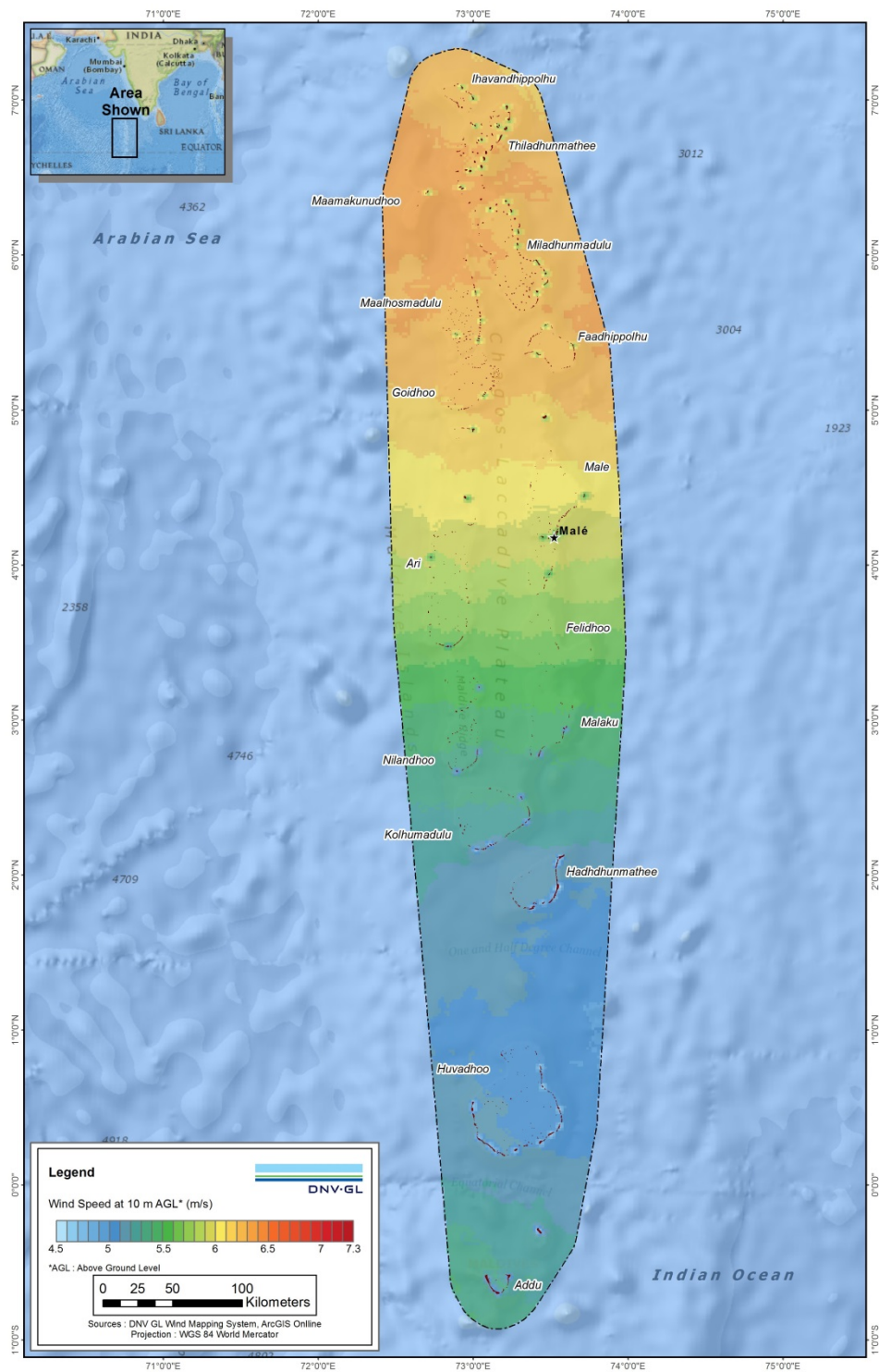


**Figure B-1 Preliminary and unvalidated mesoscale wind speed map, 10 m AGL, as simulated by the DNV GL Wind Mapping System**

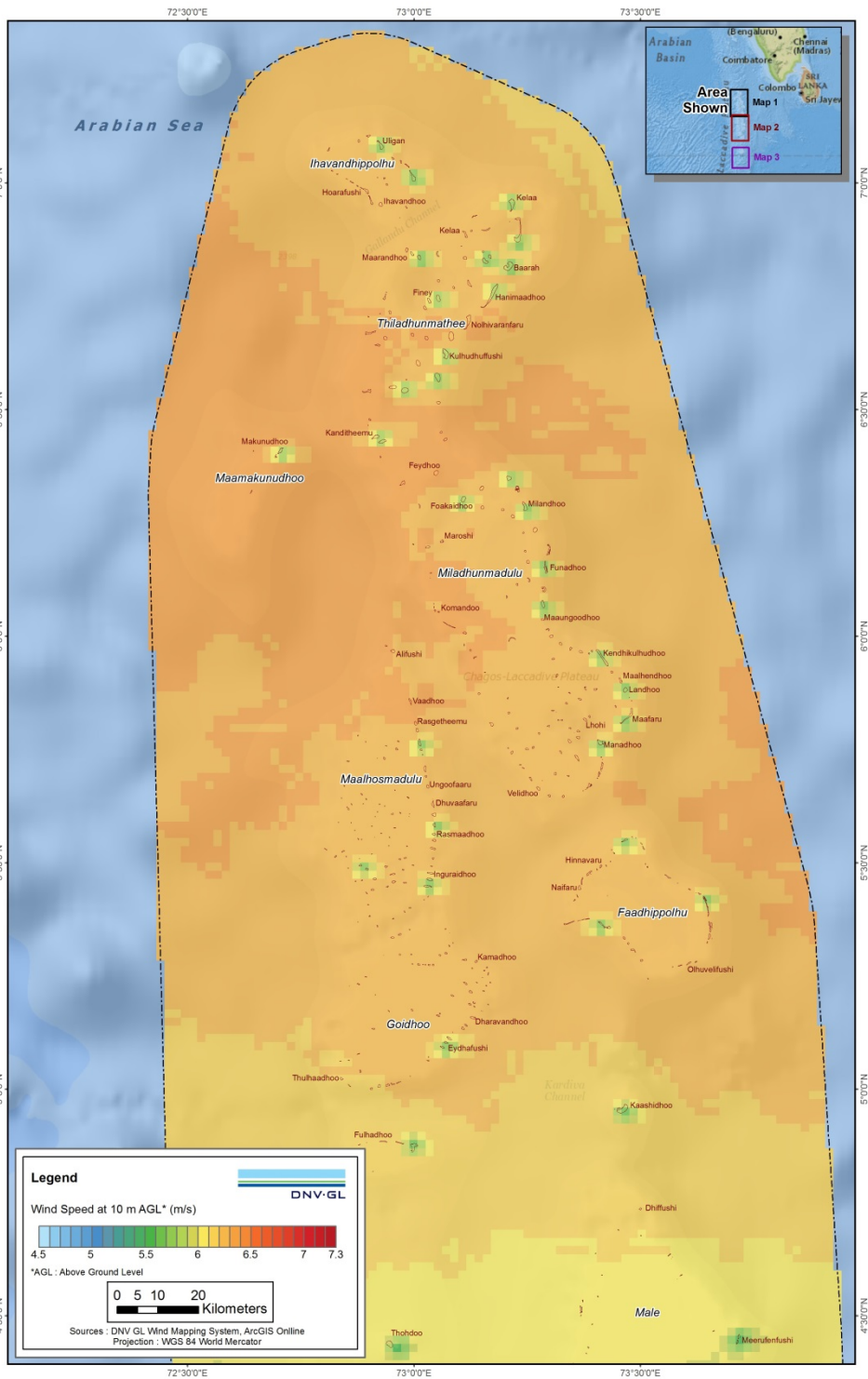


**Figure B-2 Preliminary and unvalidated mesoscale wind speed map of the north of the Maldives, 10 m AGL, as simulated by the DNV GL Wind Mapping System**

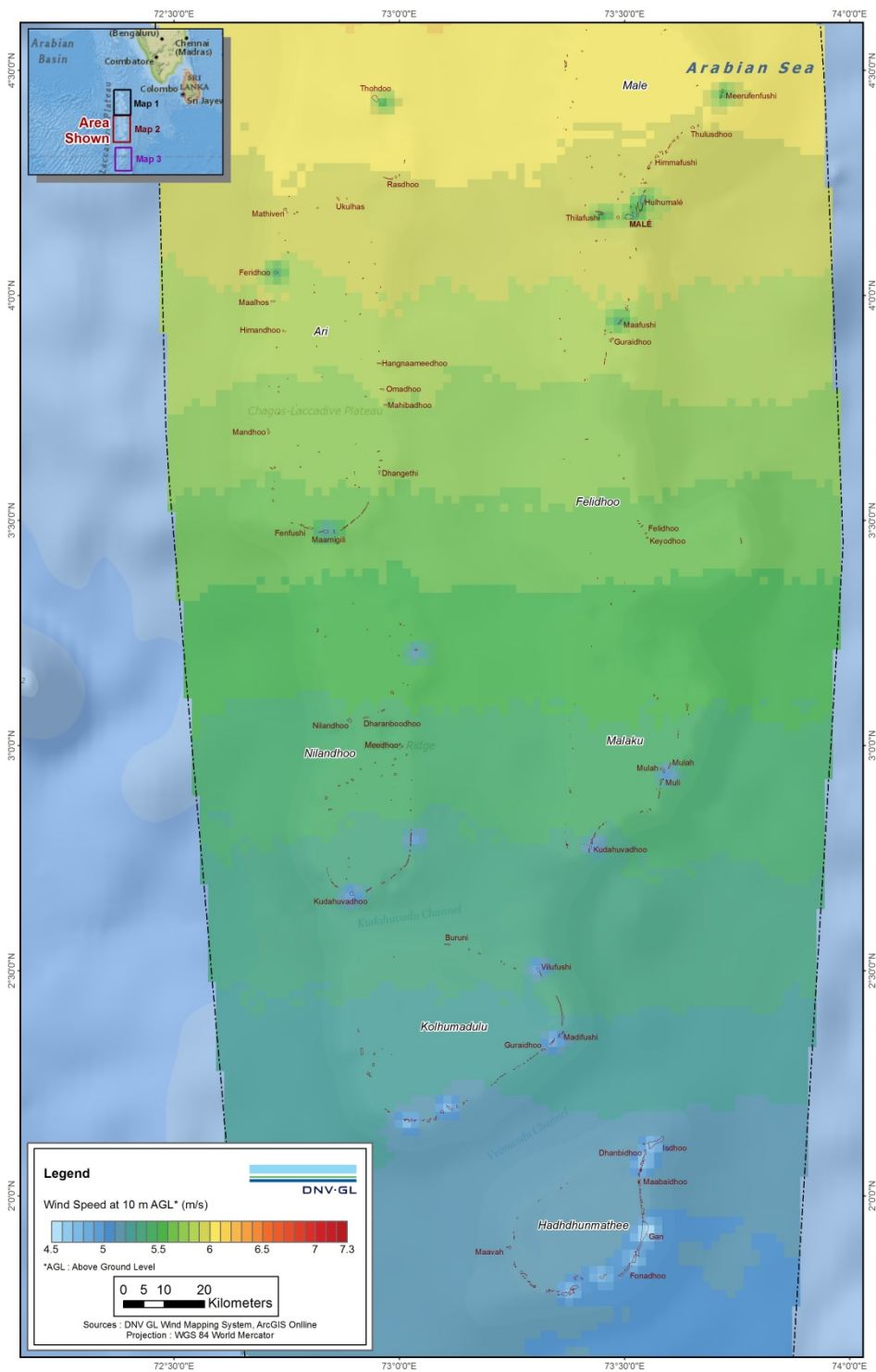


**Figure B-3 Preliminary and unvalidated mesoscale wind speed map, 10 m AGL of the center of the Maldives, as simulated by the DNV GL Wind Mapping System**

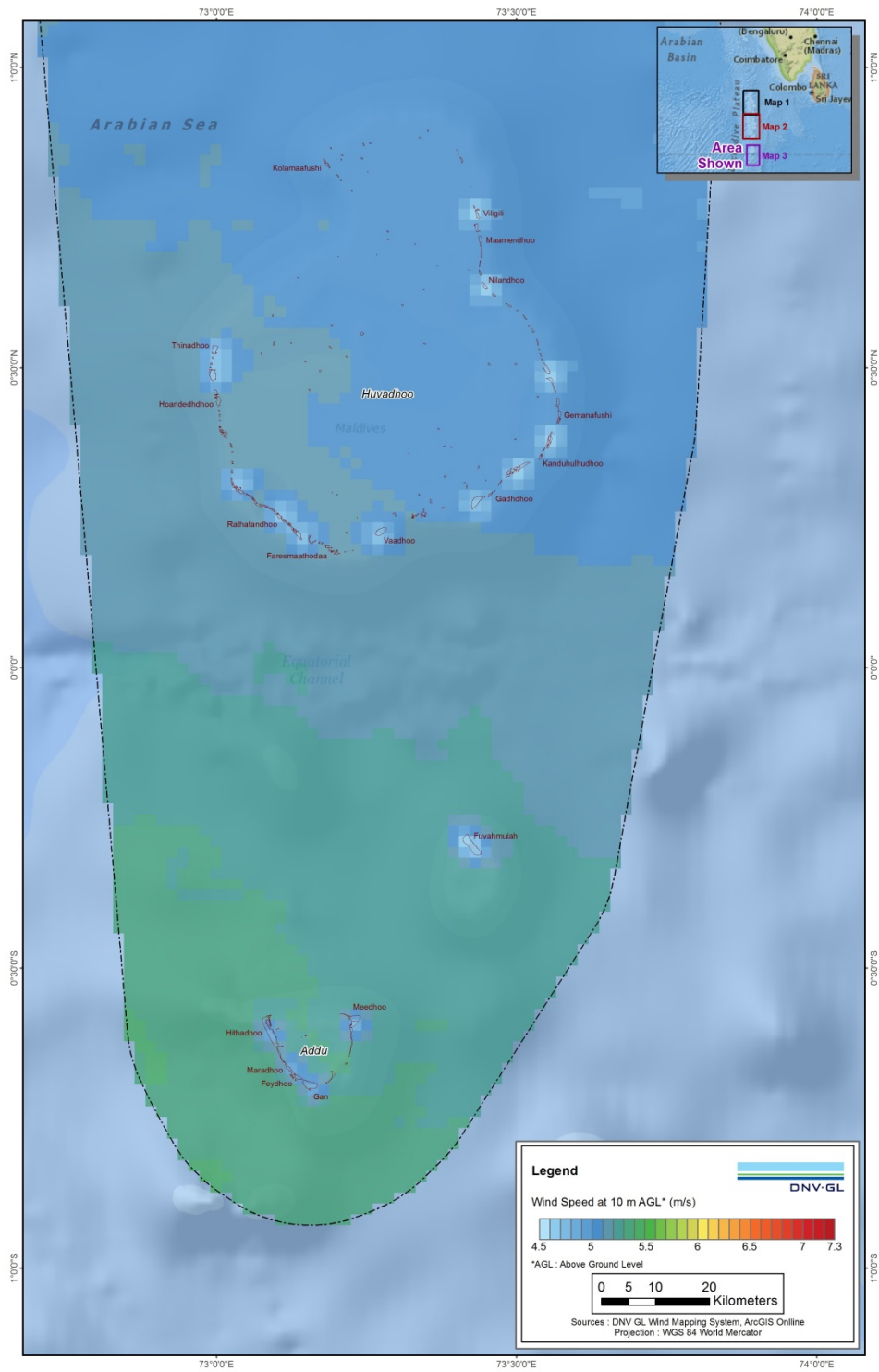


**Figure B-4 Preliminary and unvalidated mesoscale wind speed map of the south of the Maldives, 10 m AGL, as simulated by the DNV GL Wind Mapping System**



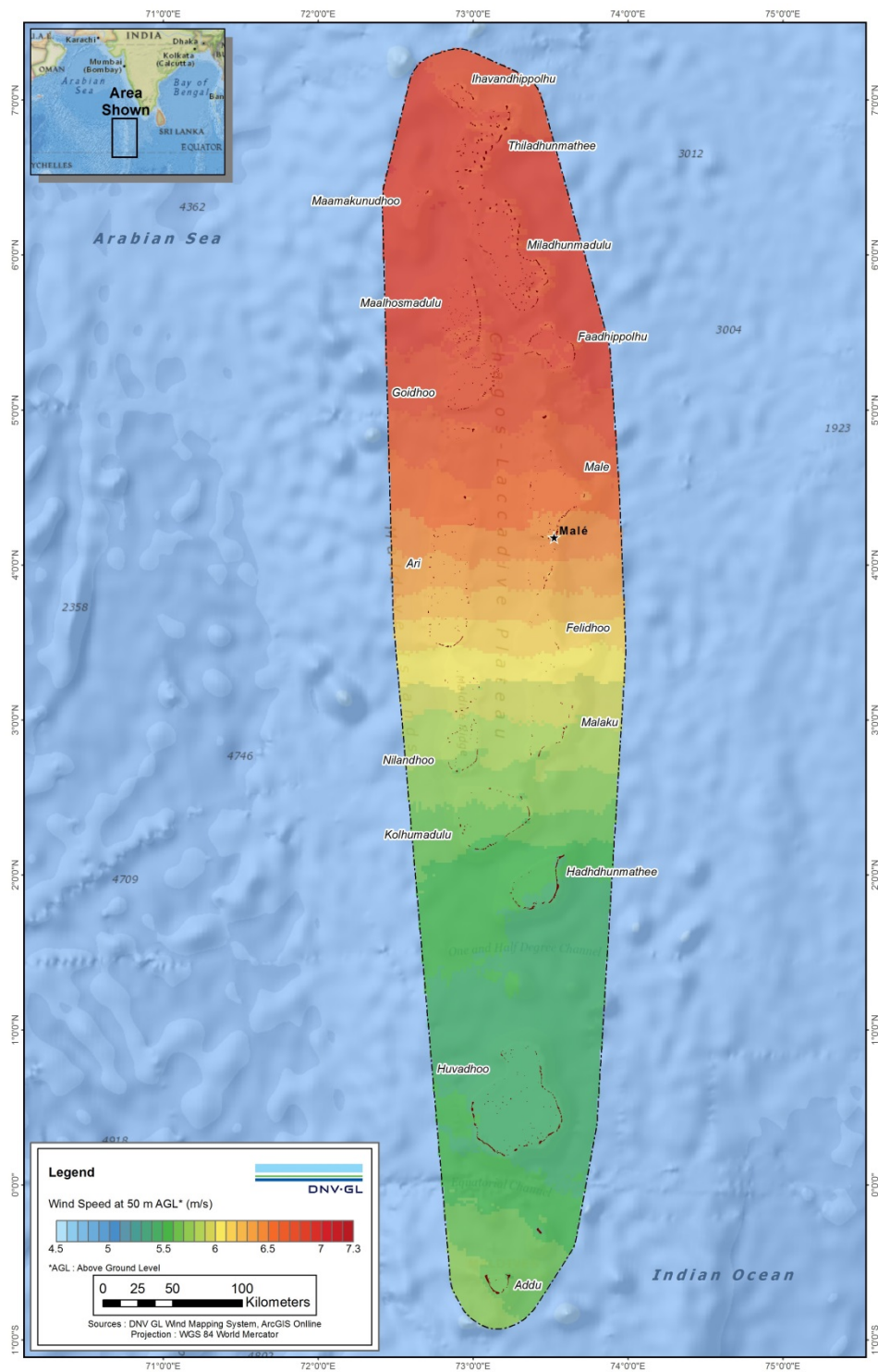


**Figure B-5 Preliminary and unvalidated mesoscale wind speed map, 50 m AGL, as simulated by the DNV GL Wind Mapping System**

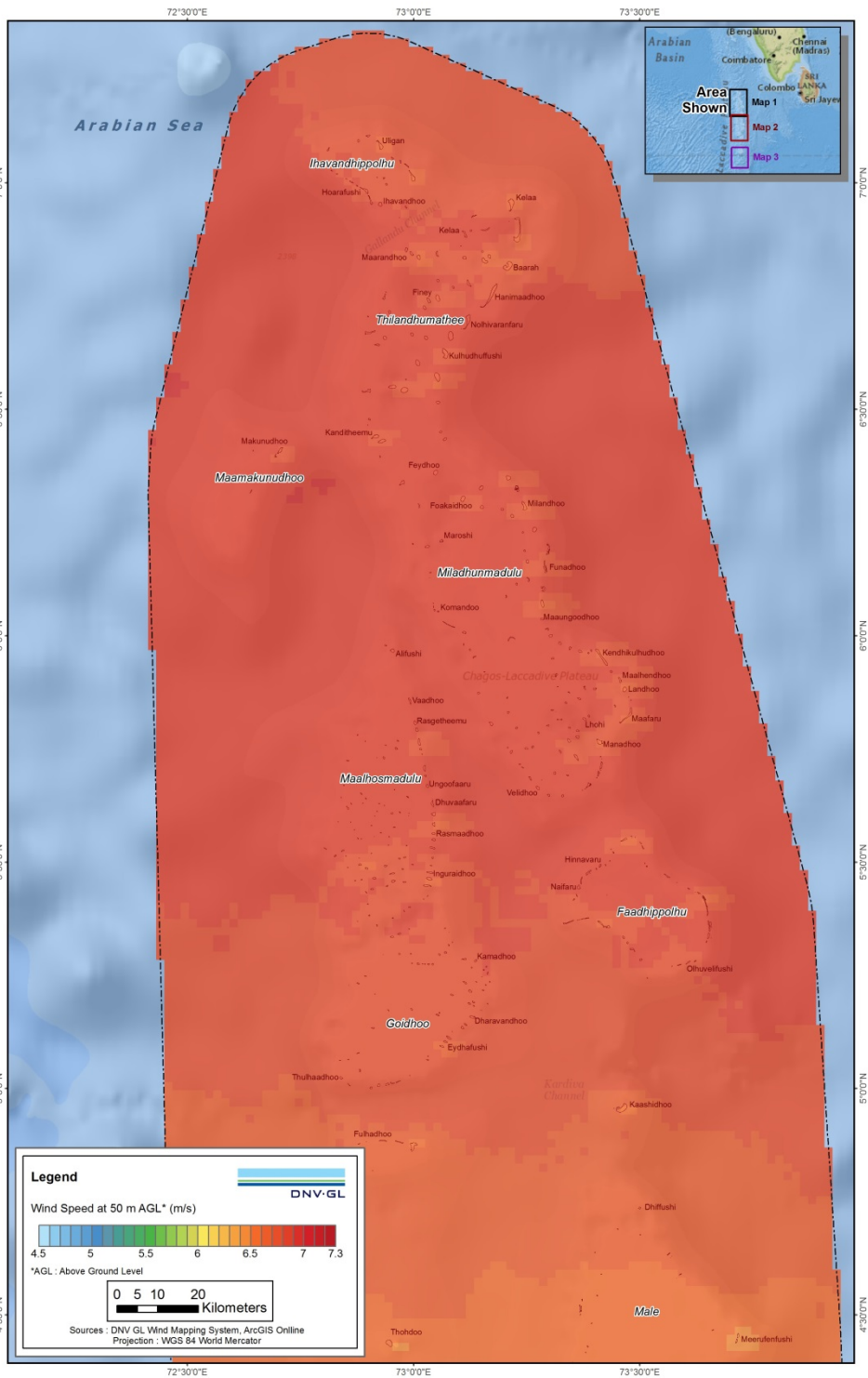


**Figure B-6 Preliminary and unvalidated mesoscale wind speed map of the north of the Maldives, 50 m AGL, as simulated by the DNV GL Wind Mapping System**

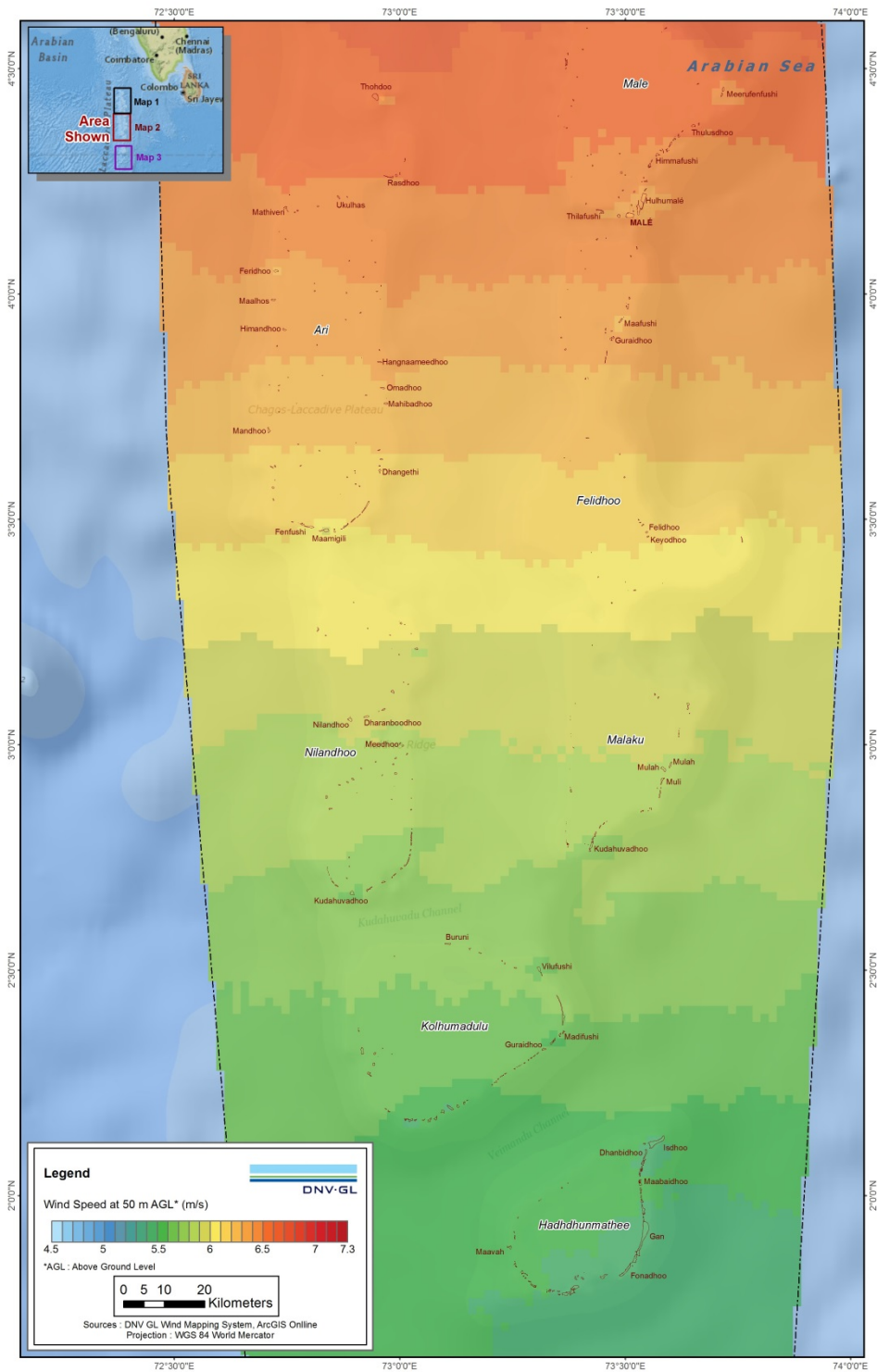


**Figure B-7 Preliminary and unvalidated mesoscale wind speed map of the center of the Maldives, 50 m AGL, as simulated by the DNV GL Wind Mapping System**

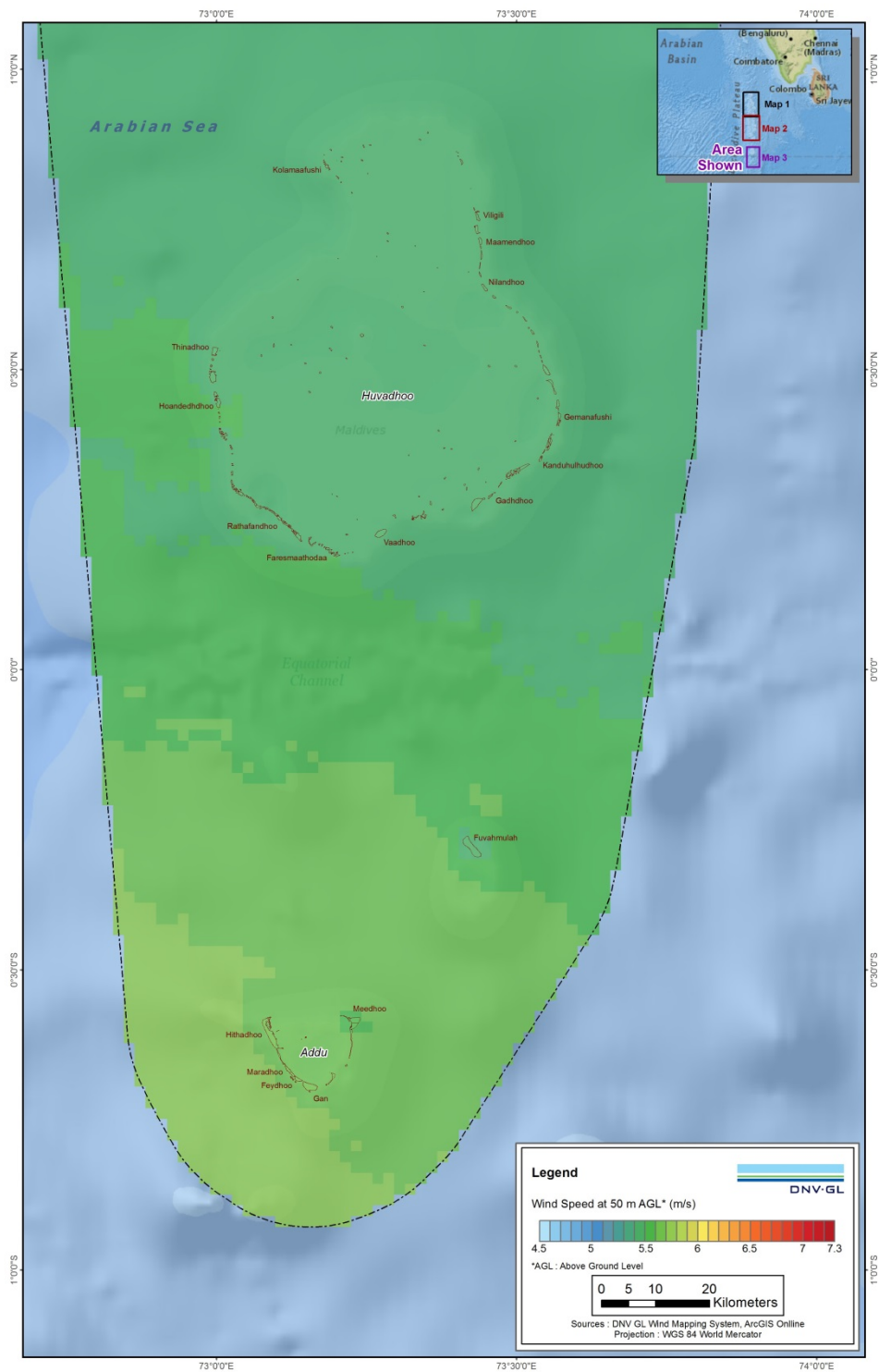


**Figure B-8 Preliminary and unvalidated mesoscale wind speed map of the south of the Maldives, 50 m AGL, as simulated by the DNV GL Wind Mapping System**

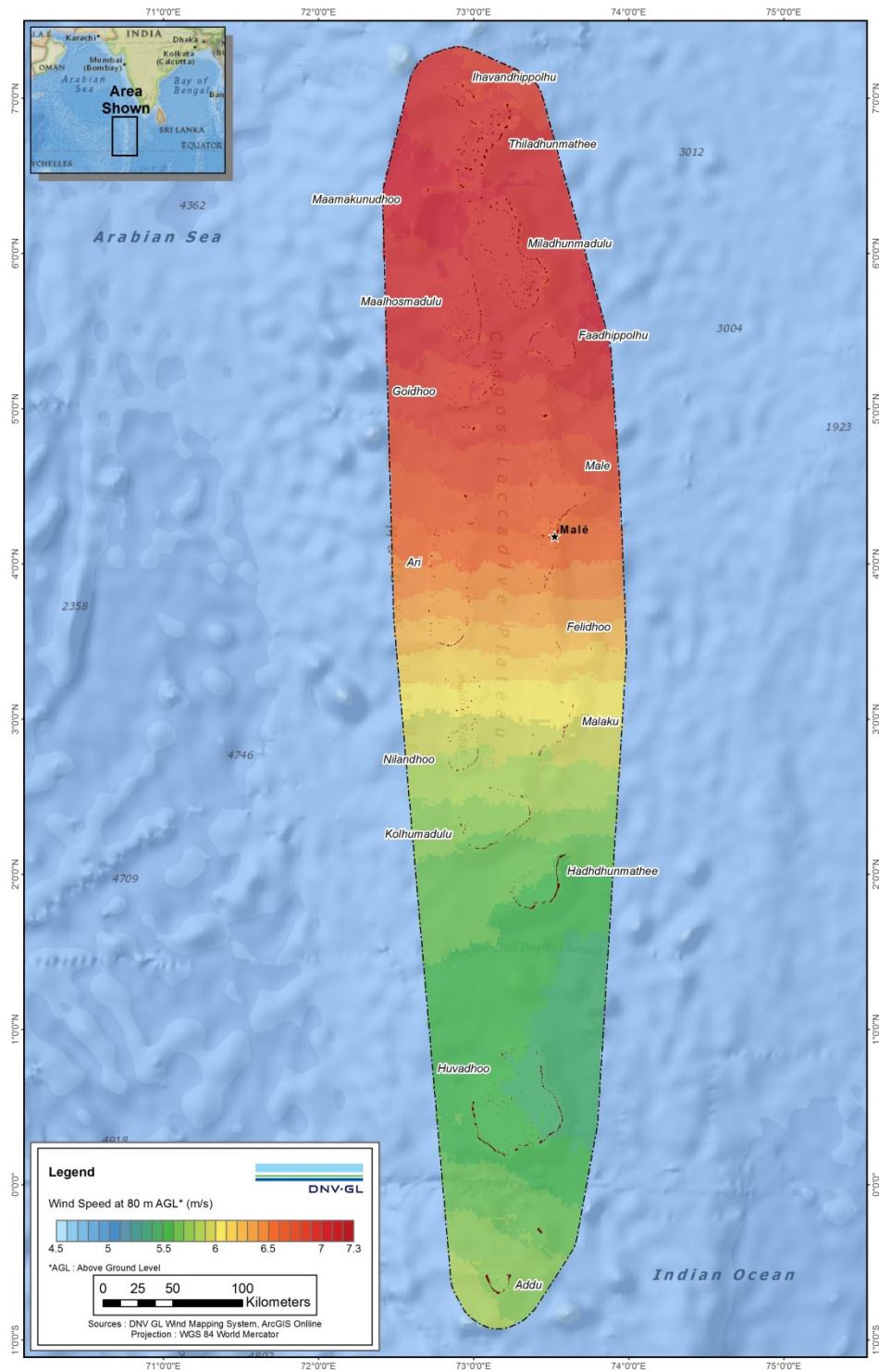


**Figure B-9 Preliminary and unvalidated mesoscale wind speed map, 80 m AGL, as simulated by the DNV GL Wind Mapping System**

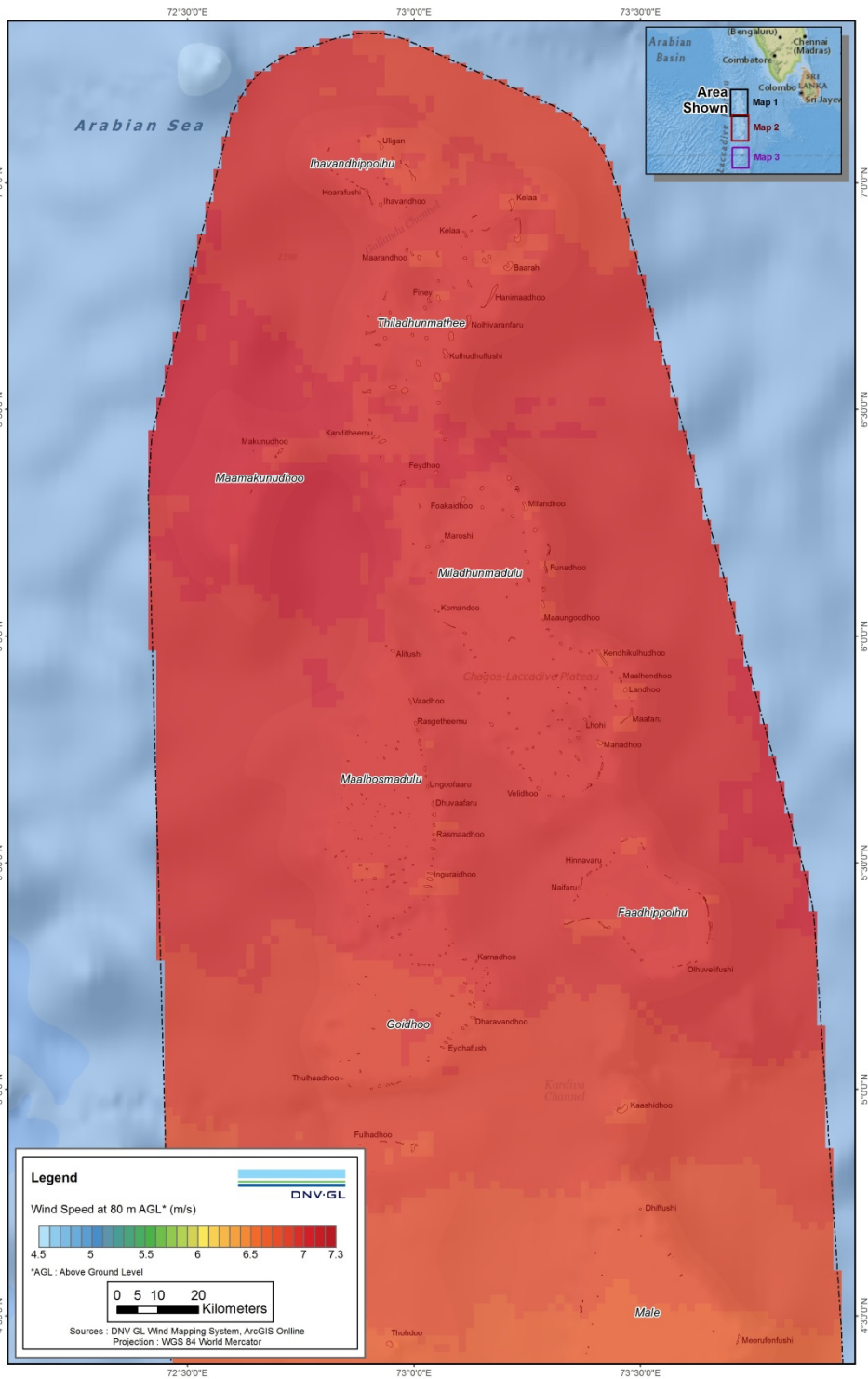


**Figure B-10 Preliminary and unvalidated mesoscale wind speed map of the north of the Maldives, 80 m AGL, as simulated by the DNV GL Wind Mapping System**

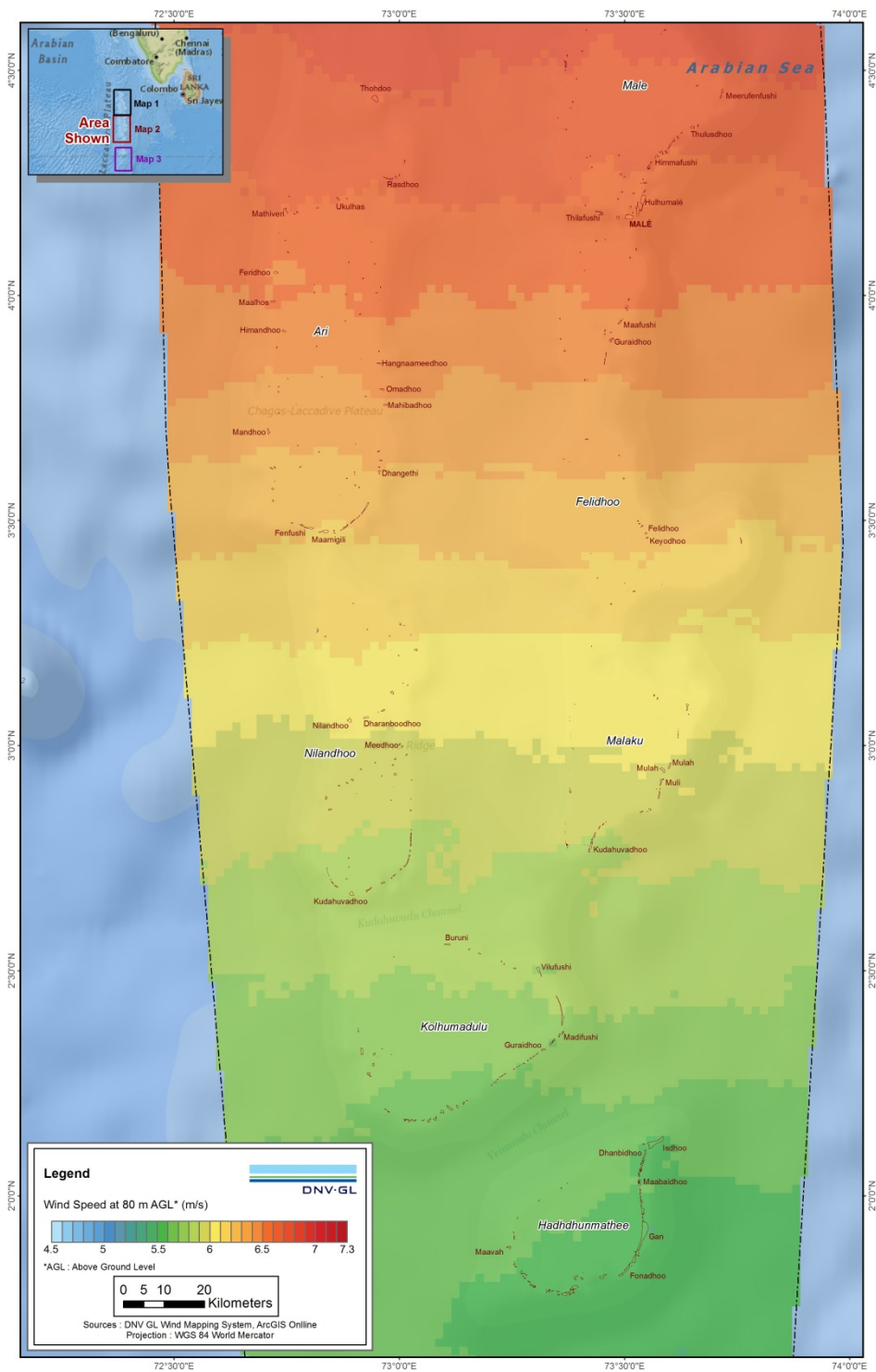


**Figure B-11 Preliminary and unvalidated mesoscale wind speed map of the center of the Maldives, 80 m AGL, as simulated by the DNV GL Wind Mapping System**

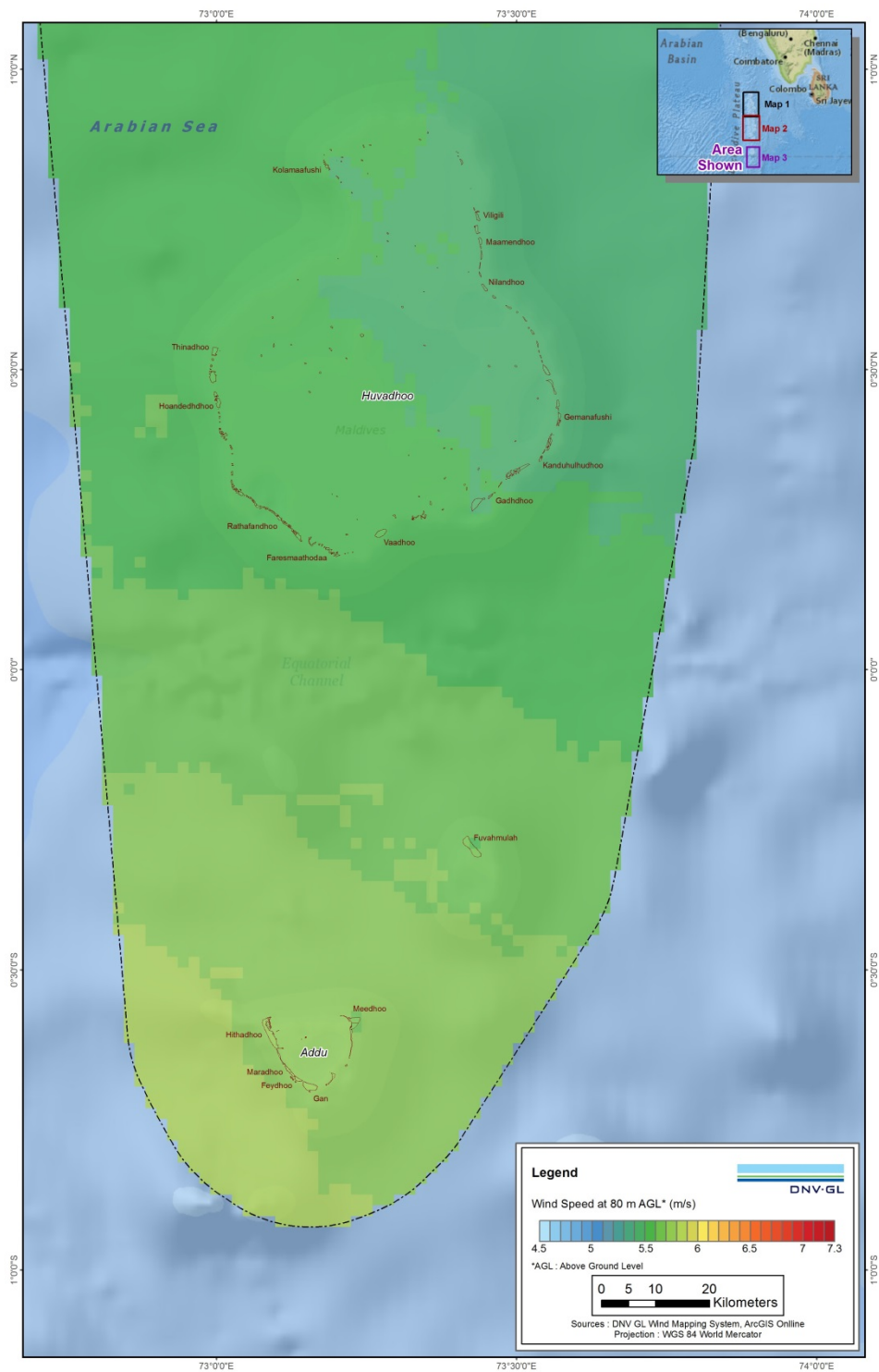


**Figure B-12 Preliminary and unvalidated mesoscale wind speed map of the south of the Maldives, 80 m AGL, as simulated by the DNV GL Wind Mapping System**



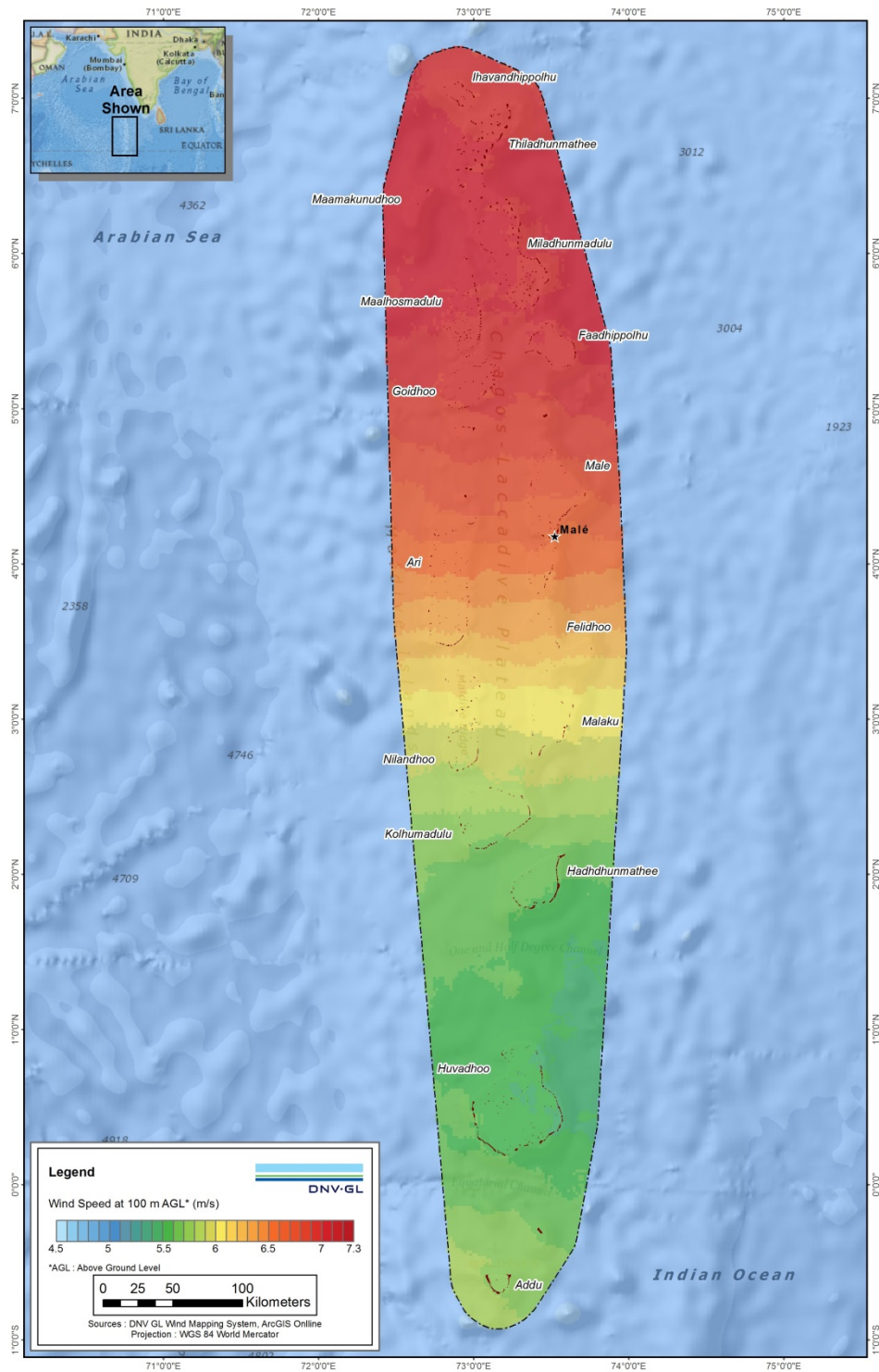


**Figure B-13 Preliminary and unvalidated mesoscale wind speed map, 100 m AGL, as simulated by the DNV GL Wind Mapping System**

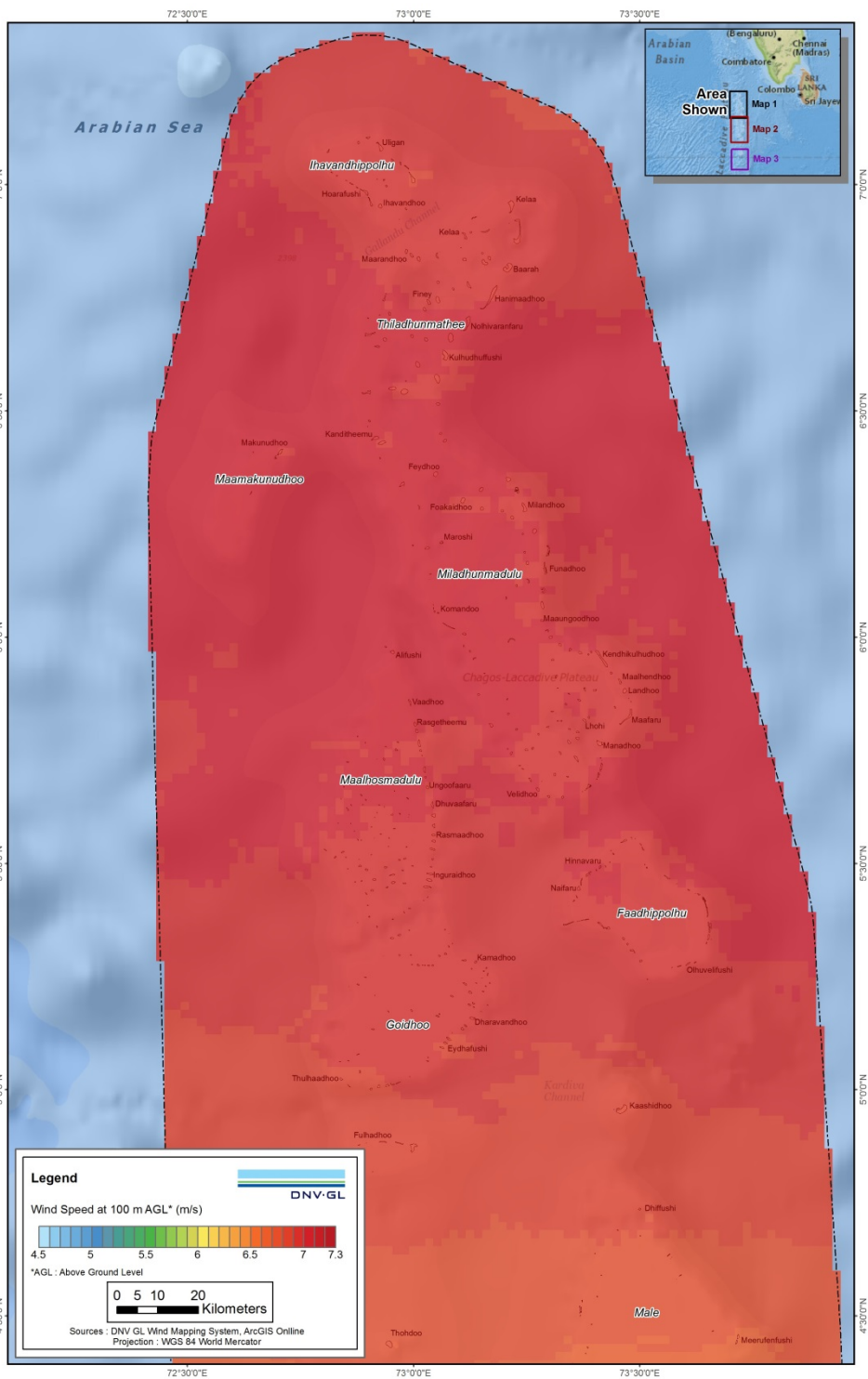


**Figure B-14 Preliminary and unvalidated mesoscale wind speed map of the north of the Maldives, 100 m AGL, as simulated by the DNV GL Wind Mapping System**

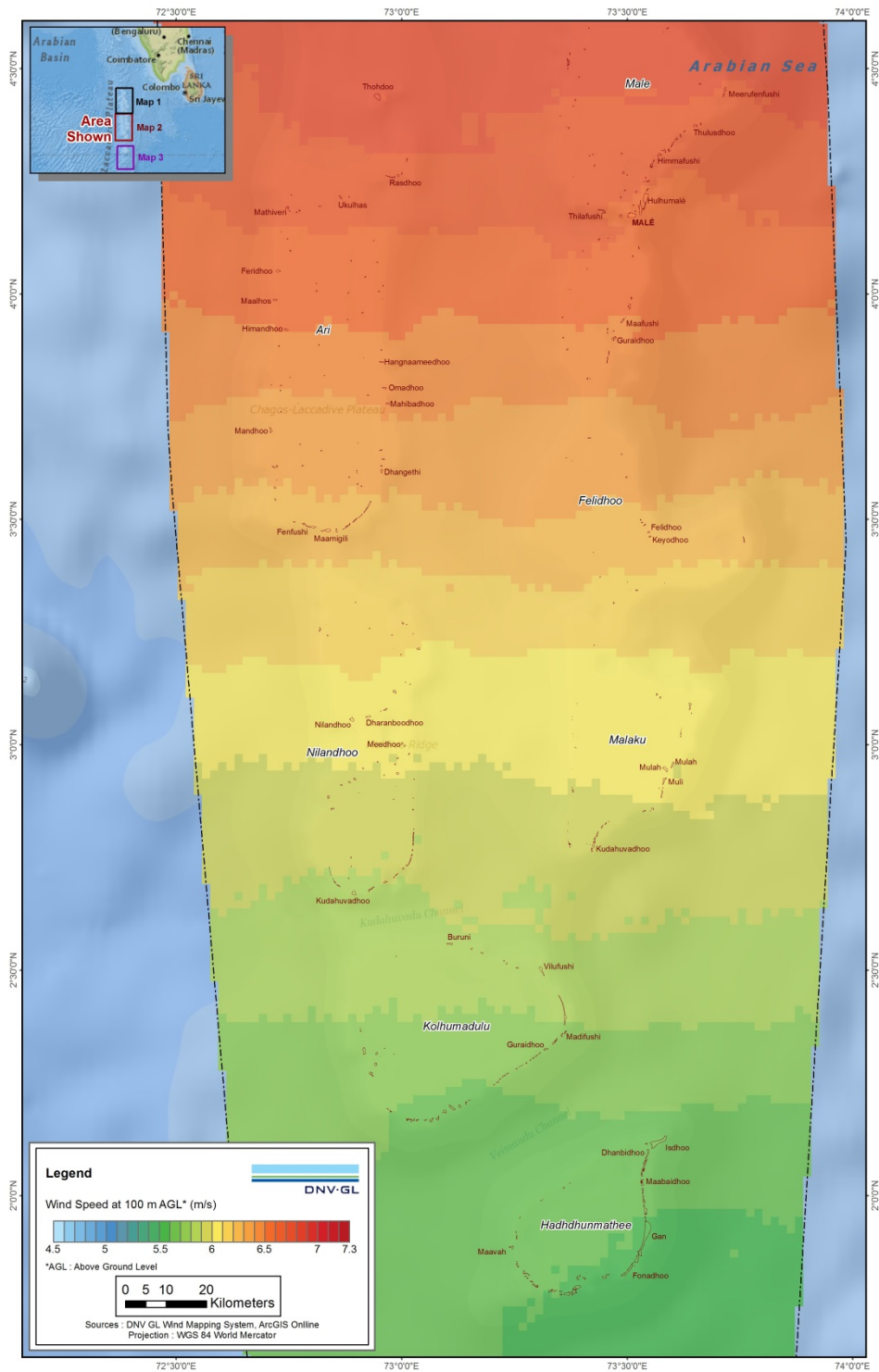


**Figure B-15 Preliminary and unvalidated mesoscale wind speed map of the center of the Maldives, 100 m AGL, as simulated by the DNV GL Wind Mapping System**

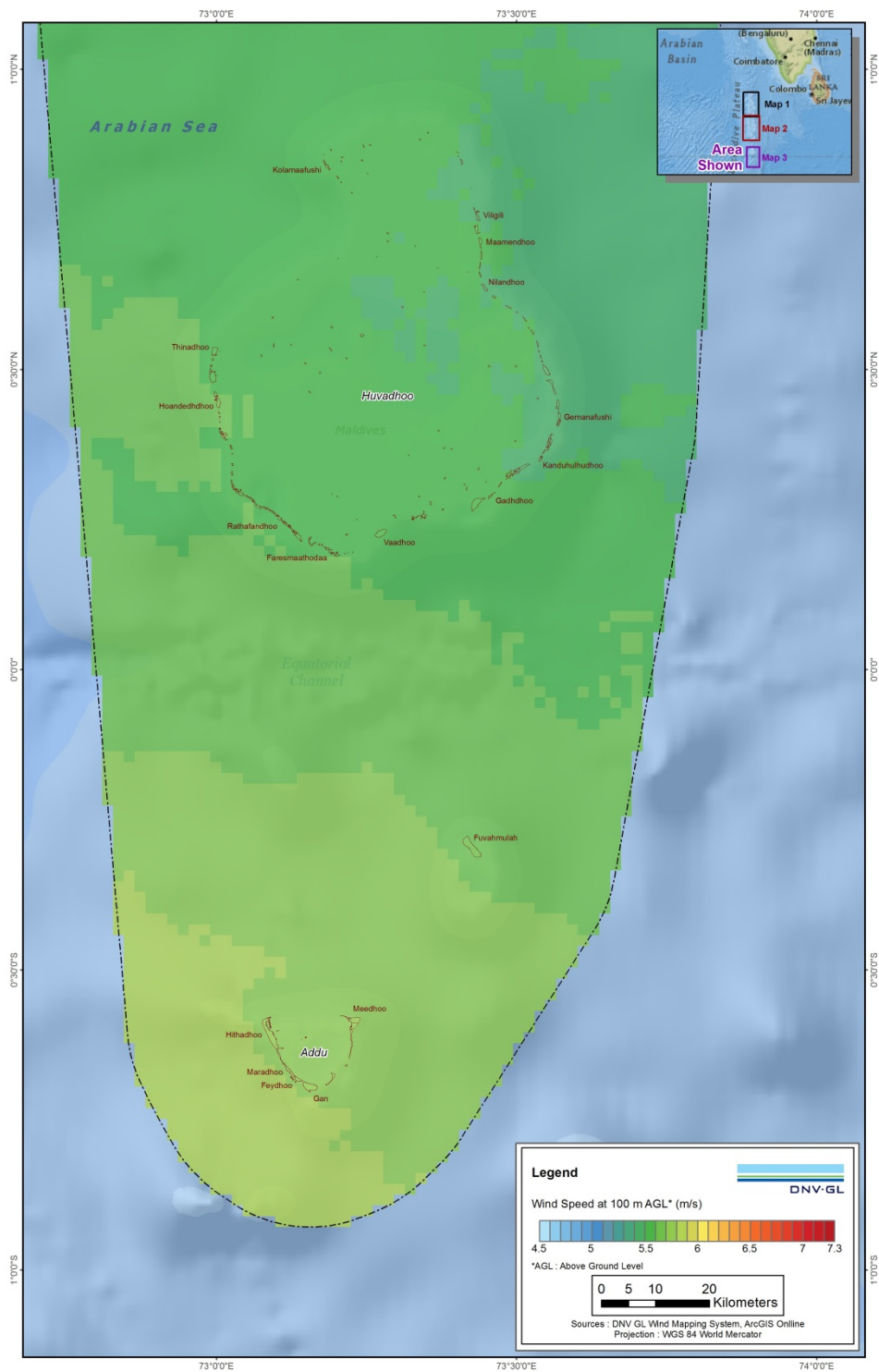


**Figure B-16 Preliminary and unvalidated mesoscale wind speed map of the south of the Maldives, 100 m AGL, as simulated by the DNV GL Wind Mapping System**

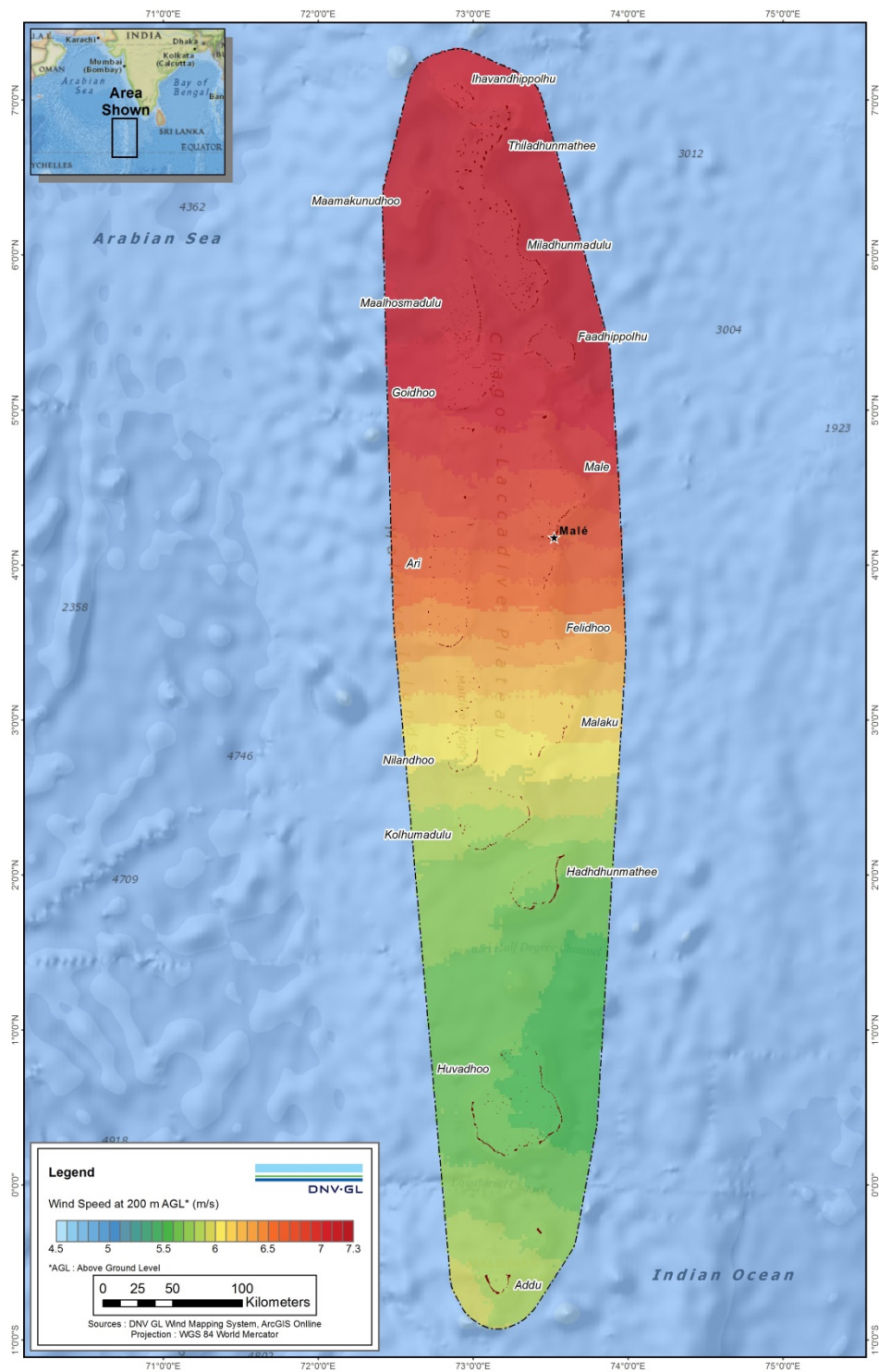


**Figure B-17 Preliminary and unvalidated mesoscale wind speed map, 200 m AGL, as simulated by the DNV GL Wind Mapping System**

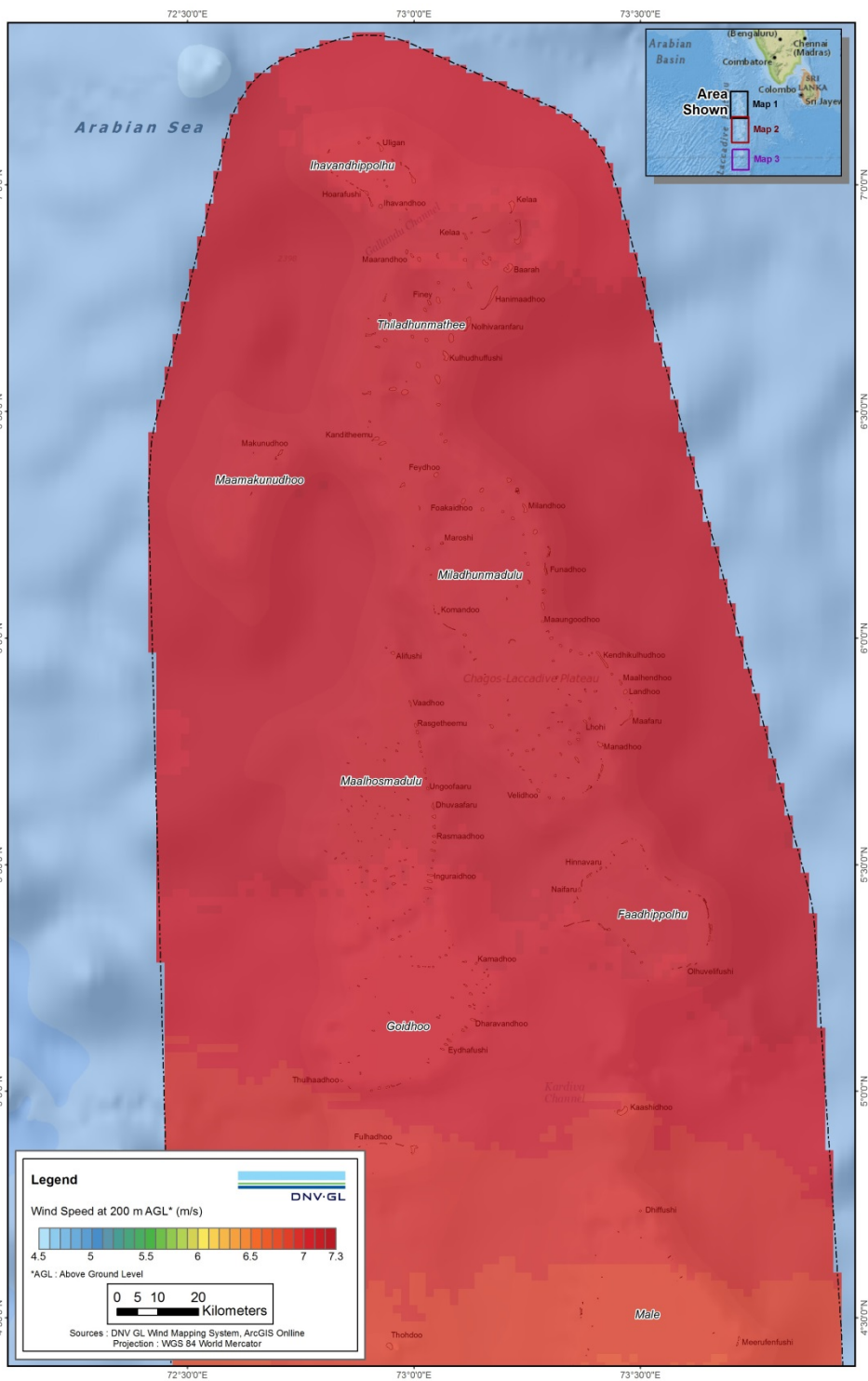


**Figure B-18 Preliminary and unvalidated mesoscale wind speed map of the north of the Maldives, 200 m AGL, as simulated by the DNV GL Wind Mapping System**

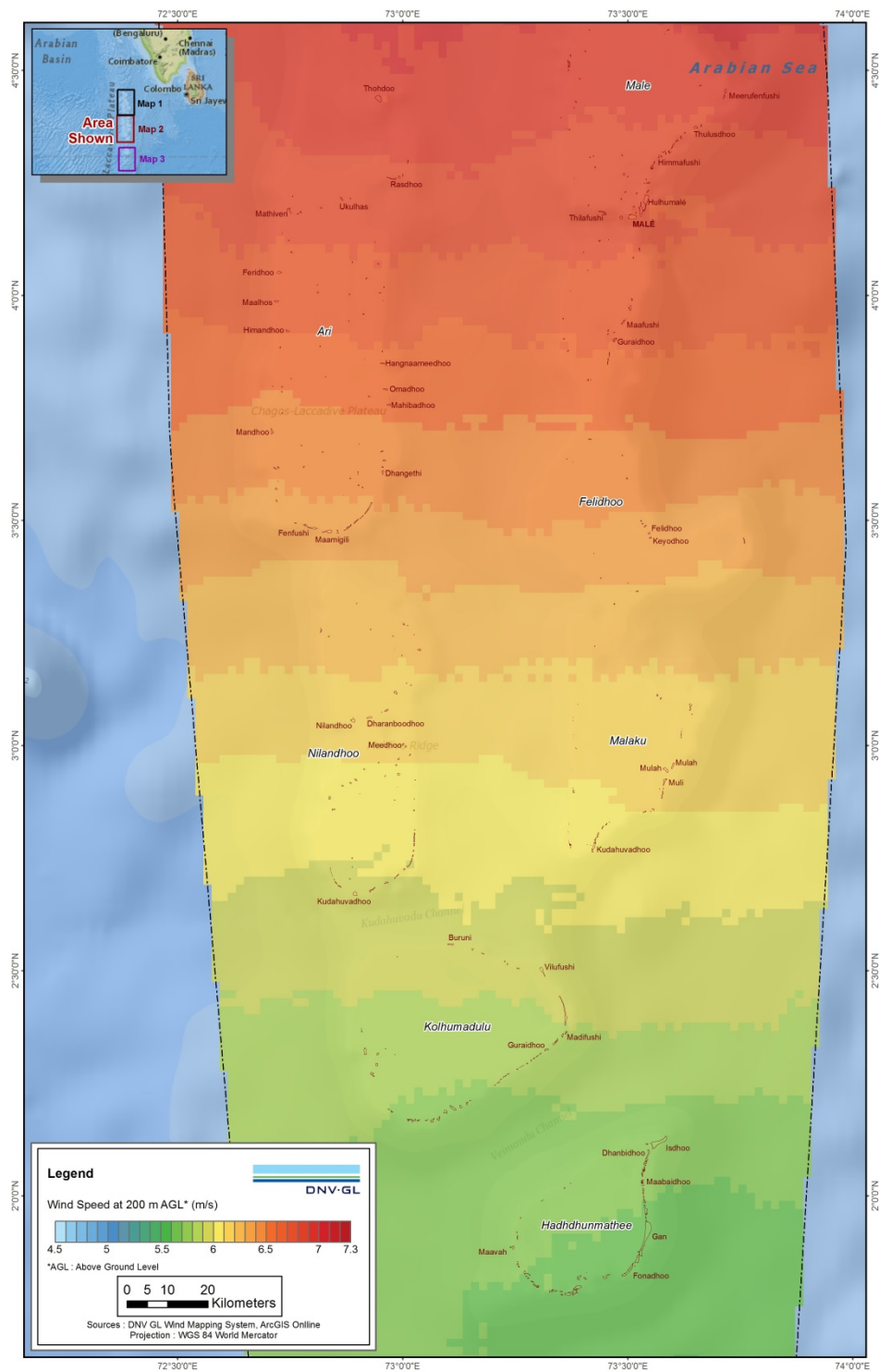


**Figure B-19 Preliminary and unvalidated mesoscale wind speed map of the center of the Maldives, 200 m AGL, as simulated by the DNV GL Wind Mapping System**

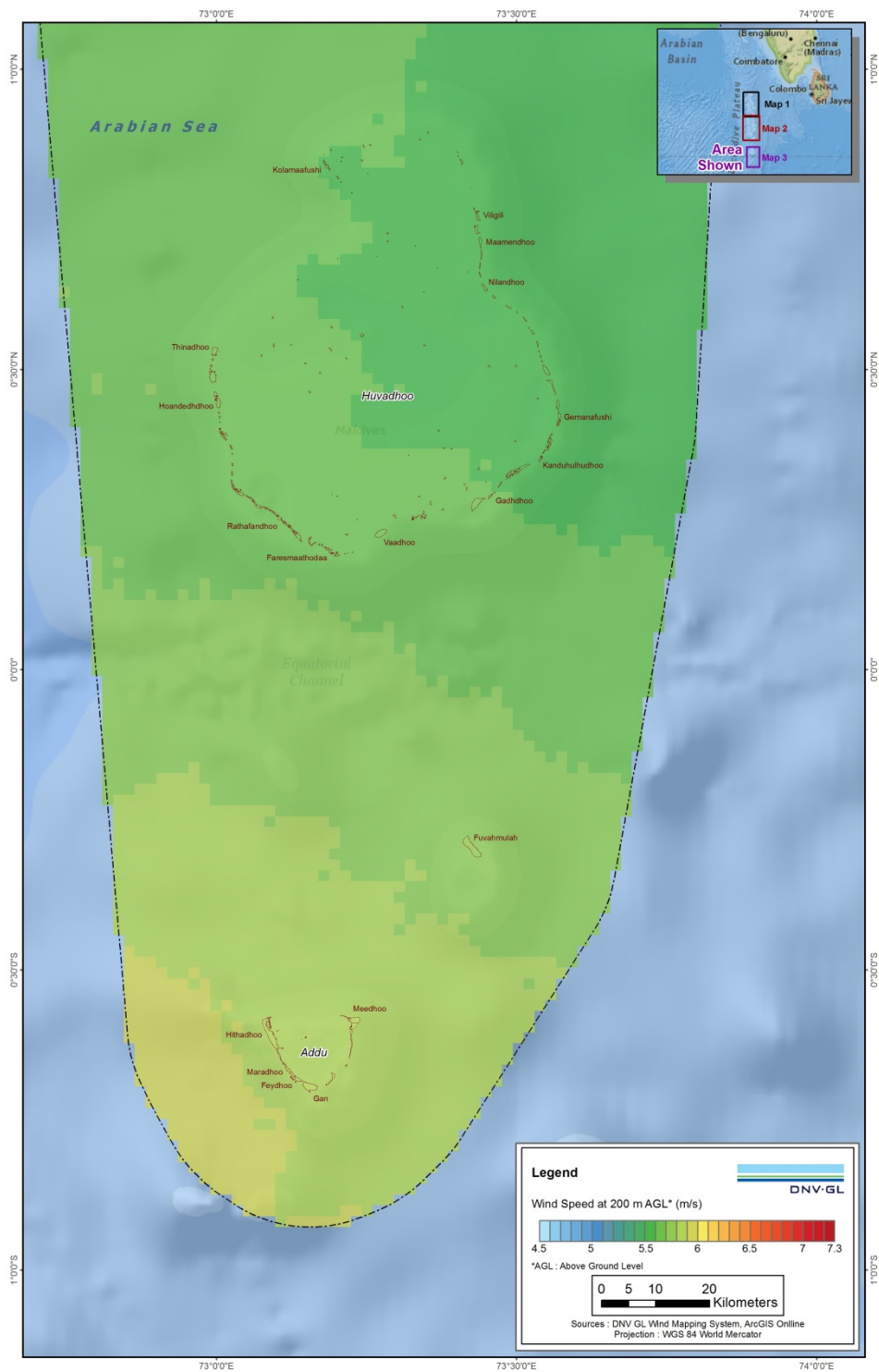


**Figure B-20 Preliminary and unvalidated mesoscale wind speed map of the south of the Maldives, 200 m AGL, as simulated by the DNV GL Wind Mapping System**



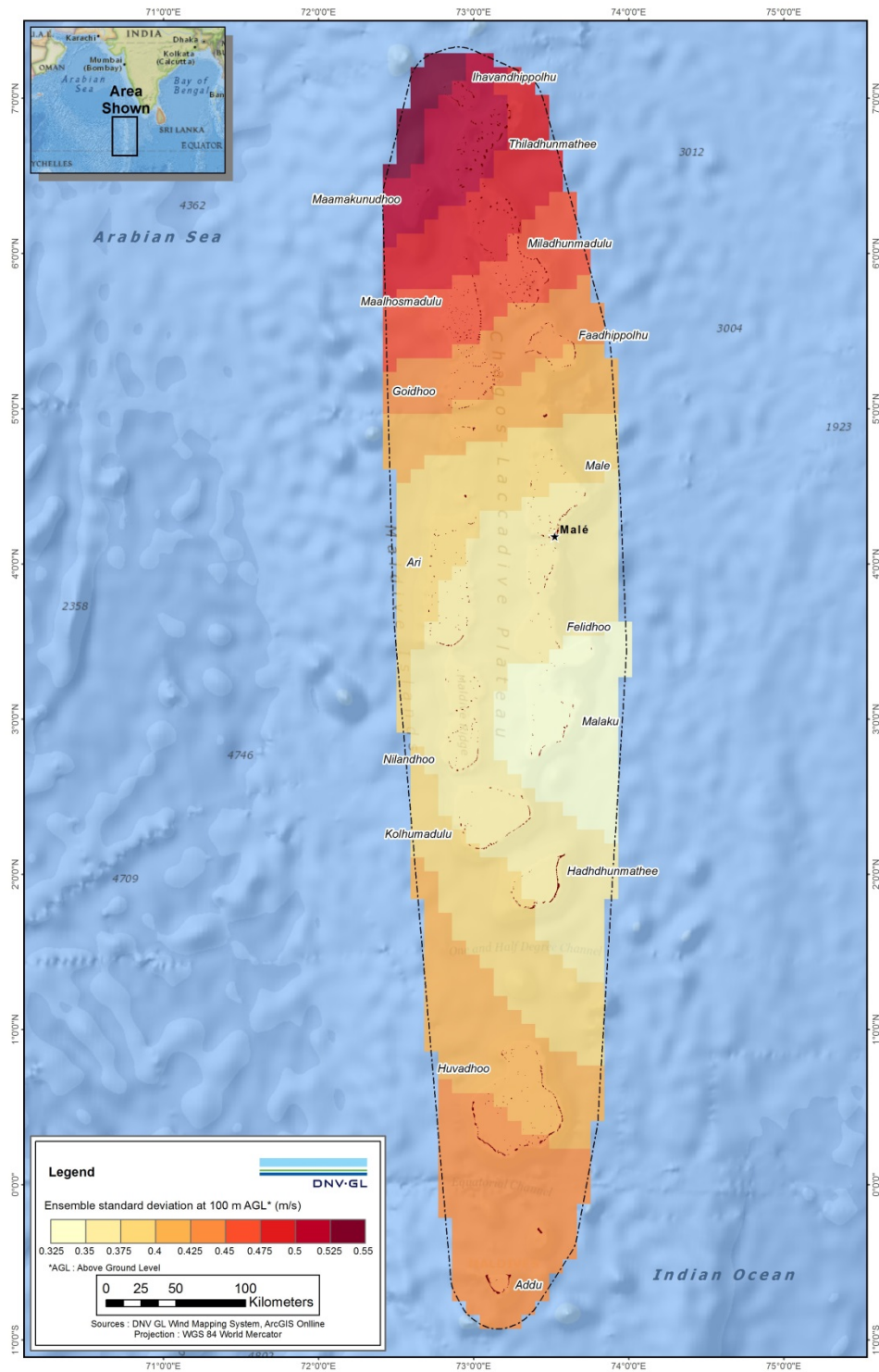


**Figure B-21 Preliminary and unvalidated wind speed uncertainty index created with the DNV GL Wind Mapping System**

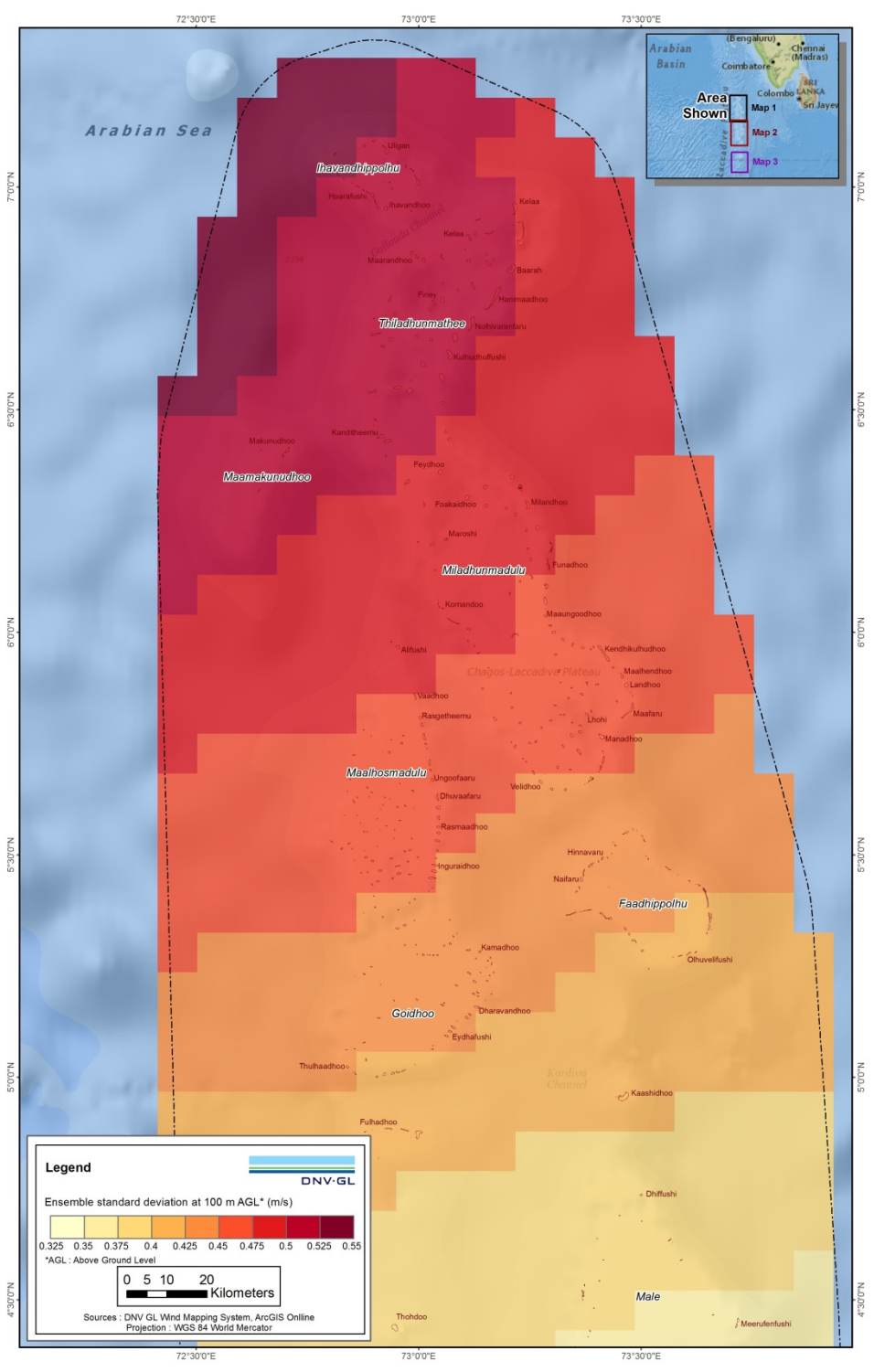


**Figure B-22 Preliminary and unvalidated wind speed uncertainty index for the north of the Maldives created with the DNV GL Wind Mapping System**

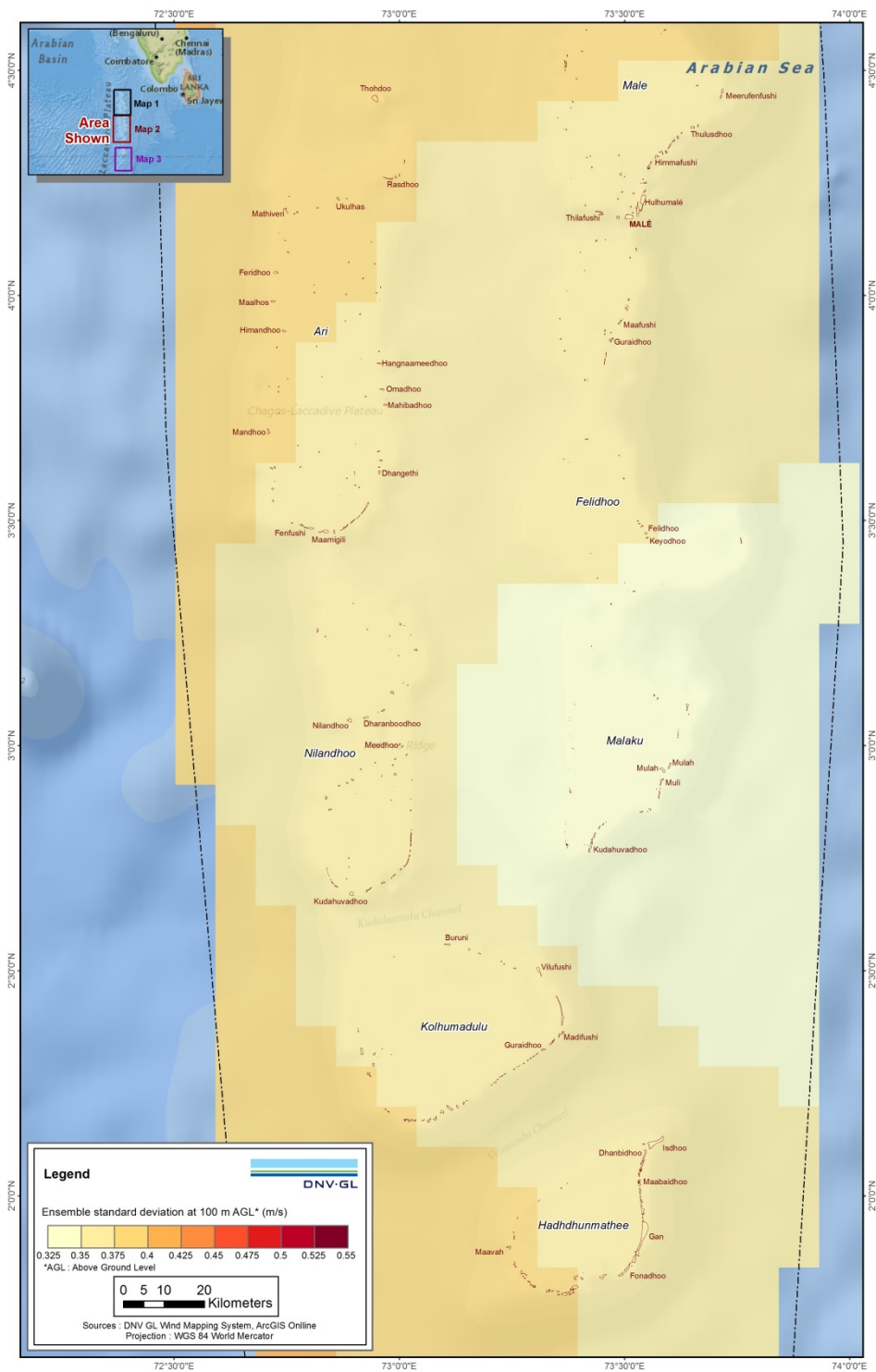


**Figure B-23 Preliminary and unvalidated wind speed uncertainty index for the center of the Maldives created with the DNV GL Wind Mapping System**

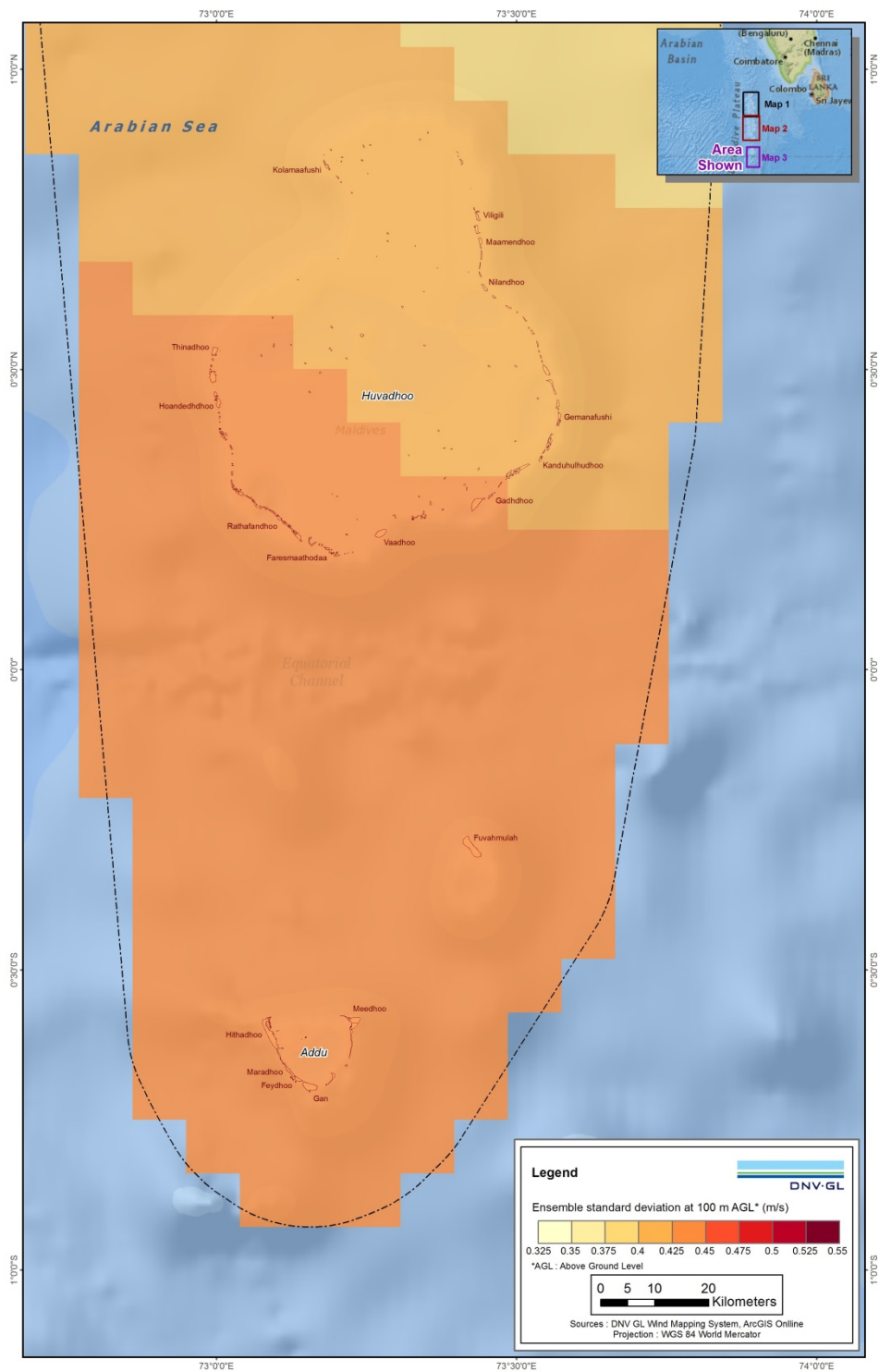


**Figure B-24 Preliminary and unvalidated wind speed uncertainty index for the south of the Maldives created with the DNV GL Wind Mapping System**

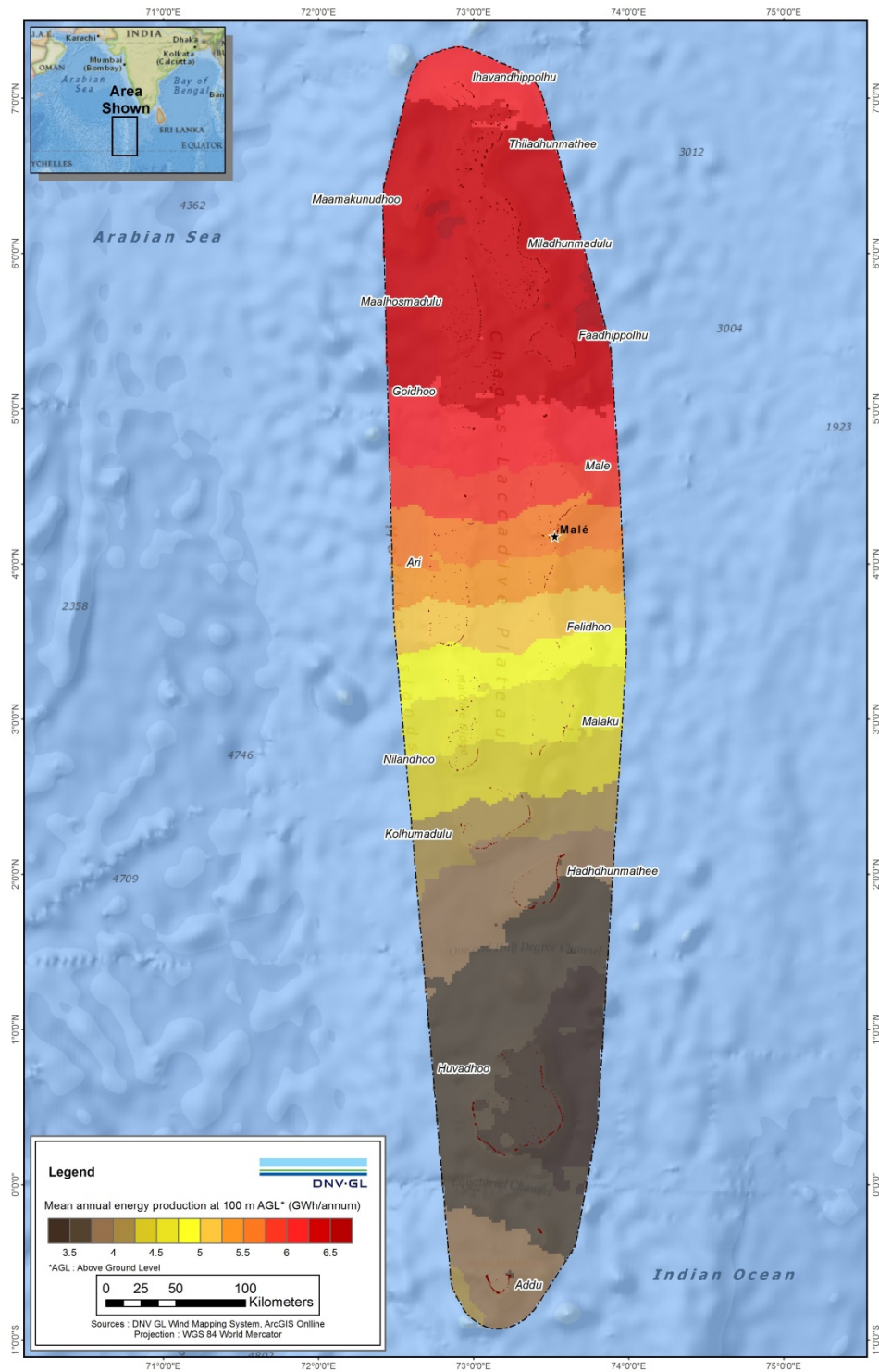


**Figure B-25 Preliminary and unvalidated wind energy map created using the DNV GL Wind Mapping System**

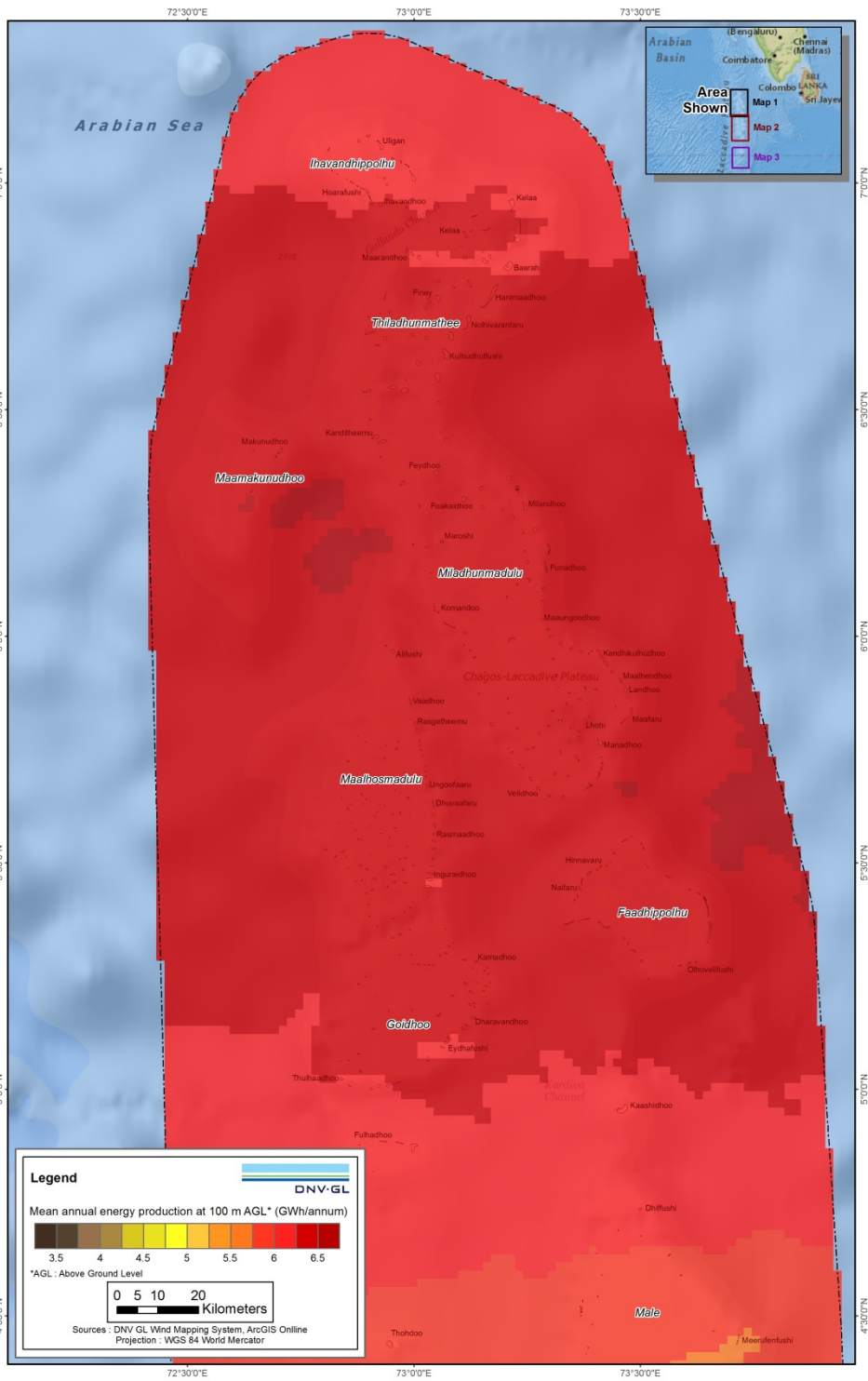


**Figure B-26 Preliminary and unvalidated wind energy map of the north of the Maldives created using the DNV GL Wind Mapping System**

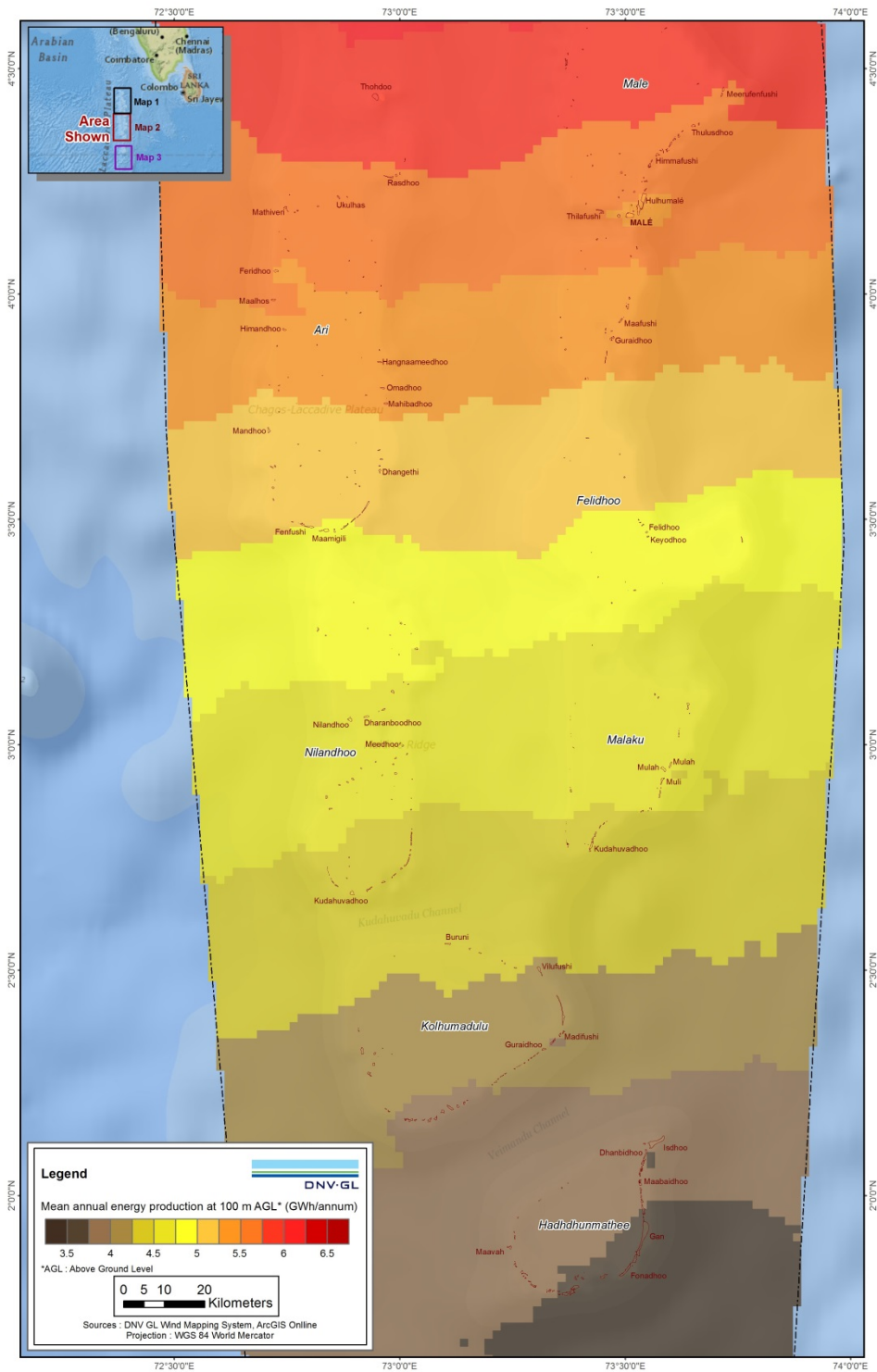


**Figure B-27 Preliminary and unvalidated wind energy map of the center of the Maldives created using the DNV GL Wind Mapping System**

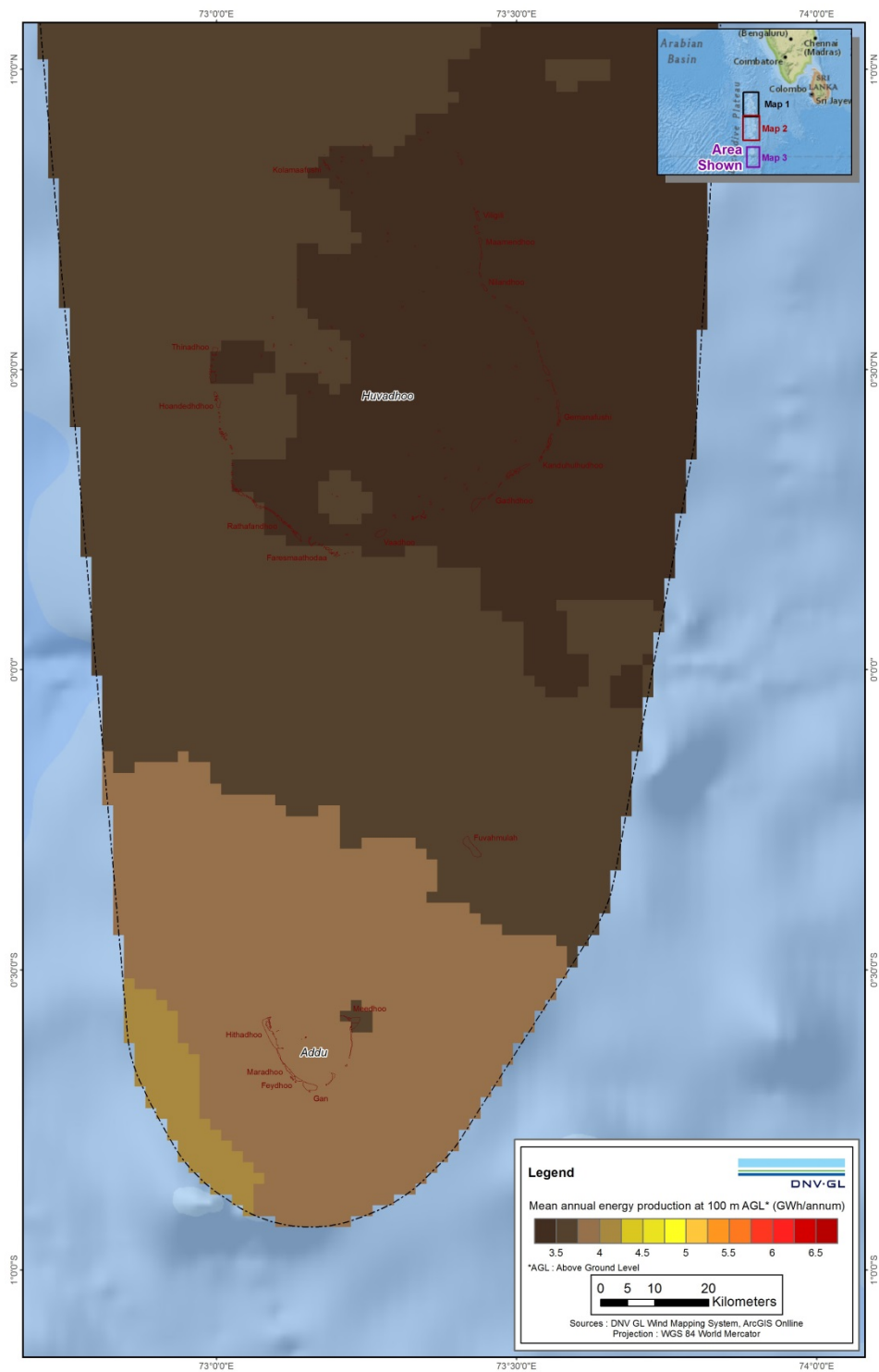


**Figure B-28 Preliminary and unvalidated wind energy map of the south of the Maldives created using the DNV GL Wind Mapping System**



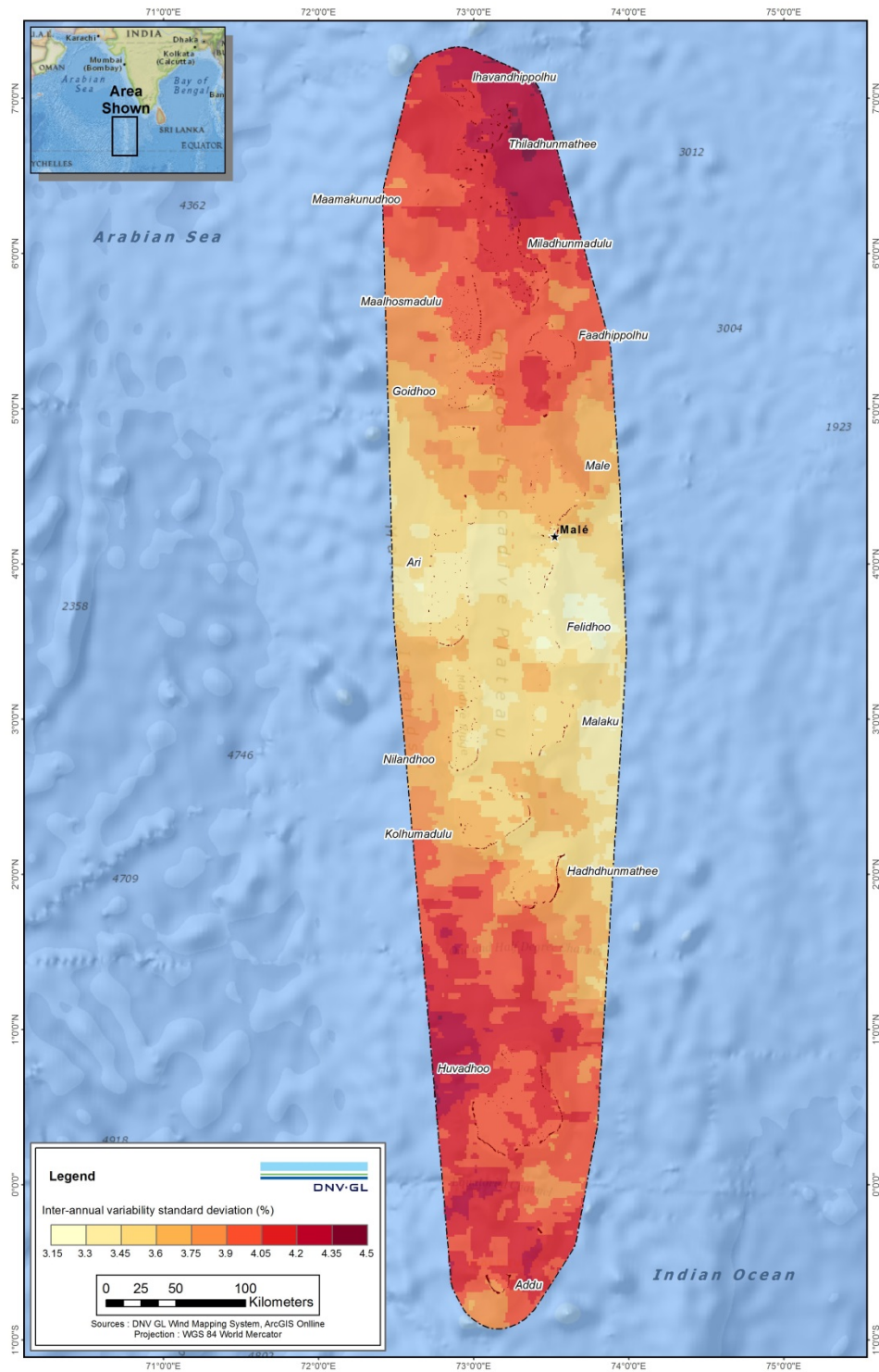
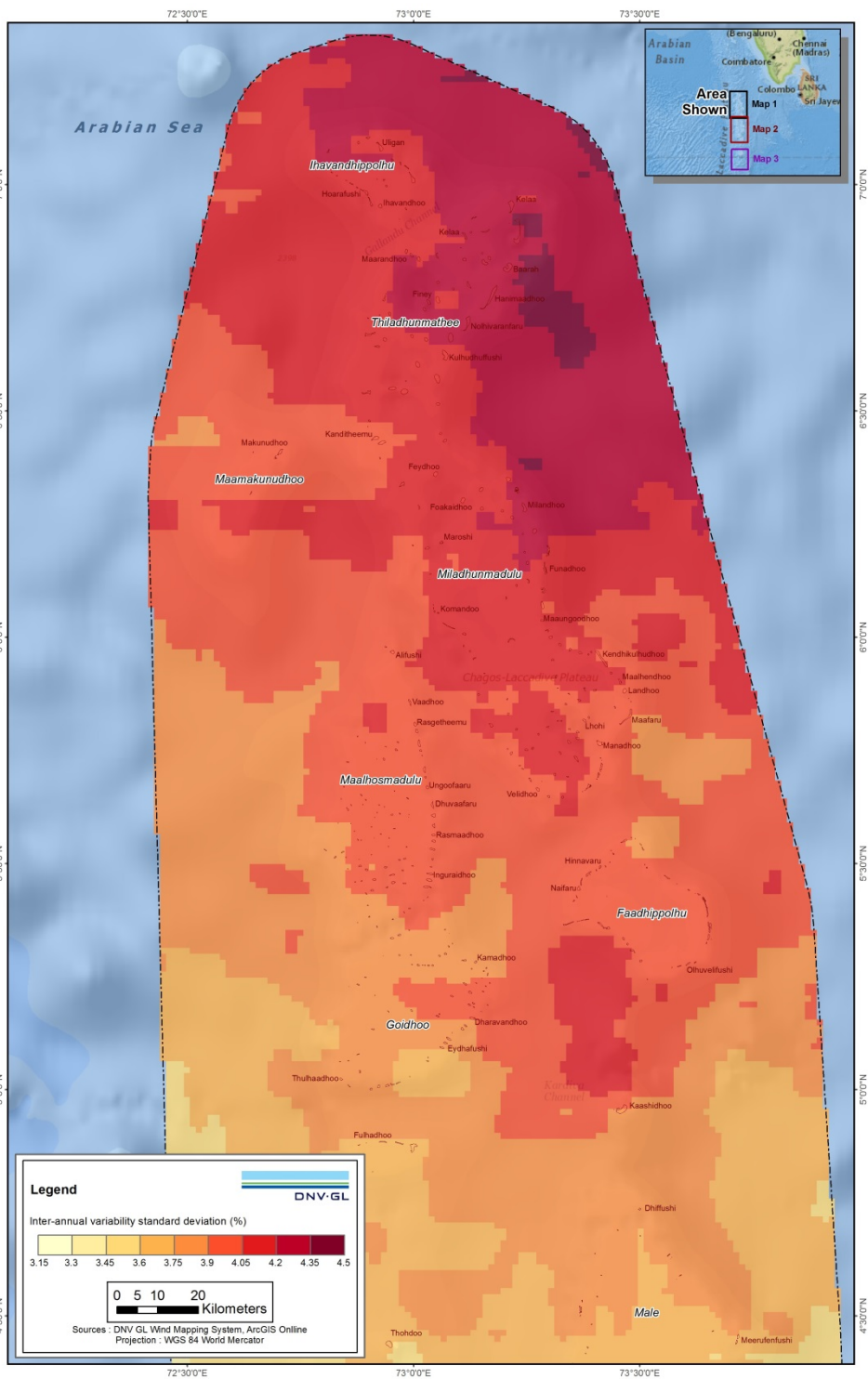
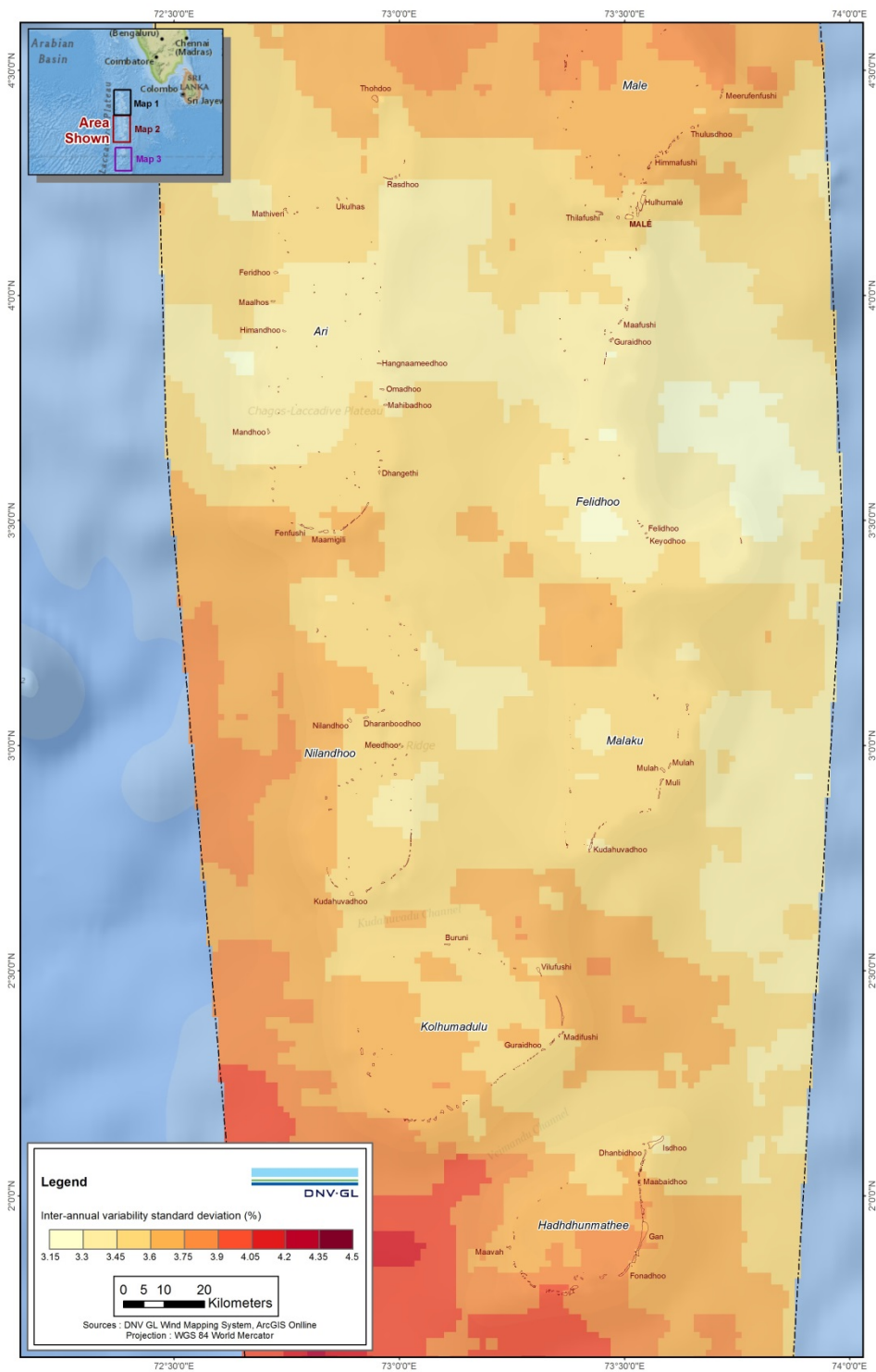


Figure B-29 Preliminary and unvalidated interannual variability index (IAVI) for wind speed



**Figure B-30 Preliminary and unvalidated interannual variability index (IAVI) for wind speed for the north of the Maldives**



**Figure B-31 Preliminary and unvalidated interannual variability index (IAVI) for wind speed for the center of the Maldives**

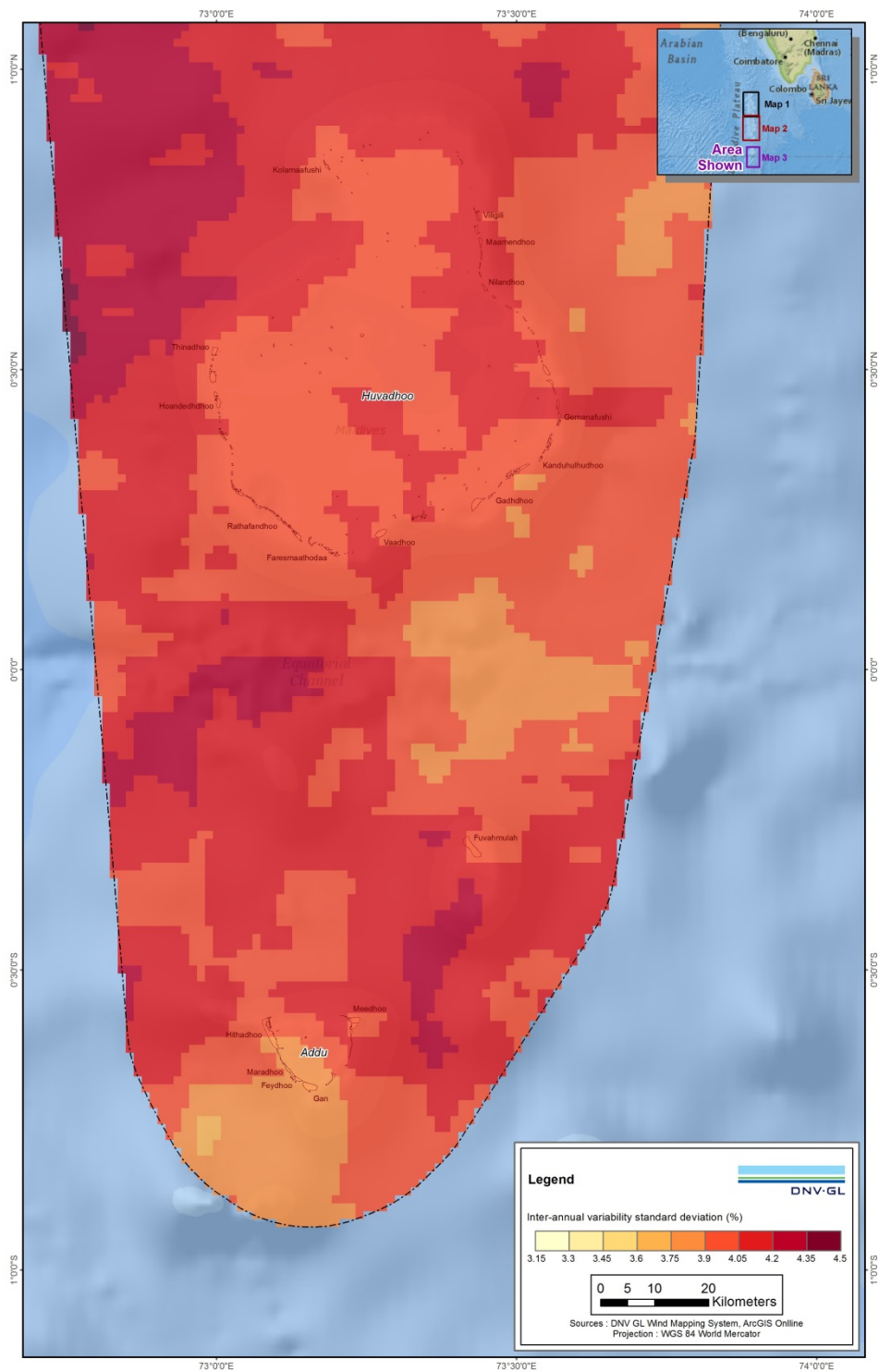


**Figure B-32 Preliminary and unvalidated interannual variability index (IAVI) for wind speed for the south of the Maldives**



## **ABOUT DNV GL**

Driven by our purpose of safeguarding life, property and the environment, DNV GL enables organizations to advance the safety and sustainability of their business. We provide classification and technical assurance along with software and independent expert advisory services to the maritime, oil and gas, and energy industries. We also provide certification services to customers across a wide range of industries. Operating in more than 100 countries, our 16,000 professionals are dedicated to helping our customers make the world safer, smarter, and greener.